

The Oregon Graduate Institute One Dimensional
Time-Dependent Radiative Convective Model:
Theory and Application

Robert Malcolm MacKay
B.A., California State University Chico, USA, 1978
M.S., Portland State University, Portland Oregon, 1983

A Thesis submitted to the faculty of the
Oregon Graduate Institute of Science
and Technology in partial fulfillment
of the requirements for the degree
Master of Science
in
Atmospheric Physics

An interdisciplinary program
between the departments of
Environmental Science & Engineering
and
Applied Physics & Electrical Engineering

October, 1990

The Thesis "The Oregon Graduate Institute One Dimensional Time-Dependent Radiative Convective Model: Theory and Application" by Robert Malcolm MacKay has been examined and approved by the following Examination Committee:

M.A.K. Khalil, Thesis Advisor
Professor

Reinhold A. Rasmussen
Professor

J. Fred Holmes
Professor

James F. Pankow
Professor

Acknowledgements

I would like to express my deep gratitude to my thesis advisor Dr. Aslam Khalil, for without his many suggestions and words of encouragement this thesis would not have been possible.

I would also like to thank the other members of my thesis committee, Dr. Rei Rasmussen, Dr. Fred Holmes, and Dr. James Pankow for their time and effort spent as committee members and reading this manuscript.

I would like to thank: Ms. Martha Shearer for her help with the many technical hurdles I have encountered while working with the computer facilities at OGI; and Paul Turner for helping me get acquainted with the OACIS hypercube system at OGI.

I would like to thank my fellow students at OGI: Mr. Yu Lu; Mr. Weining Zhao; and Mr. Francis Moraes for their constructive comments and conversations.

I would like to thank all of the library staff at OGI for their help in locating many of the references for this thesis.

I would like to thank all of my colleagues at Clark

College and the Clark College administration for their help and support during the time of this work.

Finally I would like to thank my wife Linda for her careful proof reading of this manuscript, and her never ending encouragement and patience.

This work was supported in part by grants from the Department of Energy (DE-FG06-85ER60313) and the National Science Foundation (DPP-8820632, DPP-8821320).

Dedication

This thesis is dedicated to my father, Malcom R. Mackay (1916-1984) who, through his patience and wisdom, taught me to persevere through times of frustration and to appreciate the simpler aspects of life.

Table of Contents

Chapter 1. Introduction to Climate Modeling	1
1.1 Introduction	1
1.2 The Greenhouse Effect (0-D model)	7
Chapter 2. Theory of the Absorption Spectra of Atmospheric Gases.	19
2.1 Theoretical Overview	19
2.2 Absorption for a Single Line	25
2.3 Band Models	30
Chapter 3. I.R. Absorptivities	35
3.1 Water Vapor	35
3.2 Carbon Dioxide	41
3.3 Ozone	56
3.4 Nitrous Oxide and Methane	59
3.5 Other Gases	70

Chapter 4.	Solar Absorption	72
4.1	Water Vapor	74
4.2	H ₂ O Cloudy Skies	77
4.3	Ozone	83
4.4	CO ₂ and O ₂	86
4.5	Surface Absorption	88
Chapter 5.	The OGI 1D Time Dependent RCM	91
5.1	Overview of the Model Structure	91
5.2	Atmospheric Gases (vertical profiles)	97
	H ₂ O	97
	Other Gases	98
5.3	Convective Adjustment	101
5.4	IR Flux for Cloudy Skies	106
Chapter 6.	The OGI 1D RCM	
	(Performance and Sensitivity)	109
6.1	Equilibrium Temperature Profile	109
6.2	Time Constants	113
6.3	Time Step Sensitivity	117
6.4	Model sensitivity studies	119

Chapter 7. Trace Gas Perturbations	
and Climate Sensitivity	125
7.1 Surface temperature Sensitivity	
to Trace Gas Perturbations	125
7.2 Modeled Trends in Temperature	
of the Past Century	131
Chapter 8. Conclusions	145
References.	148
Appendix A.	153
A.1 Theory of IR flux calculations	153
A.2 Theory of working equations	160
Appendix B.	167
B.1 Physical Constants	167
B.2 Conversion of Units	169
Appendix C.	170
C.1 Explanation of Input File	170

Appendix D.	173
D.1 Output When out1 Equals 1	173
D.2 Output When out2 Equals 1	177
D.3 Output When out3 Equals 1	180
D.4 Output Sent to Screen Every pout Time Steps	181
Appendix E.	
E.1 Program Source Code	182
Biographical Note	228

List of Figures

1.1	Outline of thesis structure	6
1.2	Comparative blackbody spectra for solar and terrestrial radiation	10
1.3	Zero dimensional model energy diagram	12
1.4	Feedback processes	15
1.5	Radiation flow diagram for the Earth	17
2.1	Normal vibrational modes for H ₂ O and CO ₂	21
2.2	Single line absorption	27
3.1	Water vapor emissivities	36
3.2	Water vapor continuum absorption	39
3.3	Carbon dioxide 15 μm band absorptance	47
3.4	Water vapor transmission parameters	51
3.5	Methane and nitrous oxide band absorptances	61
4.1	Solar spectrum	73
4.2	Composite cloud layer	81
5.1	Schematic of 18 layer model	92
5.2	Computational flow diagram	96
5.3	Methane and nitrous oxide vertical profiles	99
5.4	Ozone vertical profile	100
6.1	Vertical temperature profiles for different lapse rate adjustment schemes	110

6.2	Approach to equilibrium for different mixed layer depths	114
6.3a	Time constant vs ocean mixed layer depth	116
6.3b	$\ln(\Delta T)$ vs time	116
6.4a	Equilibrium temperature vs time step	118
6.4b	Outward flux at equilibrium vs time step	118
7.1	Comparison of ΔT for doubled CO_2 with other 1D RCMs	126
7.2	Vertical thermal structure for 1 x CO_2 and 2 x CO_2	128
7.3	OGI model vs WMO 1985	130
7.4	Predicted ΔT s due to CO_2 , CH_4 , N_2O , and F11 and F12 changes of the last 140 years.	134
7.5	Comparison of OGI output with the temperature record of Hansen and Lebedeff (1987)	135
7.6	Same as Figure 7.5 but with the addition of volcanos	139
A.1	Coordinate system of a plane parallel atmosphere	155
A.2	IR fluxes in the model atmosphere	161
A.3	Calculation of net heating rate	165

List of Tables

3.1	Carbon dioxide band absorption parameters	44
3.2	Water vapor transmission parameters for CO ₂ H ₂ O overlap region	52
3.3	Methane and nitrous oxide band absorption parameters	60
3.4	Methane transmission parameters for CH ₄ N ₂ O overlap	65
3.5	Band centers and band strengths of CFCs	71
4.1	Water vapor solar transmission k distribution parameters	78
6.1	Model sensitivity to doubled CO ₂ for different convective schemes	113
6.2	Summary of model sensitivity studies to perturbations in input parameters	121
7.1	Comparison of simulated and reconstructed Temperature records	140
7.2	Major volcanic eruptions of the past century	141

Abstract

The Oregon Graduate Institute One Dimensional Time-Dependent Radiative Convective Model: Theory and Application

Robert M. MacKay, M.S.
Oregon Graduate Institute, 1990

Supervising Professor: M.A.K. Khalil

A time dependent one dimensional radiative convective model (1D RCM) is developed to study the sensitivity of the Earth's vertical temperature structure to variations in external and internal components of the climate system. Special emphasis is given to the theory and development of the model so that it may be easily used and understood by others. The sensitivity of the Earth's surface temperature to variations in such parameters as the solar constant, surface albedo, cloud cover fraction, etc. is explored. The model developed is found to experience an approximate change in surface temperature of 2.0 K for a doubling of atmospheric CO₂ concentration (from 320 to 640 ppm). This compares favorably with other previously published results for similar models.

The influence on mean global temperature of variations in the atmospheric concentrations of CO₂, CH₄, N₂O, F11, and F12 over the past century is simulated with the model and compared with the record of mean global temperature reconstructed from observations. In addition the effect of volcanic aerosols on the simulated record is explored.

It is concluded that the OGI 1D RCM can serve as a valuable research tool in the future, for studying perturbations of the global average vertical thermal structure of the Earth-atmosphere system. It is also stressed that the 1D nature of the model is limited in that it offers no horizontal or seasonal resolution of the climate system.

Chapter 1

Introduction to Climate modeling

1.1 Introduction

Earth is a complex system with a physical state determined by the combined interactions between the sun, atmosphere, biosphere (including man), cryosphere (land and sea ice), hydrosphere, and geosphere. Although this list may not be exhaustive it indicates the complexity of the problem associated with a complete description of the planet. After some thought it is easily conceivable that a complete description of even a single aspect of the Earth, such as its climate, is well beyond the intellectual and computational capabilities of scientists today.

However, a complete description of the dynamics of the Earth's climate is not essential to obtaining an increased understanding of the climate system. For example the motion of a real pendulum can be modeled quite nicely by assuming that it swings at the end of a

perfectly rigid-massless rod, with all of its mass concentrated at a single point, that the sine of the angle of swing is equal to the angle, and that there is no air resistance. This model of a simple pendulum is pretty good at predicting the motion of the bob for small swings and relatively short observational times, and it also reveals many important features of the simple pendulum system. However, the motion of the pendulum eventually dies down and the pendulum modeler is compelled to increase the complexity of the model to account for this discrepancy between theory and observation.

Climate modeling can be thought of in much the same way. Start with a very simple model of the climate and see what it predicts. Even though the climate model may be grossly over simplified, many of the important larger features of the real climate can be realized in the model's behavior. Additional complexity can be added to the model in order to obtain a more detailed description of the climate and to investigate the importance of various internal and external influences to the overall state of the climate.

Several types of climate models have been used in the past, ranging from the simplified zero dimensional

model to the highly complex three dimensional general circulation models (GCMs). North et al. (1981) provide a good review of zero dimensional climate models and energy balance models. Ramanathan and Coakely (1978) offer a nice overview of climate modeling emphasizing one dimensional radiative convective models. Washington and Parkinson (1986) give a solid introduction to three dimensional climate models. Most of the climate models in use today calculate the thermal structure of the Earth's atmosphere as the primary indicator of climate.

Zero dimensional climate models are used for quick estimates of the temperature of the Earth's surface following changes in parameters such as the solar constant, atmospheric composition, or surface albedo. They are limited in that they have no spatial resolution and have little ability to accurately model the dynamical connections between the earth and the atmosphere.

Next in order of increasing complexity are the one dimensional (1D) climate models of which there are two types. One category of 1D model is the surface energy balance model (EBM) discussed by North et al. (1981). This type of model uses latitude as the spatial dimension and estimates the equilibrium surface

temperature as a function of latitude. Another type of 1D model is the radiative convective model (RCM), in which the vertical height is the only dimension considered. The development of the latter type of 1D model will be the primary focus of this thesis.

Two dimensional models considering both latitude and height are the next in model hierarchy followed by the three dimensional GCM in which all three spherical dimensions of the Earth's atmosphere are considered.

The primary purpose of this thesis is to develop and document a one dimensional time dependent radiative convective model (1D RCM) to be used to study climatic changes induced by variations in the physical and chemical properties of the sun-earth-atmosphere system. The model developed will be referred to as the OGI model throughout the rest of the text. As with most models of this type we solve for the vertical thermal structure of the atmosphere as an indicator of climate. The text to follow will provide an adequate overview of the theory behind the development of the OGI model and enough documentation so that others may use and modify the model to verify our conclusions and to explore their own questions concerning climate change.

In the next section we use a simplified zero

dimensional model to provide a brief overview of the greenhouse effect. We do this for two reasons. First, the greenhouse effect is thought to be one of the most important processes in determining the climate of the past, present, and future. Second, discussing the greenhouse effect using a simplified model offers a chance to introduce the reader to some of the terminology used in the rest of the text and in the available scientific literature.

Figure 1.1 outlines the general flow of this thesis. The rest of this chapter is devoted to a brief introduction to the theory of climate modeling. Chapter 2 gives a discussion of the quantum mechanical ideas important to the radiative transfer problem with special emphasis on the development of spectral band models. Appendix A gives the mathematical foundation for the calculation of fluxes of infrared (IR) radiation in our model atmosphere. In Chapter 3 we present the specific parameterizations used for the absorption of IR radiation due to the various greenhouse gases considered in the OGI model. Chapter 4 is devoted to a detailed description of the methods used for the calculations of solar absorption and scattering due to clouds. We outline the general structure of the OGI model

calculations in Chapter 5. Also in Chapter 5 we give

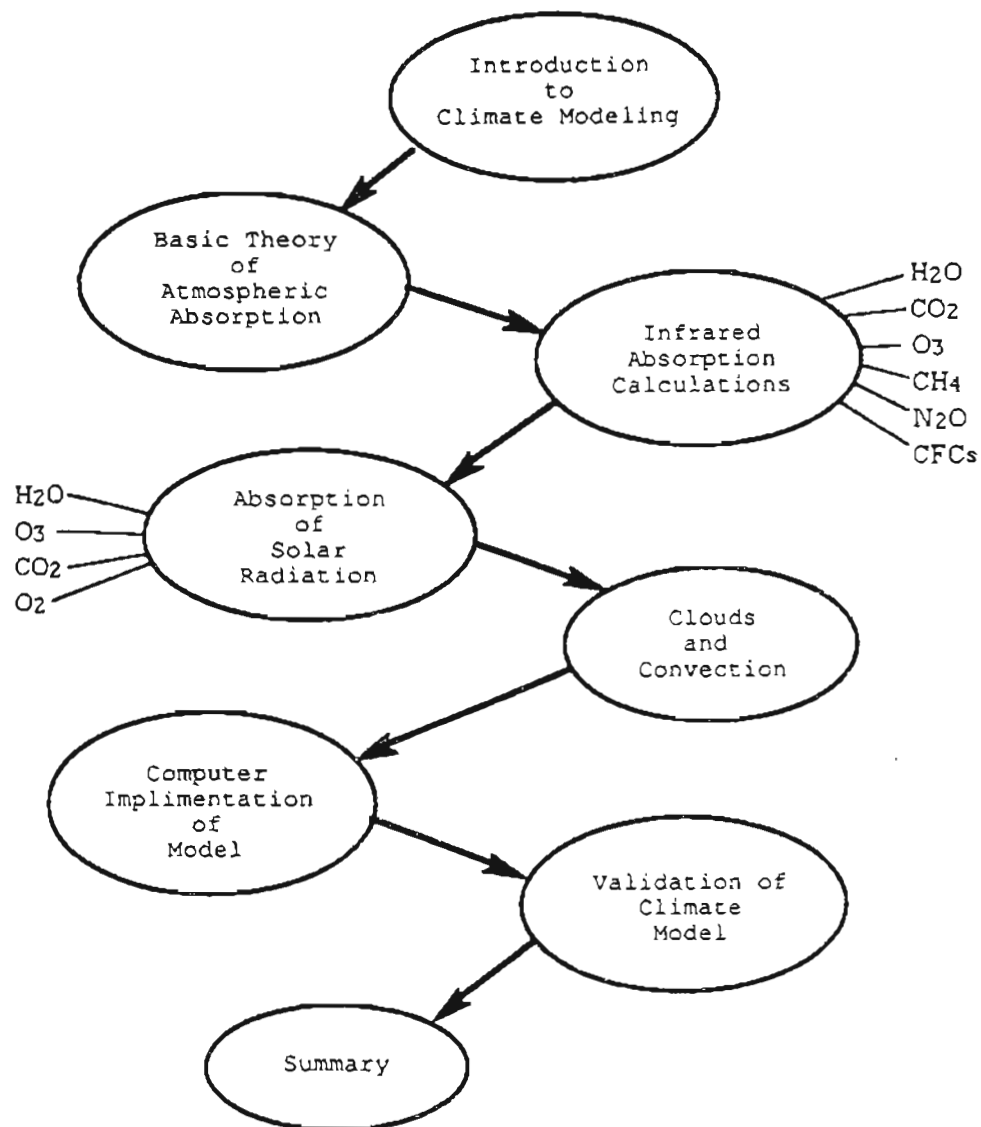


Figure 1.1. A general outline of the thesis structure.

the vertical concentration profiles of the atmospheric gases assumed for our standard model runs. In Chapter 6 we give the results of several sensitivity tests used to

understand the model's robustness or stability to variations in assumed initial conditions or calculation schemes. Chapter 7 contains the calculations of temperature and climate change that may be caused by variations in the atmospheric concentrations of CO₂ and trace gases due to human activities. In Chapter 7 we also compare the OGI results to those previously published by others using similar 1D RCMS.

1.2 The Greenhouse Effect (0-D model)

The question of changes in the thermal structure of the Earth-atmosphere system induced by variations in the atmospheric composition was addressed early on by Tyndall (1863) when he noted that water vapor absorbed 16,000 times more radiant heat than oxygen or nitrogen on an atom for atom basis. Tyndall provided one of the most elegant descriptions of the greenhouse effect when he wrote, "This aqueous vapour is a blanket more necessary to the vegetable life of England than clothing is to man. Remove for a single summer-night the aqueous vapour from the air which overspreads this country, and you would assuredly destroy every plant capable of being

destroyed by a freezing temperature. The warmth of our fields and gardens would pour itself unrequited into space, and the sun would rise upon an island held fast in the iron grip of frost. The aqueous vapour constitutes a local dam, by which the temperature at the earth's surface is deepened: the dam, however, finally overflows, and we give to space all that we receive from the sun." Thus Tyndall saw the water vapor holding in the energy that is essential for life as we know it on earth.

Arrhenius (1896) was the first to identify carbon dioxide as a strong atmospheric absorber and to estimate a surface temperature change (4 to 6 °C) for a doubling of atmospheric CO₂. Arrhenius was also quick to acknowledge that "Joseph Fourier (1823) maintained that the atmosphere acts like the glass of a hot-house, because it lets through the light rays of the sun but retains the dark rays from the ground". It thus appears that Fourier was probably the first to identify the atmosphere as a type of greenhouse due to its high transparency to visible light and relative opacity for infrared radiation.

Since the time of Fourier, many refinements and

complexities have been incorporated into the solution of the fundamental link between climatic change and atmospheric composition. A simplified model of the Earth-atmosphere system will be used below to help clarify the link between the radiative properties of the atmosphere and the climate. This model should also help the reader gain a more quantitative understanding of the greenhouse effect and will introduce some of the terminology used in the rest of the text.

We assume that both the earth and the sun are black body radiators. The total intensity $b_\nu d\nu$ (W/m²) leaving the surface of a black body radiator having a wavenumber between ν and $\nu+d\nu$ is given by Plank's radiation law,

$$b_\nu d\nu = \frac{2\pi c^2 h \nu^3 d\nu}{e^{hc\nu/kT} - 1} \quad 1.2.1$$

The wavenumber ν equals $1/\lambda$ where λ is the wavelength of the radiation, c is the speed of light (3.00×10^8 m/s), k is Boltzman's constant (1.38×10^{-23} J/K), h is Planck's constant (6.63×10^{-34} J-s), and T is the absolute temperature (K) of the radiating body. Figure 1.2 shows b_ν as a function of ν for black bodies at 5800 and 260 K, the approximate temperatures of the sun and Earth-

atmosphere respectively. It is straight forward to show that,

$$\sigma T^4 = \int_0^{\infty} b_{\nu} d\nu \quad 1.2.2$$

where $\sigma=5.67 \times 10^{-8}$ W/(m²-K⁴) is Stefan-Boltzman's constant.

5800K and 260K Black Bodies
(solar verses terrestrial)

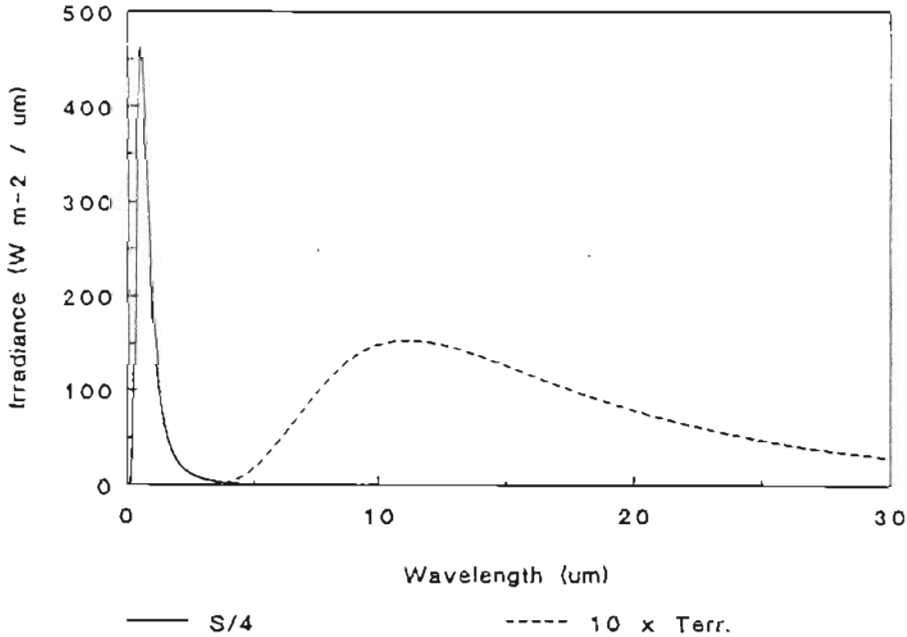


Figure 1.2. Relative irradiances of radiation from black bodies at 5800 K and 260 K. Note: the intensity of solar energy (5800 K) is normalized so that the area under the solid curve is the solar constant divided by 4. Also note that the terretrial irradiance has been multiplied by a factor of 10 to enhance the display.

The temperature of 5800 K was chosen so that when the total intensity of solar radiation S_0 is calculated at the top of the earth's atmosphere by the formula,

$$S_0 = \frac{R_s^2}{r_{es}^2} \int_0^{\infty} b_\nu d\nu \quad 1.2.3$$

we get $S_0 \approx 1380 \text{ W/m}^2$ which we use as the solar constant.

In equation 1.2.3, R_s is the radius of the sun

($6.96 \times 10^8 \text{ m}$) and r_{es} is the mean distance between the earth and the sun ($1.5 \times 10^{11} \text{ m}$).

From an inspection of Figure 1.2 it is easy to see that the domain of frequencies important for the calculation of solar radiant energy is distinct from that for the terrestrial (or IR) radiation. Thus, the calculations of fluxes of solar and terrestrial radiation through the atmosphere must be treated separately.

We assume here a simplified model of the Earth-atmosphere system (the planet). The planet has an effective albedo α of approximately 0.3. Thus the average solar energy Q coming into the planet is given by

$$Q = S_0(1 - \alpha) / 4 \approx 240 \text{ W/m}^2 \quad 1.2.4$$

where S_0 is as defined above and the factor of 4 is introduced to account for the spherical geometry of the planet. The atmosphere absorbs a fraction γ of the incoming solar energy and a fraction β of the outward IR

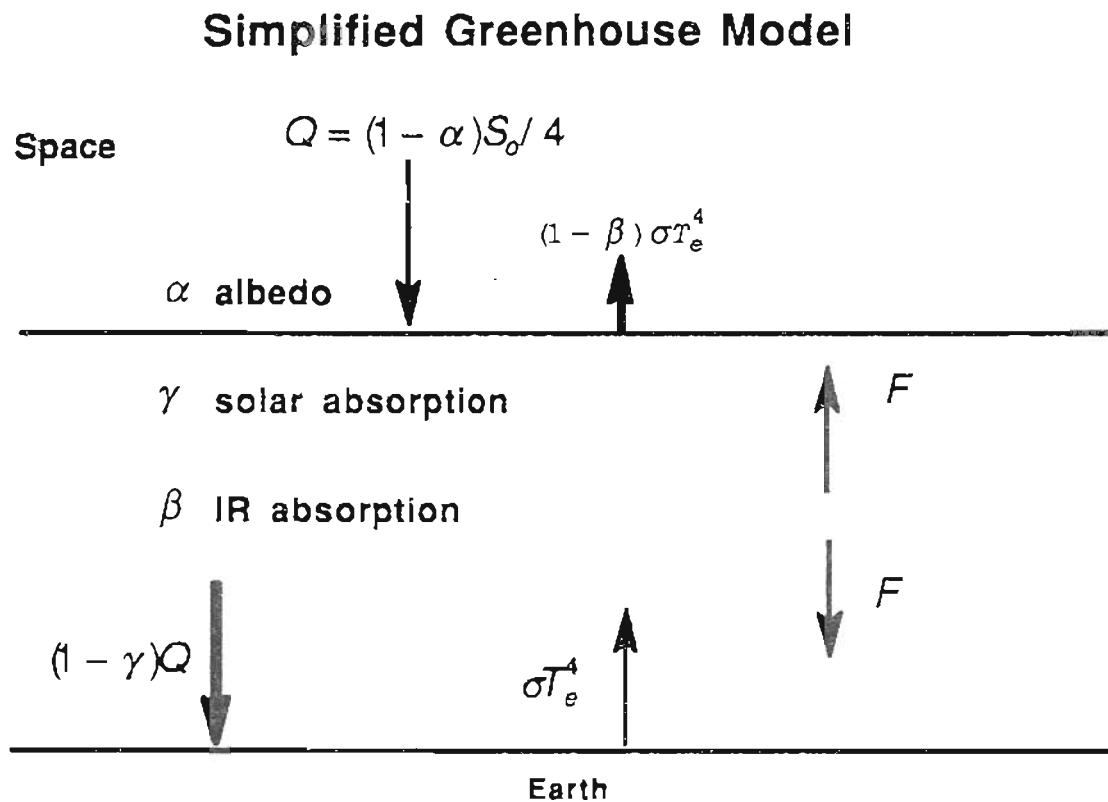


Figure 1.3. The model planet energy flow diagram.

radiation emitted from the earth's surface. In addition since the atmosphere is at some temperature T_a it emits a flux $F_a = \epsilon \sigma T_a^4$ of IR radiation in both the upward and downward directions. Here ϵ equals the emissivity of the atmosphere. Since by Kirchoff's radiation law the emissivity of a body in thermal equilibrium equals its absorptivity we can write $F_a = \beta \sigma T_a^4$.

Figure 1.3 above is a schematic energy flow diagram of a model planet. From Figure 1.3 we can see that,

$$Q = F_a + (1-\beta)F_e \quad 1.2.5$$

since in equilibrium the net flux of energy into the top of the atmosphere equals the net flux out of the top of the atmosphere. In equation 1.2.5, $F_e = \sigma T_e^4$ is the net flux of radiation leaving the surface of the earth which is assumed to be a black body at temperature T_e . In addition the net flux of energy into the earth's surface is balanced out by the net flux of energy leaving the earth's surface. Thus,

$$(1-\gamma)Q + F_a = F_e \quad 1.2.6$$

Now solving equations 1.2.5 and 1.2.6 for F_e and using

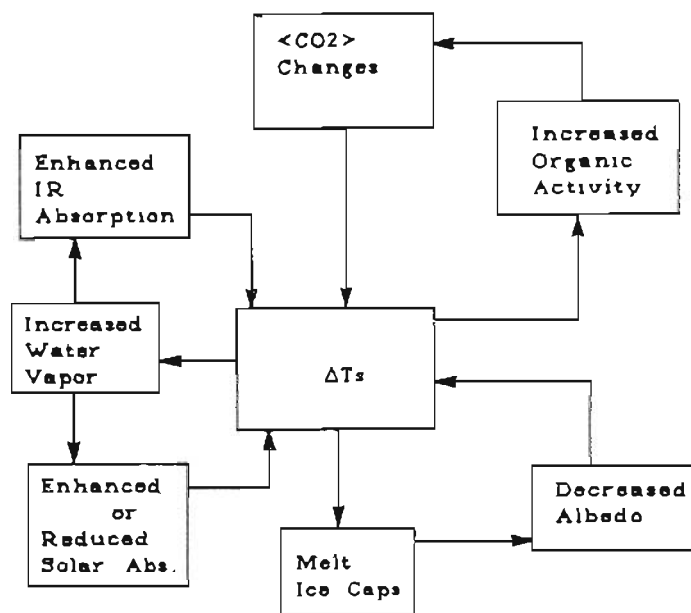
the fact that $F_e = \sigma T_e^4$, we obtain for the equilibrium surface temperature of the Earth

$$\left[\frac{(1 - \gamma/2)(1 - \alpha) S_0/4}{\sigma(1 - \beta/2)} \right]^{\frac{1}{4}} = T_e \quad 1.2.7$$

From equation 1.2.7 we can see that if there is no atmosphere, $\gamma=\beta=0$ then $T_e=255$ K (or -20°F), which is also the effective radiating temperature of the planet. Thus we can see that without an atmosphere the surface of the earth would truly be held in the "iron grip of frost". For the Earth's atmosphere, the absorbed solar energy is less than the absorbed IR energy ($\gamma<\beta$) thus $T_e > 255$ K.

If we take $\gamma=0.2$ and $\beta=0.9$ we obtain $T_e \approx 289$ K which is close to the present average surface temperature of 288 K assumed in the U.S. standard atmosphere. This increase in surface temperature due to our atmosphere is what is referred to as the greenhouse effect. The above simplified model of our planet brings out some essential features of the greenhouse effect. First we note that the greenhouse effect is a natural phenomenon, without

which life as we know it on earth today would not be possible. Secondly, the model defines the key elements of the Earth's climate, namely γ , β , α , and Q . Finally we can use this simplified model as an instrument to



Other considerations

- Temperature dependence of reaction rates
- Temperature dependence of absorption coefficients
- Cloud cover?
- Particulate matter and haze.....

Figure 1.4. Some examples of possible feedback processes for the earth-atmosphere system.

begin to understand how changes in γ , β , α , and Q can influence the equilibrium surface temperature T_e . In

particular, anything that can alter one of these parameters can affect a change in T_e and we can use equation 1.2.7 to estimate the expected magnitude of the change. In reality a change in Q , for example, will also induce a change in α and possibly γ and β thus resulting in complicated feedback processes giving rise to uncertainties in the actual change in T_e .

Figure 1.4 above shows a simplified diagram of some of the feedback processes possible in the earth climate system. The upper left-hand loop is an example of a positive feedback in that an increase in water vapor with increasing T_e will result in enhanced IR absorption by the atmosphere (β increasing) which will increase T_e further. This cycle continues until a new equilibrium is finally reached. The lower left-hand loop gives an example of a possible negative feedback loop. The increase in atmospheric water vapor due to an increase in T_e may result in an increase in cloud amount causing an increase in the planetary albedo thus reducing T_e back towards its original value. Alternately, an increased temperature may result in a decrease in total cloud amount since warmer air can hold more water in the vapor phase than cool air. This increase in water vapor

with decreasing cloud cover would result in a warming of the atmosphere and hence would constitute a positive feedback. The uncertainty of this lower left hand loop is an example of the type of unanswered questions puzzling atmospheric scientists today.

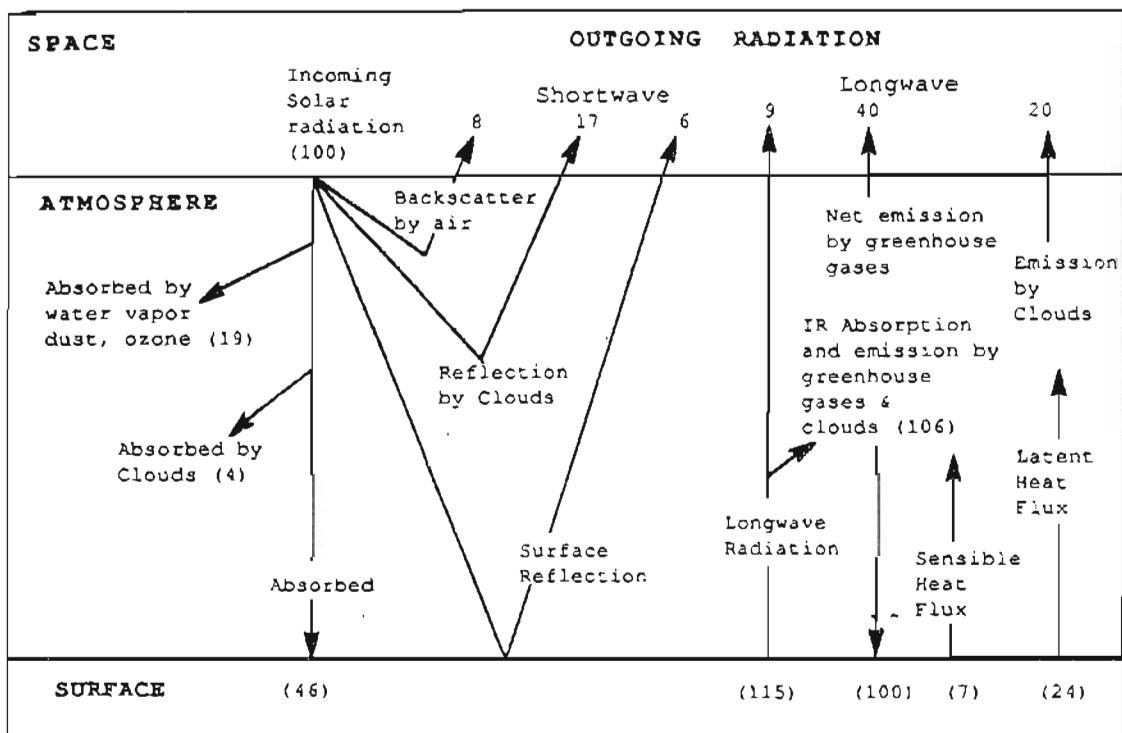


Figure 1.5. Schematic representation of the flow of solar and terrestrial energies for the earth atmosphere system. After Mitchell (1989).

In Figure 1.5 we present a more realistic account of the energy exchanges for the earth atmosphere system.

This figure has been modified slightly from that presented by Mitchell (1989). As is evident from the figure there are many complications that have been omitted by the simplified model described above. One way to increase the ability of a climate model to incorporate more of the physical processes involved in determining the climate state is to increase the model's spatial resolution. The rest of the text to follow is written with this goal in mind.

The next three chapters are devoted to an explanation of the nuts and bolts of calculating fluxes of solar and terrestrial radiation through the atmosphere. Appendix A would be worthwhile reading for anyone interested in the basic theoretical development of radiative transfer. In Chapter 5 we will return again to the problem of climate modeling where we outline the development of the OGI 1D time dependent RCM. The last two chapters will give the results of experiments performed with the model. Appendix B contains the values of useful physical constants and conversion factors. Appendix C and D give examples of the input and output formats respectively, and a complete listing of the source code can be found in Appendix E.

Chapter 2
Theory of the
Absorption Spectra of Atmospheric Gases

2.1 Theoretical Overview

Since Neils Bohr introduced his idea that the sharp spectral lines emitted by the hydrogen atom were related to the transitions of electrons between discrete energy states, we have realized that many forms of energy are quantized. The rules determining the particular quantization conditions for more complicated atoms and molecules were more completely developed along quantum mechanical principles by physicists in the mid to late 1920's. Although the quantum mechanical state of the atoms and molecules in the atmosphere is very complicated, it is important only to realize that atmospheric molecules do have discrete energy states associated with: 1) electronic energy levels about the molecule; 2) vibrational energy levels of the molecule; and 3) rotational energy levels for molecules that have

asymmetries (natural or induced) causing the molecule to possess a non-zero electric dipole moment.

Goody (1989) notes that the wavelengths ($\lambda = hc/\Delta E$) associated with electronic transitions are typically of the order of 0.1 to 10 μm (uv, visible, and near infrared); vibrational transitions 1 to 100 μm (near to far infrared); and rotational transitions 10^1 to 10^4 μm (far infrared to microwave region). Thus the electronic transitions are most important when discussing transmission of solar radiation through the atmosphere; and vibrational, rotational, or vibrational-rotational transitions are important to the transmission of terrestrial (or IR) radiation through the atmosphere.

Since rotational or vibrational-rotational transitions are the most important for the transfer of terrestrial radiation through the atmosphere we give here a brief outline of the quantum mechanical theory for an harmonic oscillator-rigid rotator. Figure 2.1 shows the normal vibrational modes for CO_2 and H_2O . For simplicity we will restrict our attention to the CO_2 molecule.

Because of linear symmetry, the CO_2 molecule has no static electric dipole moment and hence no pure

rotation band. The symmetrical motion of the ν_1 mode of vibration does not give rise to an induced dipole moment and hence this mode is relatively optically inactive.

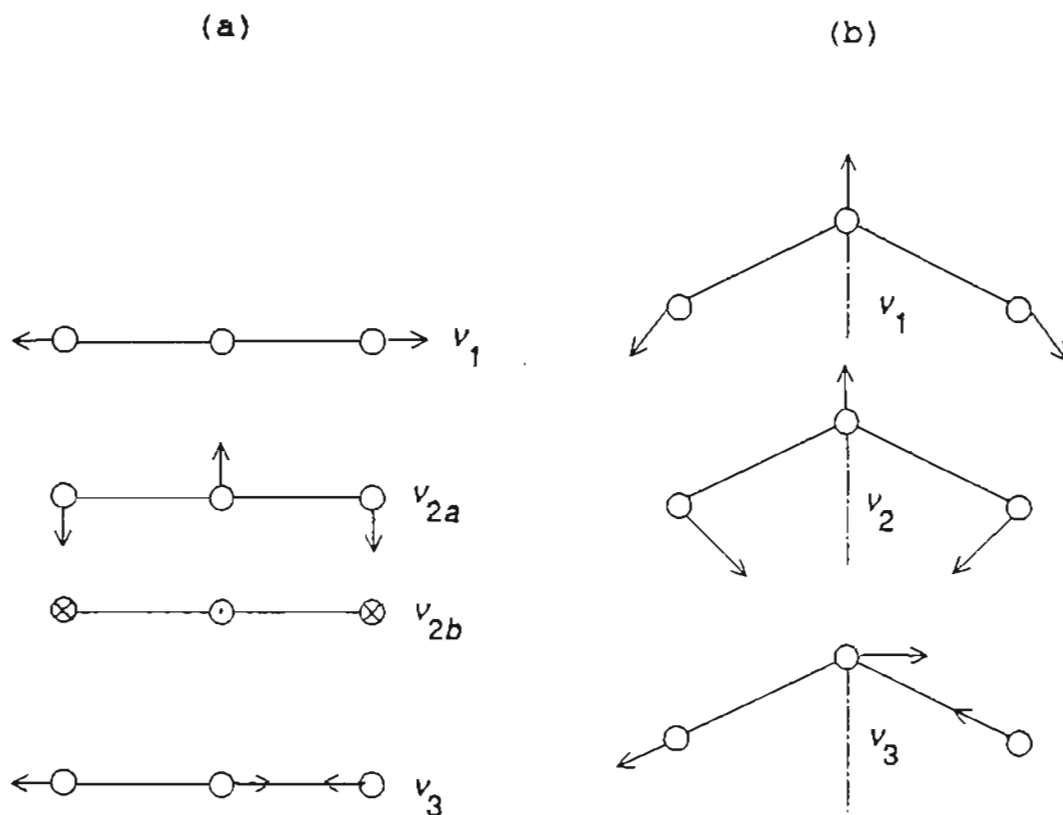


Figure 2.1. Normal modes of vibration for a linear (a) molecule such as CO₂ and a triangle (b) molecule such as H₂O.

In the ν_2 modes of vibration a dipole moment is induced

perpendicular to the linear axis of the molecule resulting in a vibration-rotation band being formed around the ν_2 vibrational frequency. This fundamental frequency corresponds to a wavelength of 15 μm . Since the IR radiation leaving the earth has a maximum intensity near this wavelength, this absorption band is of primary importance when considering atmospheric energy flux calculations. The ν_3 vibration also has an induced dipole moment and thus forms a very strong vibration-rotation band. However this band is centered at 4.3 μm and since the intensity of solar radiation and terrestrial radiation are both small in this region (see Figure 1.2) the absorption due to the ν_3 band is of little consequence for our model.

Goody (1989) gives,

$$\nu = \nu_k \pm 2Bc(J + 1) \quad 2.1.1$$

for the quantum mechanical solution for the allowable wave numbers ν associated with a harmonic oscillator-rigid rotator transition from $(n_{k+1}, J+1)$ to (n_k, J) . In equation 2.1.1, $B = h/(8\pi^2cI)$ is the rotational constant,

$I = 2 m_o d_{o-c}^2$ is the moment of inertia of the CO₂ molecule about an axis through its center and perpendicular to the line of the molecule, m_o is the mass of an oxygen atom, $d_{o-c} = 1.1632 \text{ \AA}$ is the carbon oxygen bond length, c is the speed of light, h is Plank's constant, n_k is the vibrational quantum number, J is the rotational quantum number, and ν_k is the wave number associated with the vibrational transition. For CO₂, $B = .39 \text{ cm}^{-1}$.

From equation 2.1.1 it can be seen that there are many allowable wave numbers symmetrically located about each ν_k due to the accompanying rotational transitions. Thus it becomes apparent why the vibration-rotation bands are so much more important than a purely vibrational band such as that due to the ν_1 vibrational mode of Figure 2.1. For future reference a vibrational level is specified as (k, j, m) where the integers k , j , and m correspond to the vibrational energy levels of ν_1 , ν_2 , and ν_3 respectively. Sometimes a superscript is included with j to include the angular momentum quantum number 1 associated with the angular momentum due to ν_{2a}

and v_2 vibrating out of phase.

The natural linewidth, $\Delta\nu$, associated with a spectral line of energy E_0 is related to the lifetime τ , by Heisenberg's uncertainty principle ,

$$\Delta\nu \propto \frac{1}{\tau} \quad (2.1.2)$$

If the molecule is undisturbed its lifetime is relatively long and hence its line width is very narrow. This is the natural line width. The line width of a spectral line will increase as the temperature of the gas increases. The reason for this is that the molecules in a gas move randomly in all directions with an rms speed of

$$v_{rms} = \sqrt{\frac{3kT}{m}} \quad (2.1.3)$$

where k is Boltzman's constant, T is the temperature of the gas and m is the mass of the gas molecule. Thus as the temperature increases the rms speed of the molecules increases and hence the range of frequencies observed becomes larger due to the Doppler effect. This increase in line width above the natural line width is referred

to as Doppler broadening.

The lifetime of a molecule in a particular energy state can also be shortened by collisions with other molecules. The collision of an excited molecule with another molecule can induce an energy transition and hence the emission of a photon. Thus if the molecule is in an environment where there is a high probability of collision with other molecules (high pressure) its lifetime becomes shorter and hence its line width is much broader than its natural line width or even its Doppler width. This type of broadening is called collision broadening or pressure broadening and, as noted by Liou (1980), is the most important source of broadening in the troposphere and lower stratosphere (<40 km).

2.2 Absorption for a Single Line

The monochromatic transmission function for a single line is given by,

$$T_{\nu} = e^{-k_{\nu}u} \quad 2.2.1$$

where k_{ν} is the mass absorption coefficient at wave

number ν and u is the absorber amount. The shape of the pressure broadened line is taken to be Lorentzian i.e.,

$$k_\nu = \frac{S\alpha}{\pi[(\nu - \nu_0)^2 + \alpha^2]} = S f(\nu - \nu_0) \quad 2.2.2$$

where α is the half width at half maximum(which is a function of temperature and pressure) , ν is the wave number (1/wavelength) at the center of the spectral line, $f(\nu - \nu_0)$ represents the shape factor of the line, and the line strength or line intensity S is defined to be,

$$S = \int_{-\infty}^{+\infty} k_\nu d\nu \quad 2.2.3$$

The line strength is a parameter that is often cited in the literature in reference to the absorbing properties of a gas. The pressure P and temperature T dependence of α is often taken to be

$$\begin{aligned} \alpha &= \alpha_0 \frac{n \nu_{rms}}{n_0 \nu_{rms_0}} \\ &= \alpha_0 \frac{P T_0 \sqrt{T}}{P_0 T \sqrt{T_0}} \\ &= \alpha_0 \left(\frac{P}{P_0} \right) \sqrt{\frac{T_0}{T}} \end{aligned} \quad 2.2.4$$

where n is the number density which is equal to $P/(kT)$

from the ideal gas law. P_0 and T_0 correspond to the pressure and temperature conditions for the measurement of α_0 .

Combining equations 2.2.1 and 2.2.2 gives the frequency dependent absorption for a single line as

$$A_\nu = 1 - T_\nu = 1 - \exp\left\{-\frac{S\alpha u}{\pi[(\nu - \nu_0)^2 + \alpha^2]}\right\} \quad 2.2.5$$

Figure 2.2 shows A_ν versus ν for fixed α and S with various absorber amounts u .

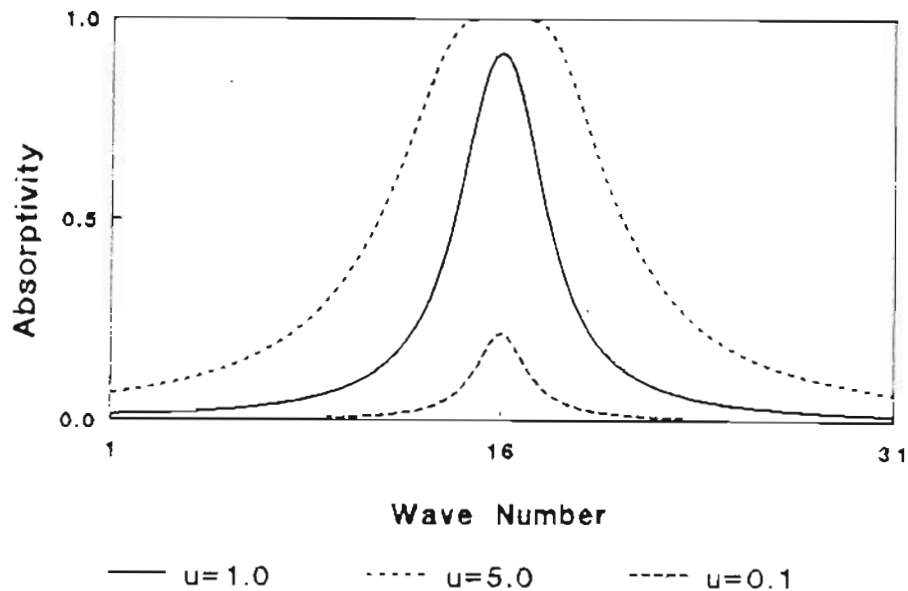


Figure 2.2. Monochromatic Absorption function as a function of wave number for a single line of Lorentz line shape.

Notice that for very large values of u , the middle of the line becomes saturated and an increase in total absorption $\int A dv$ with increasing u can only come from the "wings" of the line. This is the strong line limit to be discussed below. When u is small all wave numbers of the line can contribute to the increase in total absorption. This is the weak line limit and is characterized by a linear increase in total absorption with absorber amount.

The transmission function for an interval $\Delta\nu$ is defined to be

$$T_{\nu}(u) = \frac{1}{\Delta\nu} \int_{\Delta\nu} e^{-k_{\nu} u} d\nu \quad 2.2.6$$

where we have assumed that the atmospheric path is short enough to be considered homogeneous so that k_{ν} does not depend on path length. For a single line with a Lorentz line shape (see equation 2.2.3),

$$T_{\nu}(u) = \frac{1}{\Delta\nu} \int_{\Delta\nu} d\nu \exp\left[\frac{S\alpha u/\pi}{(\nu - \nu_0)^2 + \alpha^2}\right] \quad 2.2.7$$

Liou (1980) shows that integration of equation 2.2.2 gives , for the absorptivity function,

$$A_{\nu}(u) = 1 - T_{\nu}(u) \quad 2.2.8$$

$$A_{\nu}(u) = \frac{2\pi\alpha}{\Delta\nu} x e^{-x} [I_0(x) + I_1(x)]$$

where $x = Su/2\pi\alpha$, S is the line intensity, u is the absorber amount, α is the half width at half maximum, and I_0 and I_1 are the modified Bessel functions. For small path lengths ($x \rightarrow 0$) $I_0(x) \approx 1$, $I_1(x) \approx x/2$ and, $e^{-x} \approx 1 - x$. Thus,

$$A_{\nu} \approx \frac{2\pi\alpha}{\Delta\nu} x(1-x)(1-\frac{x}{2}) = \frac{2\pi\alpha}{\Delta\nu} x \approx \frac{2\pi\alpha}{\Delta\nu} \frac{Su}{2\pi\alpha} = \frac{Su}{\Delta\nu} \quad 2.2.9$$

The net absorptance $A_{\nu}\Delta\nu$ is thus seen to be a simple linear function of absorber amount u ,

$$A_{\nu}\Delta\nu \approx S u \quad 2.2.10$$

Ramanathan (1976b) notes that this "weak line" limit is valid when addressing the influence of varying concentrations of CFCs and other low concentration gases ($[C] < 5$ ppbv) on global warming.

For large absorber amounts $x \rightarrow \infty$ $I_0 \approx I_1 \approx e^x/\sqrt{2\pi x}$ and so 2.2.4 may be written as

$$A_{\nu}\Delta\nu \approx 2\sqrt{S\alpha u} \quad 2.2.11$$

for the strong line limit. The strong line limit is

sometimes referred to as the limit of square root absorption or logarithmic absorption.

2.3 Band Models

As discussed previously there are typically many spectral lines contained within a frequency band. The purpose of a band model is to determine the net absorptivity (or band absorptance) $\int A_{\nu} d\nu$ over a spectral interval by assuming something about the shape of the individual lines and the distribution of the line strengths throughout the interval. A variety of band models have been developed, some are purely empirical while others have some theoretical bases. Liou (1980) describes the theoretical justification of the regular or Elsasser model developed by Elsasser in 1938 and the Goody statistical band model developed by Goody in 1952. We have made extensive use of the Goody band model in the OGI model and will hence outline the arguments given by Liou (1980) below.

Let $\Delta\nu$ be a spectral interval containing n lines of mean line spacing $\delta = \Delta\nu/n$. Define $P(S_i)$ to be the probability that the i^{th} line has a line strength S_i .

$p(S)$ is normalized according to,

$$\int_0^{\infty} P(S) dS = 1 \quad 2.3.1$$

Each line is assumed to be randomly located in the spectral interval Δv . Thus the probability of a line being in the spectral interval dv is, $dv/\Delta v$. Hence the probability of a line being in the interval dv with line intensity in the interval dS is the joint probability given by

$$\frac{dv}{\Delta v} P(S) dS \quad 2.3.2$$

The average transmission function for the i th spectral interval is

$$T_{v_i} = \frac{1}{\Delta v} \int_{\Delta v} \int_0^{\infty} dv_i dS_i e^{-k_i u} P(S_i) \quad 2.3.3$$

Now if we assume that the lines are not correlated (i.e. they are completely randomly distributed) then the total average transmission function due to all lines is the product of the individual transmission functions, i.e.

$$\begin{aligned}
T_{\nu} &= \prod_{i=1}^n \frac{1}{\Delta \nu} \int_{\Delta \nu 0}^{\infty} \int d\nu_i dS_i e^{-k_i \nu_i} P(S_i) \\
&= \left[\frac{1}{\Delta \nu} \int_{\Delta \nu 0}^{\infty} \int d\nu dS e^{-k\nu} P(S) \right]^n \\
&= \left[1 - \frac{1}{\Delta \nu} \int_{\Delta \nu 0}^{\infty} \int d\nu dS (1 - e^{-k\nu}) P(S) \right]^n
\end{aligned} \tag{2.3.4}$$

The subscript i was dropped since it is just a subscript on the dummy variables ν , S , $k=k(\nu, S)$. Since $\Delta \nu = n\delta$ and

$(1-x/n)^n \approx \exp(-x)$ we can rewrite the transmission function as,

$$T_{\nu} = \exp\left(-\frac{1}{\delta} \int_{\Delta \nu 0}^{\infty} \int d\nu dS (1 - e^{-k\nu}) P(S)\right) \tag{2.3.5}$$

We now assume that the probability density function $P(S)$ has the form

$$P(S) = \frac{1}{S_a} \exp\left(-\frac{S}{S_a}\right) \tag{2.3.6}$$

where S_a is the mean line intensity. We further assume that all lines have a Lorentz shape

$$k_{\nu} = \frac{S\alpha\pi}{(\nu - \nu_0)^2 + \alpha^2} \tag{2.3.7}$$

Inserting these two conditions into equation 2.3.5 and

integrating S from 0 to ∞ and v from $-\infty$ to $+\infty$ gives,

$$T_v = \exp \left\{ - \frac{S_a u / \delta}{\sqrt{1 + \frac{S_a u}{\pi \alpha}}} \right\} \quad 2.3.8$$

Goody (1964) and Rodgers and Walshaw (1966) have

published values of S_a/δ and $\pi\alpha/\delta$ for many of the spectral intervals of water vapor. We have used this information extensively in the OGI model to calculate the transmissivities of water vapor over comparatively narrow spectral intervals to apply in the overlap corrections required when the spectral band of another gas overlaps that of water.

As mentioned earlier other band models have been developed to estimate the band absorptance $\int A_v dv$ of a spectral interval. As with the Goody model some have a theoretical foundation, others are purely empirical in nature, while many combine aspects of both observations and theoretical considerations. Cess and Ramanathan (1972) used the latter approach to justify the formula,

$$A(u) = 2A_o \ln \left\{ 1 + \frac{u}{\sqrt{4 + u(1 + 1/\beta)}} \right\} \quad 2.3.9$$

for the absorptance of CO_2 in the atmospheres of Mars

and Venus, where $\beta = 2\alpha/\delta$, and $u = 1.66 S w/A_0$. The parameter A_0 (units of $\text{cm}^{-1}(\text{atm-cm})^{-1}$) is an adjustable parameter, while β is related to the line width α (calculated using the pressure and temperature correction given by equation 2.2.4) and the mean line spacing δ . The effective absorber amount u includes the diffusivity factor 1.66 (see appendix A), the mean line intensity S (same units as A_0), the actual amount of CO_2 (in cm-atm), and the adjustable parameter A_0 . Since 1972 this formula has been extended for IR flux calculations in the Earth's atmosphere by: Ramanathan (1976) for carbon dioxide ; Ramanathan and Dickenson (1979) for ozone; and Donner and Ramanathan (1980) for methane and nitrous oxide. In the OGI model we have followed Ramanathan's work by using equation 2.3.9 (or something similar) for the calculation of the band absorptance of CO_2 , CH_4 , and N_2O . The details of the specific parameterizations used for the IR absorptivities are presented in the following chapter.

Chapter 3

I.R. Absorptivities

Presented in this chapter are the specific parameterizations used in the calculation of broadband I.R. absorptivities or emissivities for each of the atmospheric gases considered (H_2O , CO_2 , O_3 , N_2O , and CH_4). Throughout this chapter subroutines (from Appendix E) utilized to carry out the specific calculations are given along with the appropriate references. It should be stressed that we present only the parameterizations in this chapter, and that a discussion of the calculations of IR fluxes using these parameterizations is postponed until Chapter 5.

3.1 Water Vapor

The absorption of terrestrial radiation due to water vapor is attributed to three spectral bands: 1) the vibration-rotation band centered at $6.3 \mu\text{m}$, 2) pure rotation for wavelengths greater than $12 \mu\text{m}$, and 3) the

continuum band extending from 8.3 to 20.83 μm . The emissivity formulas given by Ramanathan (1976) and the transmissivity formulas given by Roberts (1976) are utilized in our model and are outlined briefly below.

Comparison of H₂O Emissivities Analytical vs Experimental

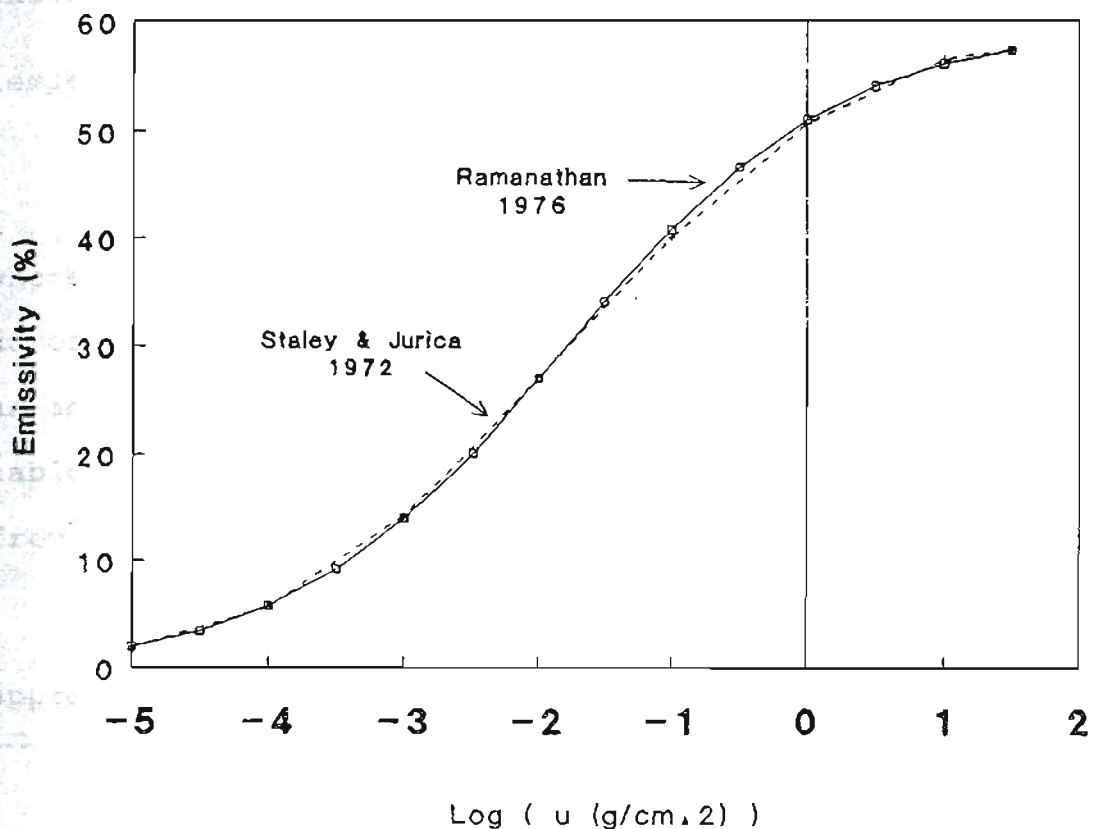


Figure 3.1. Comparison of water vapor emissivity calculated using equation 3.1.1 (Ramanathan 1976) with values published by Staley and Jurica (1970).

The emissivity for vibration-rotation and pure rotation bands $E_1(\tilde{U}_1, T)$ is given by

$$E_1(\tilde{U}_1, T) = 0.59 \left(\frac{T_0}{T} \right)^{\frac{1}{2}} \left[1 - \frac{1}{2} \sum_{n=1}^2 \frac{1}{1 + A_n (\tilde{U}_1)^{\frac{1}{2}}} \right] \quad 3.1.1$$

where $A_1 = 19$, $A_2 = 3.5$ and \tilde{U}_1 is the pressure and temperature corrected path length (in g cm^{-2}) defined by

$$\tilde{U}_1 = \int \left(\frac{P}{P_0} \right) \left(\frac{T_0}{T} \right)^{\frac{1}{2}} dU_1 \quad 3.1.2$$

where $P_0 = 1$ atm and $T_0 = 293$. P and T are the atmospheric pressure and temperature. Equation 3.1.1 is an analytical expression designed to fit the emissivity tables of Staley and Jurica (1970) and as can be seen from Figure 3.1 below does so very well.

The modified emissivity E_1^1 is calculated using the approximate relationship given by Ramanathan (1983)

$$E_1^1 = E_1 \left(.847 (\tilde{U}_1)^{.022} \right) \quad 3.1.3$$

After obtaining E_1 and E_1^1 we use the theory developed in Appendix A to calculate the net heating (or cooling) due to water vapor. Since the emissivity method is only used for water vapor the above calculations are

performed in the one subroutine "water" listed in Appendix E.

Staley and Jurica have omitted the influence of the water vapor continuum from 1200 to 480 cm^{-1} (8.3 to 20.83 μm) in their emissivity formulation and hence this spectral region is treated separately. We use the parameterization given by Roberts (1976) to calculate the mean transmission for the continuum region. Roberts (1976) give for the average transmission $T_{\Delta\nu}$ over a wavenumber interval $\Delta\nu$

$$T_{\Delta\nu} = \exp(-1.66K_{\nu}U) \quad 3.1.4$$

$$K_{\nu} = k_{\nu} \times \left(\frac{e}{e_0}\right)$$

$$k_{\nu} = [4.2 + 5588 \exp(-.00787\nu)] \times \exp\left\{1800\left(\frac{1}{T} - \frac{1}{296}\right)\right\}$$

where k_{ν} is the absorption coefficient for e type absorption, U is the total amount of water vapor (g/cm^2) in the path, e is the partial pressure of H_2O (atm), e_0 is the reference pressure of 1 atmosphere, and T is the average temperature of the path weighted by water vapor content. Figure 3.2 below shows the wavenumber dependence of k_{ν} .

The partial pressure of water vapor e (atm) in

equation 3.1.4 above is calculated using the Clausius Clapeyron relation (see Washington and Parkison 1986 page 112) for the saturated vapor pressure of water e_s ,

$$e_s = (6.03 \times 10^{-3}) \exp\left(\frac{.622L}{R} \left(\frac{1}{273} - \frac{1}{T}\right)\right) \quad 3.1.5$$

where R is the ideal gas constant $0.287 \text{ J g}^{-1}\text{K}^{-1}$ and L is

Water Vapor Continuum Absorption k (at 296 K)

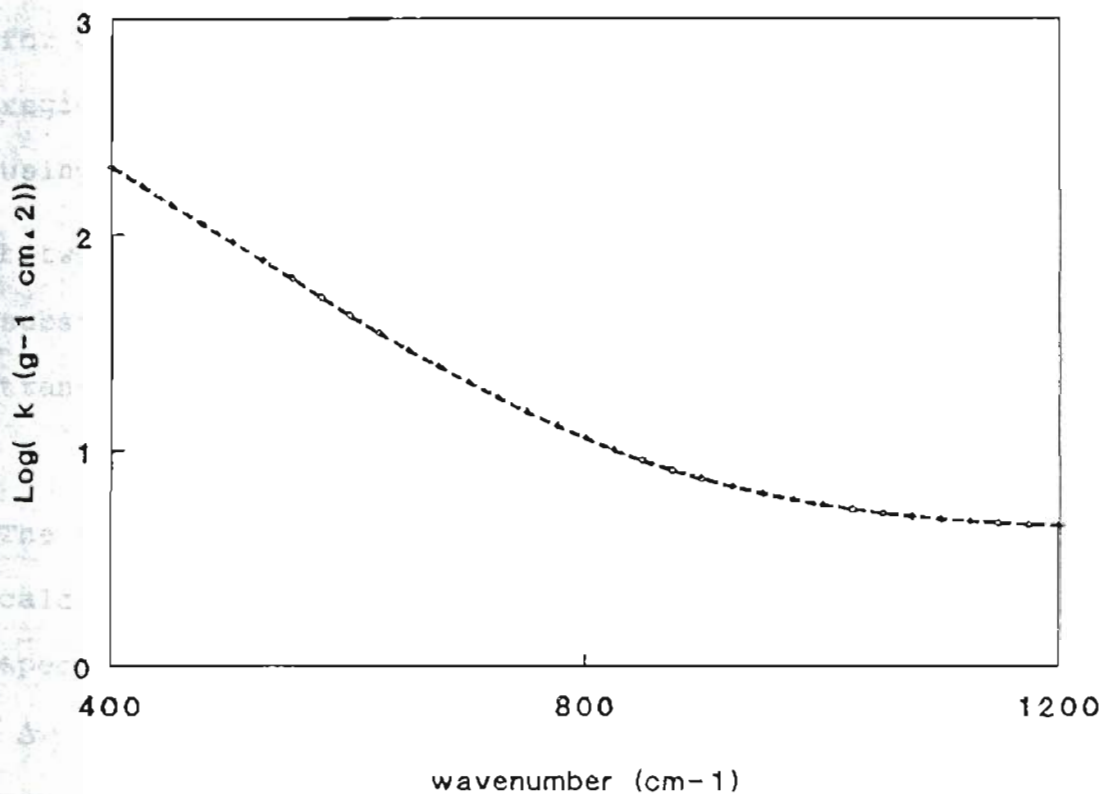


Figure 3.2. The absorption coefficient $k\nu$ versus ν for the water vapor continuum. After Roberts (1976).

the latent heat of vaporization ($J g^{-1}$) given by Stone and Carlson (1982) to be $L = 2510 - 2.38 (T-273)$.

For a relative humidity h the partial pressure of water vapor is calculated as.

$$e = h * e_s$$

The function "esat" (Appendix E) is used to calculate the partial pressure of water vapor.

The continuum region is broken into two subregions for computational efficiency. The transmission of the region between 1200 and 800 cm^{-1} , TR1 is calculated using subroutine "trc1". This subroutine assumes that between 1200 and 800 cm^{-1} the function k_v does not vary substantially and hence uses for the average transmission the transmission at 1000 cm^{-1} , i.e.

$$TR1 = \exp(-1.66 k_{1000} U) \quad 3.1.6$$

The transmission TR2, for the 800 to 480 cm^{-1} region is calculated using subroutine "trcont" which divides the spectral interval into eight subintervals of equal width

$\Delta\nu_j$ (40 cm^{-1}) and performs the average according to equation 3.1.7 below

$$TR2 = \frac{1}{320} \sum_{j=1}^8 T_{\Delta v_j} \Delta v_j \quad 3.1.7$$

After calculating the average transmissions TR1 and TR2 over each interval the mean band absorptance $A_v \Delta v$ over each interval is calculated by,

$$A_v \Delta v = (1 - TR_i) \Delta v_i \quad 3.1.8$$

where Δv_i is the width of each spectral interval (400 or 320 cm^{-1}). The above calculations are performed in subroutines "h2oir" and "h2otrans" of Appendix E.

In the rest of Chapter 3 we outline the specific methods of calculating the integrated absorptivity (or band absorptance) of the other gases considered by the model as IR absorbers. Once the band absorptance is calculated the subroutine "acool" (Appendix E) is always used to calculate the net heating (or cooling) due to the particular gas under consideration.

3.2 Carbon Dioxide

The band absorptance $\int A_v dv$ for the $15\mu\text{m}$ band of CO_2 is calculated using a method first employed by Cess and Ramanathan (1972) for IR flux calculations in the

atmospheres of Mars and Venus. Ramanathan (1976) extended this method to include the hot and minor isotopic bands in the $15\mu\text{m}$ (667 cm^{-1}) region of CO_2 in the flux calculations of a 1D RCM designed for the Earth's atmosphere. Kiehl and Ramanathan (1983) described the model in some detail and also include additional weaker bands in the $15\mu\text{m}$ region. We give only a brief outline of the model here.

As noted in Chapter 2 a semi-empirical formula used to calculate the band absorptance of several atmospheric gases is

$$A = 2A_0 \ln \left[1 + \frac{u}{\sqrt{4 + u(1 + 1/\beta)}} \right] \quad 3.2.1$$

where A_0 is an empirical constant called the effective band width parameter ($A_0 = \partial A / \partial \ln u$), u the dimensionless optical depth, and β the mean line-width parameter. The parameters u and β are defined as,

$$u = \frac{SW}{A_0}$$

$$\beta = \frac{2\gamma}{\delta}$$

where S is the band strength, W is the amount of gas times 1.66 to account for diffuse radiation (see Appendix A), γ is the mean line width, and δ is the mean line

spacing. Ramanathan (1976) and Kiehl and Ramanathan (1983) give the equation,

$$A = 2A_o \ln \left[1 + \sum_{i=1}^4 \sum_{j=1}^{14} \frac{U_{ij}}{\sqrt{4 + U_{ij}(1 + 1/\beta_{ij})}} \right] \quad 3.2.2$$

for the total band absorptance due to the $i = 4$ isotopes of CO_2 and the $j = 14$ bands of CO_2 in the $15 \mu\text{m}$ spectral region. Equation 3.2.2 assumes complete band overlap of the individual bands. In equation 3.2.2 above,

$$u_{ij} = q_i \int \frac{S_j(T)}{A_o(T)} P_a dz$$

and

$$\beta_{ij} = \frac{4}{\delta_{ij} u_{ij}} \int \gamma(T) P du_{ij} \quad 3.2.3$$

where P_a is the partial pressure of CO_2 (atm), q_i is the isotopic abundance relative to $\text{C}^{12}\text{O}_2^{16}$, $S_j(T)$ ($\text{cm}^{-2}\text{atm}^{-1}$) is the band strength of $\text{C}^{12}\text{O}_2^{16}$ at temperature T , P is the atmospheric pressure (in atm), and z is the height (cm).

To use equation 3.2.2 the four quantities S_j , γ , δ_{ij} , and A_o must be specified. Kiehl and Ramanathan (1983) provide a table of the S_j , δ_{ij} , and the band

location, ν_j , for the 14 bands in the 15 μm region of CO_2 . We have reproduced many of the important features of their table as Table 3-1 below.

Table 3.1. CO_2 15 μm Band parameters as given by Kiehl and Ramanathan 1983. † For $\text{C}^{12}\text{O}^{16}\text{O}^{18}$ and $\text{C}^{12}\text{O}^{16}\text{O}^{17}$ the mean line spacing is 0.78 for all bands. Band strengths were from those listed by Kiehl and Ramanathan (1983) except where a * indicates that the author of this paper used band strengths given by Goody and Yung (1989).

Band Number	Band Center ν_j, cm^{-1}	Strength at 300K $\text{cm}^{-2}\text{atm}^{-1}$	Lower State E_j, cm^{-1}	Mean Line Spacing † $\delta_{ij}, \text{cm}^{-1}$
1	667.381	222.0 *	0.0	1.56
2	618.029	3.87 *	667.381	1.56
3	720.805	5.0	667.381	1.56
4	667.751	17.4 *	667.381	0.78
5	647.063	0.6 *	1285.410	1.56
6	791.446	0.022	1285.410	1.56
7	597.342	0.14	1335.131	0.78
8	741.724	0.144	1335.131	0.78
9	668.107	1.0 *	1335.131	0.78
10	544.288	0.01	1388.185	1.56
11	668.670	0.4 *	1388.185	1.56
12	652.529	0.045	1932.473	0.78
13	720.286	0.005	2076.855	1.56
14	615.887	0.015	1932.473	1.56

Note that $\delta_{ij} = 4B$ or $2B$, where $B = .39 \text{ cm}^{-1}$ is the quantum mechanical rotation constant discussed in Chapter 2. The mean line width γ and A_0 are assumed to be the same for all lines and are written as,

$$\gamma = 0.067(300/T)^{0.667} \text{ (cm}^{-1}\text{)}$$

and

3.2.4

$$A_0 = 22.18(t/296)^{0.5} \text{ (cm}^{-1}\text{)}$$

respectively. Goody (1989) gives $q_1=1.0$, $q_2 = 0.0113$, $q_3 = 0.00414$, $q_4 = 0.00066$ for the relative abundances of the four isotopes $\text{C}^{12}\text{O}_2^{16}$, $\text{C}^{13}\text{O}_2^{16}$, $\text{C}^{12}\text{O}^{16}\text{O}^{18}$, and $\text{C}^{12}\text{O}^{16}\text{O}^{17}$ respectively. The temperature dependence of the band strengths is given by Kiehl and Ramanathan (1983) to be,

$$S_j(T) = S_j(T_0) \left(\frac{T_0}{T} \right) \frac{Q_v(T_0) \left\{ 1 - e^{-1.439 \nu_j / T} \right\}}{Q_v(T) \left\{ 1 - e^{-1.439 \nu_j / T_0} \right\}} \times \exp\{1.439 E_j [1/T_0 - 1/T]\} \quad 3.2.5$$

(Note that 1.439 equals hc/k and T_0 is the reference temperature of 300 K). As noted by Kiehl and Ramanathan

(1983) the fourth term on the right-hand side of equation 3.2.5 accounts for stimulated emission and the last term is a Boltzman factor, which accounts for the population of higher vibrational transitions (hot bands). Also if the CO₂ molecule is assumed to behave as a harmonic oscillator we can write Q_v(T) as,

$$Q_v(T) \approx \left(1 - e^{-1.439\nu_j/T} \right)^{-2}$$

A slightly modified form of equation (3.2.2) is used in the OGI model to account for bands that are not completely overlapped, see Kiehl and Ramanathan (1983) for specific details or subroutine "co2" in Appendix E. Equation 3.2.2 is useful since it is directly applicable to the temperatures, pressures, and absorber amounts present in the Earth's atmosphere and, as noted by Kiehl and Ramanathan (1983), agrees well with the laboratory data. For computational efficiency the band absorptance is calculated every tenth time step since the temperature dependence of 3.2.2 is not very strong. Subroutine "co2ir" is used for the above calculation of the 15μm band absorptance for CO₂. Figure 3.3 shows the band absorptance for the 15 μm band of CO₂ as calculated by the OGI model for T=300 K and P=1.0 atm.

CO₂ Band Absorptance (15 μ m Band)

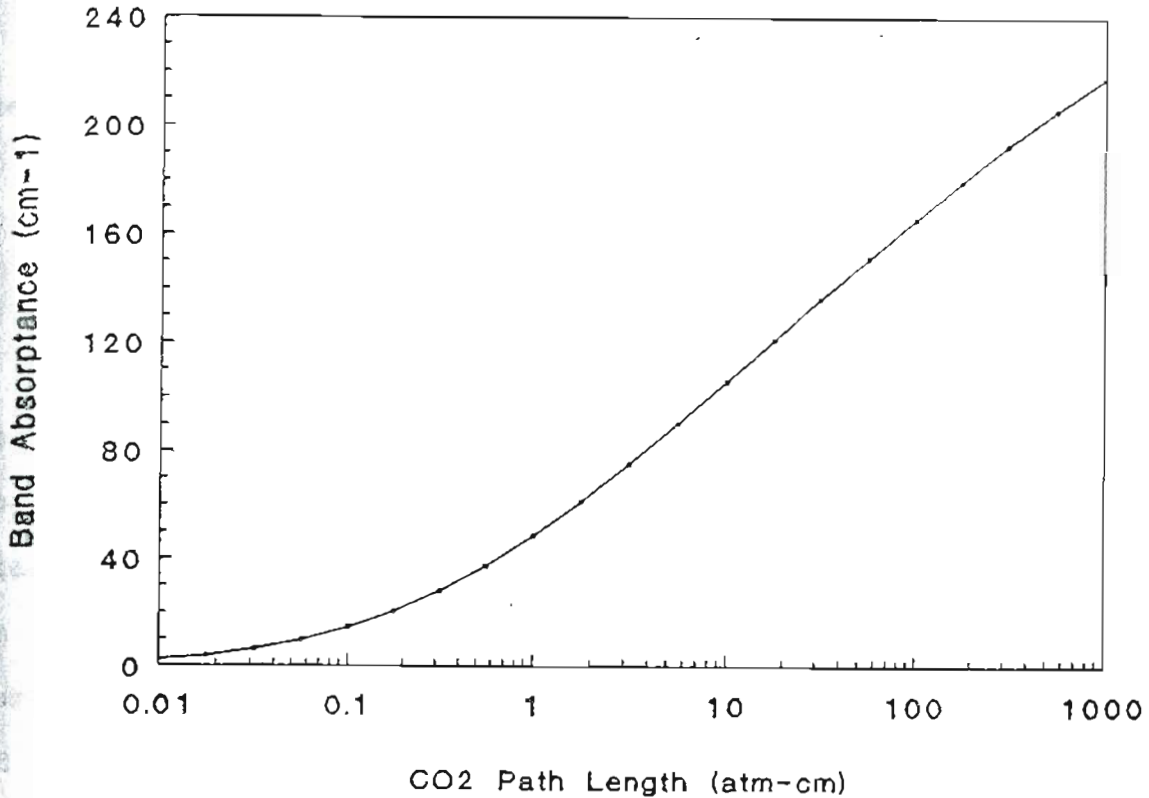


Figure 3.3. Integrated band absorptance of CO₂ 15 μ m band versus absorber amount (cm-atm) as calculated using equation 3.2.5.

Water vapor is also a strong absorber in the 15 μ m region and hence a correction is needed for the overlap of CO₂ with water vapor. If in a spectral interval there is absorption due to two different gases x and y that do not interact then the total monochromatic

transmission of the mixture is the product of the individual transmissions i.e.

$$T_{xy}^v = T_x^v T_y^v \quad 3.2.6$$

the absorptivity over the spectral interval is given by,

$$\begin{aligned} A_{xy} &= \int (1 - T_x^v T_y^v) dv \\ &= \int [(1 - T_x^v) + (1 - T_y^v) T_x^v] dv \\ &= A_x + A_y \bar{T}_x \end{aligned} \quad 3.2.7$$

assuming that T_x and T_y are not correlated over the spectral interval. Use of equation 3.2.7 is the standard method of dealing with the overlap of two gases in climate models (see Staley and Jurica (1970) or Ramanathan (1976)). That is, the absorption due to one of the gases is calculated using the standard absorptivity for that gas and the absorption due to the second gas is calculated by multiplying its absorptivity by the mean transmission T_x of the first gas.

Since we calculate the heating due to water vapor without any overlap correction we must multiply the absorptivity of CO_2 given in 3.2.5 by the transmission of water vapor in the 12-18 μm interval. Following Kiehl and Ramanathan (1983) we calculate the transmission of the H_2O pure rotation band (TRR) using

the method given by Kuo (1977) and the transmission of the H₂O continuum (TRC) is calculated from the formulation given by Roberts (1976). Subroutine "h2oco2" performs the above calculations which are outlined below.

Kuo (1977) starts with the Goody statistical model (see Section 3.4 or Chapter 2) for the mean transmissivity in a spectral interval $\Delta\nu$ given by,

$$\bar{T} = \exp\left[-\frac{Sm\delta}{\delta}\left(1 + \frac{Sm}{\pi\alpha}\right)^{-1/2}\right] \quad 3.2.8$$

where S is the mean line intensity $S = \int k_\nu d\nu$, α is the line half width at half maximum, δ is the mean line spacing, m is the absorber amount in g/cm² for water vapor, and k_ν is the monochromatic mass absorption coefficient. Defining the generalized absorption coefficient f to be,

$$f = \frac{\pi S \alpha}{\delta^2} = \left[\frac{2}{\Delta\nu} \sum_i \sqrt{S_i \alpha_i} \right]^2 \quad 3.2.9$$

equation 3.2.8 can be rewritten as,

$$\bar{T}(m, \nu) = \exp\left\{-\left[\frac{fm}{1 + \pi^2 \alpha^2 / fm \delta^2}\right]^{1/2}\right\} \quad 3.2.10$$

From 3.2.10 it is easy to see that for the strong line limit ($f m \gg \pi^2 \alpha^2 / \delta^2$)

The

$$\bar{T}_s(m, \nu) \approx \exp - \sqrt{f(\nu)m} \quad 3.2.11$$

and that for the weak line limit ($f m \ll \pi^2 \alpha^2 / \delta^2$)

$$\bar{T}_w(m, \nu) \approx \exp\left[\frac{-S(\nu)}{\delta} m\right] = \exp[-k(\nu)m] \quad 3.2.12$$

where $k=S/\delta$.

From an inspection of the $\log_{10}(f\nu)$ versus ν graph shown below in Figure 3.4 it is evident that

$$f(\nu, T) = f_0 e^{2B(T)(\nu - \nu_0)} \quad 3.2.13$$

where $f_0 = f(\nu_0, T)$ and $2B(T)$ equals the slope of the graph which is temperature dependent. Similar arguments apply to the $k(\nu, T)$ profile, so that an accurate representation of $k(\nu, T)$ is given by

$$k(\nu, T) = k_0 e^{2B'(T)(\nu - \nu_0)} \quad 3.2.14$$

Kuo (1977) notes that since $\pi\alpha/\delta$ does not vary appreciably with ν and T , using $B(T) = B'(T)$ is a good approximation. $B(T)$ expresses the temperature dependency of $f(\nu, T)$ and is represented by a quadratic formula in the temperature departure $T' = T - T_0$ where T_0 is the

reference temperature i.e.

$$B(T) = b(T_0) (1 - cT' - c'T'^2) \quad 3.2.15$$

The values of b , c , and c' used for the intervals of interest ($0-800 \text{ cm}^{-1}$) are listed below in Table 3.2.

H₂O Absorption Coefficients f_ν (From Kuo 1977)

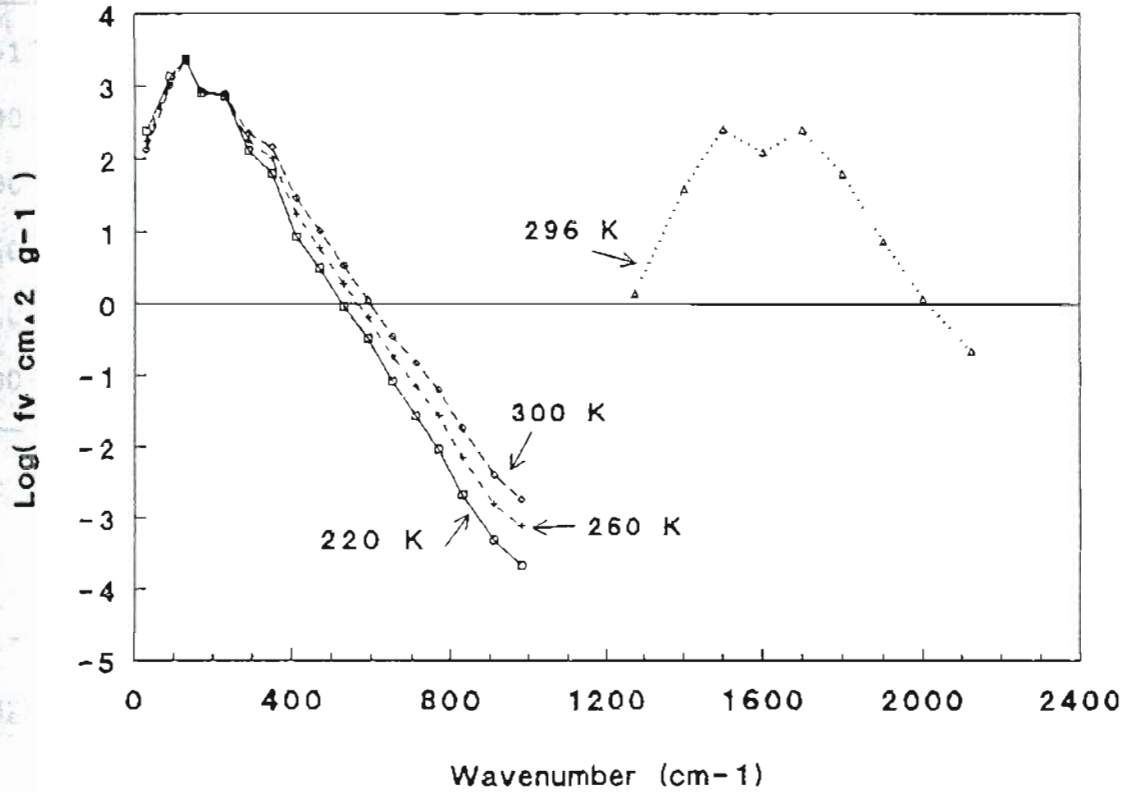


Figure 3.4. $\text{Log}(f_\nu)$ versus ν showing the exponential character of f_ν . After Kuo (1977).

Table 3.2. Values of b , c , and c' as given by Kuo (1977) to calculate the temperature dependence of f_v ($T_0=260$ K). The columns f_1 and f_2 are the values of the generalized absorption coefficients at the beginning and end of each spectral interval. For example in the first row f_1 corresponds to $\nu=0$ cm^{-1} .

Wave number range, cm^{-1}	b 10^{-2} cm	c 10^{-2} K $^{-1}$	c' 10^{-4} K $^{-2}$	f_1 g^{-1}cm^2	f_2 g^{-1}cm^2
0-130	1.3607	-.2647	0.0448	177.1	2692.0
130-290	0.8457	0.2569	-.1191	2692.0	179.8
290-350	0.4643	0.6739	-.3600	179.8	103.0
350-410	1.4640	0.2605	-.1307	103.0	17.8
410-500	0.9270	0.1641	-.0255	17.8	3.354
500-800	0.9270	.1641	-.0255	3.354	0.0129

From equations 3-22 and 3-24 we can write the strong line transmissivity (applicable for the water vapor rotation band) as,

$$\bar{T}(\nu, m^*) = \exp\left\{-\sqrt{f_0 m^*} e^{B(\nu-\nu_0)}\right\} d\nu \quad 3.2.16$$

where $m^* = 5/3 \int p dm$ is the pressure corrected absorber amount for diffuse radiation and p is the pressure in atmospheres. The mean transmissivity T for the interval

$\Delta v = v_1 - v_0$ is given by

$$\bar{T}(m^*, \Delta v) = \frac{1}{\Delta v} \int_{v_0}^{v_1} \exp\left\{-\sqrt{f_0 m^*} e^{B(v-v_0)}\right\} dv \quad 3.2.17$$

Setting $x = e^{B(v-v_0)}$, $x_1 = e^{B\Delta v}$ and $y = \sqrt{f_0 m^*}$,

we can rewrite 3.2.17 as,

$$\begin{aligned} \bar{T}(m^*, \Delta v, T) &= \frac{1}{B(T)\Delta v} \int_1^{x_1} \frac{1}{x} e^{-yx} dx \\ &= \frac{1}{B(T)\Delta v} \{E_1(y) - E_1(x_1 y)\} \end{aligned} \quad 3.2.18$$

where $E_1(U)$ is the first order exponential integral defined by

$$E_1(u) = \int_u^{\infty} \frac{1}{u} e^{-u} du$$

and is calculated in subroutine "expon" (Appendix E) using a numerical procedure outlined in Abramowitz and Stegun (1970).

From an inspection of Table 3.2 it can be seen that the pure rotation band is broken into 6 intervals and the interval of interest for the H₂O - CO₂ overlap correction is the last (500-800 cm⁻¹). Starting at the rotational band center of (130 cm⁻¹) $y_1 = \sqrt{2692m^*}$

$= 51.88\sqrt{m^*}$. All other values of y_i can be obtained from $y_i = y_{i-1} e^{B_i(v_i - v_{i-1})}$ (See Figure 3.3) and the transmission in the 500-800 cm^{-1} range can be calculated from equation 3.2.18 as

$$\text{TRR} = \frac{1}{B_6 \Delta v_6} [E_1(y_6) - E_1(y_5)] \quad 3.2.20$$

In the OGI model the values of b_j , c_j , c_j' and Δv from Table 3.2 are used to calculate

$$y_5 = y_1 \exp\left\{-\sum_2^5 B_j (v_j - v_{j-1})\right\}$$

and

$$y_6 = y_1 \exp\left\{-\sum_2^6 B_j (v_j - v_{j-1})\right\}$$

during each time step (new temperature) via subroutine "bcalc" (Appendix E). Equation 3.2.20 is then used to calculate the transmission of the H_2O pure rotation band TRR to be used in the H_2O CO_2 overlap correction.

As noted by Kiehl and Ramanathan the transmission of the H_2O continuum (TRC) in the 15 μm band of CO_2 must also be accounted for when calculating the net absorption due to CO_2 and water vapor. The total transmission due to water vapor TRC2 is given by the

product of the continuum and pure rotational transmission

$$TRC2=TRC \times TRR \quad 3.2.21$$

TRC is calculated following the method described by Roberts (1976), see equation 3.1.4.

To calculate the average transmission of the H₂O continuum for the CO₂ spectral band, TRC, we break the interval from 560 cm⁻¹ to 840 cm⁻¹ into 7 smaller intervals of equal width Δv_j (40 cm⁻¹) and perform the average according to equation 3.2.22 below

$$TRC = \frac{1}{280} \sum_{j=1}^7 T_{\Delta v_j} \Delta v_j \quad 3.2.22$$

Finally combining 3.2.22, 3.2.21 and 3.2.20 we can obtain the mean transmission of water vapor over the CO₂ spectral interval. We multiply the absorptivity of CO₂ calculated by equation 3.2.5 by the transmission as suggested by equation 3.2.7 to complete the overlap correction.

As noted by Augustsson and Ramanathan (1977), CO₂ also contains a weak absorption band in the atmospheric window region around 10 μ m. We use equation 3.2.1 with $A_0=22.18$ cm⁻¹, $S=.03$ atm⁻¹ cm⁻² from Goody and Yung

(1989), $B = (2 * .084 / 1.56) (p/p_0) (298/T)^{.56}$ from Goody (1964). To correct for the overlap with the water vapor continuum we multiply the band absorptance of the 10 μm CO_2 band by the transmission of water vapor in the 10 μm region as calculated in the next section for the ozone overlap correction. This band contributes to roughly 5 percent of the global warming due to a doubling of CO_2 but is important since it is not near saturation at present.

3.3 Ozone

We employ the method of Kuo (1977) to calculate the IR band absorptance for the ozone 9.6 μm (1040 cm^{-1}) band. The theoretical justification of this method is identical to that outlined in section 3.2 for the calculation of the water vapor rotation band transmission used for the $\text{CO}_2\text{-H}_2\text{O}$ overlap correction. Hence we present here the specific parameterization only.

Kuo (1977) notes that the generalized absorption coefficient f_v is nearly symmetric about the O_3 1040cm^{-1}

band center. He uses this simplifying assumption to derive the semi-empirical expression for the average transmission of IR radiation for this spectral band given by,

$$T_{O_3} = .3476[E_1(y) - E_1(17.78y)] \quad 3.3.1$$

where $y = .5183m_o^* / \sqrt{(1 + 3.7145m_o^*)}$, and $E_1(y)$ is the first order exponential integral as defined in Section 3.2.

The pressure corrected optical path length m_o^* is defined by,

$$m_o^* = \frac{5}{3}m \left(\frac{p}{p_o} \right)^\alpha \quad 3.3.2$$

where m is the optical path length of O_3 in atm-cm, p is the atmospheric pressure, and p_o is the standard pressure of 1 atmosphere. Kuo (1977) notes that equation 3.3.1 is in good agreement with experimental observations for values of m_o^* between 0.0 and 0.4 atm-cm, which is the typical range of values encountered in the atmosphere. The value of α in equation 3.3.2 depends on the pressure $p^* = p/p_o$ and the absorber amount in a complicated way. The following representations for α are found to agree well with observations for values

of m between 0.0 and 0.65 atm-cm.

$$\begin{aligned} \alpha &= (1.085 - 0.085p^*)\alpha_u & 0 \leq p^* \leq 0.015 \\ &= \alpha_u^{1-\beta} \alpha_1^\beta & 0.015 \leq p^* \leq 0.25 \\ \text{where} \quad &= 0.667(1.75 - p^*)\alpha_1 & 0.25 \leq p^* \leq 1.0 \end{aligned}$$

$$\alpha_u = \frac{4.1m}{1 + 9.5m} \quad \alpha_1 = \frac{.8467m(1.9 - m)}{1 + 2m} \quad \beta = \sqrt{\frac{p^* - .015}{.235}}$$

Using equation 3.3.1 to calculate T_{O_3} we then calculate the band absorptance A_{O_3} for the 9.6 μm band of O_3 to be,

$$A_{O_3} = (1 - T_{O_3})\Delta\nu \quad 3.3.3$$

where $\Delta\nu = 137\text{cm}^{-1}$ is the band width. The above procedures are performed by subroutine "o3ir" in Appendix E.

The water vapor continuum band also absorbs IR energy in the 9.6 μm region. Thus the absorptance calculated by equation 3.3.3 must be multiplied by the transmission of water vapor in this region T_H to correct for this overlap. To calculate T_H we used the formula given by Roberts (1976), see equation 3.1.4 using $\nu = 1042\text{cm}^{-1}$.

3.4 Nitrous Oxide and Methane

Following Ramanathan et al. (1987) and Donner and Ramanathan (1982), we use an equation similar to equation 3.2.1 to calculate the band absorptance for methane (CH₄) and nitrous oxide (N₂O) respectively. In particular the band absorptance is given by,

$$A = 2A_o \ln \left[1 + \frac{u}{D + \sqrt{E + u(1 + 1/\beta)}} \right] \quad 3.4.1$$

where

$$u = 1.66 Sw/A_o$$

$$\beta = \beta_o \left(\frac{P}{P_o} \right) \quad \text{and} \quad \beta_o = \frac{2\gamma}{\delta}$$

S is the band intensity (cm⁻² atm⁻¹), W is the absorber amount (cm STP), A_o is the effective bandwidth parameter (cm⁻¹), γ is the mean line width at pressure $p_o=1$ atm, δ is the mean line spacing, 1.66 is the diffusivity factor, $E=(2-D)^2$, where $D=0.106$ and 0.0 for methane and both bands of nitrous oxide respectively.

Methane has a single absorption band centered at 1306 cm⁻¹ (950-1650 cm⁻¹) and nitrous oxide has two

bands; one at 589 cm^{-1} ($520\text{-}660\text{cm}^{-1}$) and another at 1285 cm^{-1} ($1200\text{-}1350 \text{ cm}^{-1}$). The values of A_0 and B_0 used in the OGI model are taken from Donner and Ramanathan (1982) or Ramanathan et al. (1987) and are shown in Table 3.3. Also shown in Table 3.3 are the band intensities used in the OGI model obtained from Goody (1989).

Table 3.3. Absorption parameters for Methane and Nitrous oxide. Values for both N₂O bands are from Donner and Ramanathan (1982), and the CH₄ band parameters are from Ramanathan et al (1987).

Parameter	CH ₄ (1306cm ⁻¹)	N ₂ O (1285cm ⁻¹)	N ₂ O (589cm ⁻¹)
A ₀ (cm ⁻¹)	$68.2(T/300)^{.858}$	$20.4(T/300)^{.5}$	$23(T/300)^{.5}$
B ₀	$0.211(300/T)$	$1.12(300/T)^{.5}$	$1.08(300/T)^{.5}$
S (cm ⁻² atm ⁻¹)	135	268	32

Figure 3.5 below shows the band absorptances for the 1306 cm^{-1} band of methane, and the two 1285 cm^{-1} and 589 cm^{-1} bands of nitrous oxide.

Integrated Band Absorptivities
(For CH₄ and N₂O at 1 atm & 300 K)

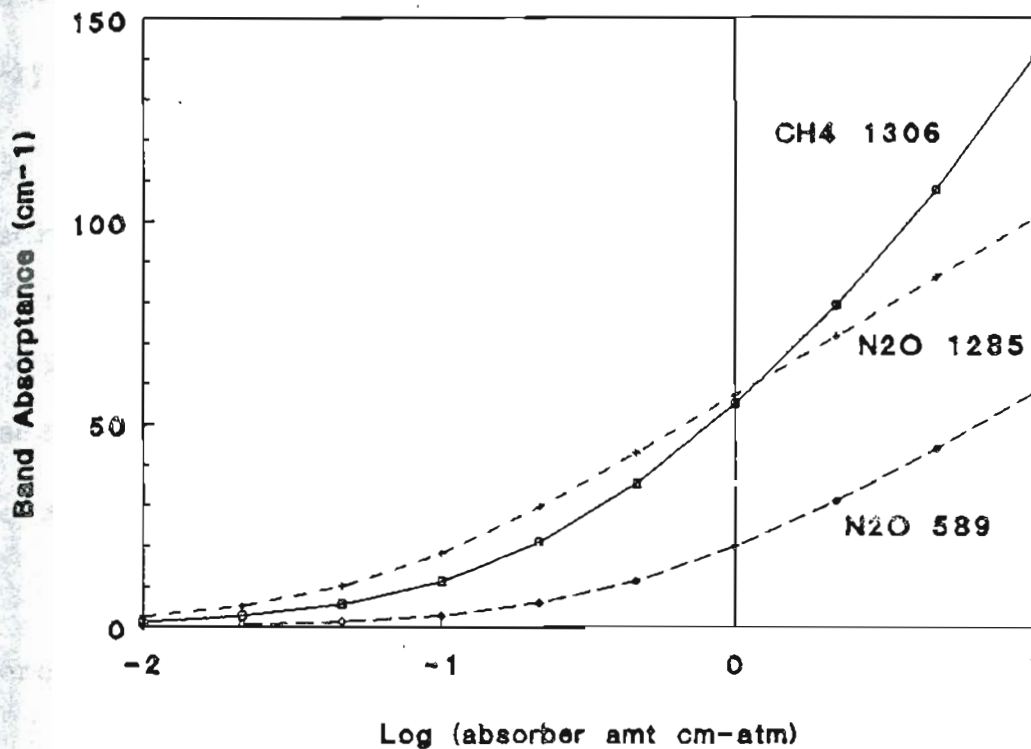


Figure 3.5. The band absorptances as calculated by equation 3.4.1 for the, a) 1306 cm⁻¹ CH₄, b) 1285 cm⁻¹ N₂O, and c) 589 cm⁻¹ N₂O bands

Methane

Equation 3.4.1 with the parameters listed in Table 3.3 are used in subroutine "ch4ir" of Appendix E to calculate the IR atmospheric cooling(or heating) due to

methane. The 1306 cm^{-1} region of the spectrum also has absorption due to the water vapor continuum ($950\text{-}1200\text{ cm}^{-1}$) and the water vapor vibration-rotation band ($1200\text{-}1650\text{ cm}^{-1}$). Following the procedure for CO_2 the absorptance of methane as calculated by equation 3.4.1 is multiplied by the average water vapor transmissivity T_4 to account for the overlapping bands of the two gases. The average transmissivity of water vapor for the $950\text{-}1650\text{ cm}^{-1}$ band interval is taken to be

$$T_4 = \{260 * T_{41} + 450 * T_{42}\} / 710 \quad 3.4.2$$

where T_{41} is the transmissivity of the water vapor continuum from $940\text{-}1200\text{ cm}^{-1}$ and T_{42} is the transmissivity of the water vapor vibration-rotation band from $1200\text{-}1650\text{ cm}^{-1}$. T_{41} is calculated using the parameterization given by Roberts (1976) for the water vapor continuum. Subroutine "trcont" is used for the calculations and the details of the method are as described in Section 3.1 for the H_2O continuum transmissivity. The Goody statistical model (see Chapter 2 or the more detailed discussion given at the end of this section) is used to calculate T_{42} for the $1200\text{-}1650$

cm⁻¹ region. The values of S/δ and $S/(\pi\alpha)$ are taken from Rodgers and Walshaw (1966) and are 248.3 g⁻¹cm² and 1276 g⁻¹cm² respectively and the dependency of S/δ and $S/(\pi\alpha)$ on temperature assumed to be negligible.

Nitrous oxide (1285 cm⁻¹)

Equation 3.4.1 along with Table 3.3 are used in subroutine "n2o1285" (Appendix E) to calculate the IR cooling due to the N₂O band extending from 1200-1350 cm⁻¹. The vibration-rotation band of water vapor and the absorption band of methane both overlap this band of N₂O and hence the transmissivity of each must be calculated. The total transmissivity of this interval T₅ due to methane and water vapor is taken to be

$$T_5 = T_{CH_4} * T_{H_2O} \quad 3.4.3$$

where T_{CH₄} and T_{H₂O} are the transmissivities due to methane and water vapor respectively. The band absorptance of N₂O as calculated by equation 3.4.1 is then multiplied by T₅ to correct for the band overlap.

T_{H₂O} is calculated using the Goody statistical band

model (see Chapter 2 and the detailed discussion given below at the end of this section). The values of S/δ and $S/(\pi\alpha)$ are taken from Rodgers and Walshaw (1966) and are $12.65 \text{ g}^{-1}\text{cm}^2$ and $142.3 \text{ g}^{-1}\text{cm}^2$ respectively. The temperature dependence of S/δ and $S/(\pi\alpha)$ is again assumed to be negligible for this spectral region. This calculation is performed in subroutine "n2oh2o1285" of Appendix E. T_{CH_4} is calculated using the spectral data given by Green (1964) which is briefly outlined below.

Green (1964) gives,

$$T = \exp[-(w'/w_e)\eta] \quad 3.4.6$$

for the transmission T of IR radiation through an atmosphere containing methane where

$$w' = w(P_e/P_s) \quad 3.4.7$$

w_e is an empirical constant, P_e is the effective atmospheric pressure (atm), w is the absorber amount (cm-
STP), P_s is a standard pressure (1 atm), and the exponent η is an empirical constant ($\eta = .46$). Table 3.4 gives the values of w_e for the 5 spectral intervals of CH_4 that are used to span the N_2O interval from 1200-

1350 cm^{-1} .

To calculate the average transmissivity of CH_4 for the 1200-1350 cm^{-1} band of N_2O we use,

$$T_{\text{CH}_4} = [\sum (T_j \Delta\nu_j)] / 150 \quad 3.4.8$$

where T_j is calculated using equation 3.4.6 and the values of w_{ej} and $\Delta\nu_j$ are as given in table 3.4. The above calculation is performed by subroutine "n2c41285" of Appendix E.

Table 3.4. Values of w_e and $\Delta\nu_j$ for the five spectral intervals of CH_4 between 1200 and 1350 cm^{-1} .

j	Spectral interval (cm^{-1})	$\Delta\nu_j$ (cm^{-1})	w_e (atm-cm)
1	1200-1272	72	14.95
2	1272-1285	13	6.47
3	1285-1304	19	2.60
4	1304-1315	12	9.08
5	1316-1350	34	18.4

Nitrous oxide (589 cm^{-1})

As with CH_4 we again use equation 3.4.1 along with the values given in Table 3.3 to calculate the band absorptance of N_2O for the spectral interval between 520 and 660 cm^{-1} . This calculation is performed by subroutine "n2o590" of Appendix E. Since the water vapor rotation band and CO_2 ν_2 band both absorb in this spectral region their respective transmissivities $T_{\text{H}_2\text{O}}$ and T_{CO_2} must be calculated to correct for the overlap of these bands with that of N_2O at 589 cm^{-1} .

We employ the Goody statistical model again, but now with a temperature correction, to calculate $T_{\text{H}_2\text{O}}$. We give here a brief description of the implementation of the model since the temperature correction formulation developed by Rodgers and Walshaw (1966) and Rodgers (1967) is much more detailed than the no temperature correction version utilized in previous sections of this chapter.

The band formulation given by Rodgers and Walshaw

(1966) and Rogers (1967) to calculate the mean transmissivity of water vapor TH₂O over this spectral interval is (see Chapter 2),

$$T_{H_2O}(U, T) = \exp - \left[\frac{S\bar{m}}{\delta} \left(1 + \frac{S\bar{m}}{\pi\alpha_0\bar{p}} \right)^{-\frac{1}{2}} \right] \quad 3.4.9$$

where $\bar{m} = \int \Phi(T) dm$ is the temperature corrected amount of water vapor ($g \text{ cm}^{-2}$), $\bar{m}\bar{p} = \int \chi(T)p \, dm$, \bar{p} is an average pressure over the atmospheric path, S is the mean line intensity, δ the mean line spacing, and α_0 is the line half width at $p = p_0 = 1 \text{ atm}$. $\chi(T)$ and $\Phi(T)$ are functions of temperature T (k) and are defined as

$$\Phi(T) = \frac{\sum S_i(T)}{\sum S_i(T_0)} \quad 3.4.10$$

$$\chi(T) = \left[\frac{\sqrt{\sum [S_i(T) \alpha_0(T)]}}{\sqrt{\sum [S_i(T_0) \alpha_0(T_0)]}} \right]^2 \quad 3.4.11$$

and are used as temperature corrections to the quantum mechanical data S and α_0 . Rodgers and Walshaw (1966) gave the empirical expressions,

$$\begin{aligned} \ln(\Phi(T)) &= a(T-260) + b(T-260)^2 \\ \ln(\chi(T)) &= a^1(T-260) + b^1(T-260)^2 \end{aligned} \quad 3.4.12$$

Note if no temperature correction is applied, as was the case in previous sections, $\chi(T)$ and $\Phi(T)$ are both just set to unity.

The above method is used several other times by the model when calculating the correction due to the overlap of water vapor with other gases. It is based upon the Goody statistical model described in Chapter 2 and hence transmissions calculated using equation 3.4.9 are referred to as Goody Statistical transmissions. The values of $S/\delta = \sum S_i/\Delta\nu$ and $\pi\alpha_0/\delta$ can be calculated by using the tabulated values of $\sum S_i$ and $\sum\sqrt{[\alpha_i S_i]}$ given by Goody (1964 Chapter 5) for every 20 cm^{-1} interval (from 0 to 1000 cm^{-1}) where $\Delta\nu$ is the total wave number interval. (Note: Goody's S_{mi} are equivalent to Rodgers and Walshaws k_i). For the rotational band under consideration 15.2-19.3 μm (520-660 cm^{-1}) $\Delta\nu = 140 \text{ cm}^{-1}$ and $S/\delta = 9.706 \text{ (g}^{-1}\text{cm}^2)$ at $T_0 = 260\text{K}$. The term $\pi\alpha_0/\delta$ can be obtained from Goody's tabulated values as

$$\pi\alpha_0/\delta = \frac{\left[\frac{2\sum\sqrt{[\alpha_i S_i]}}{\Delta v} \right]^2}{(S/\delta)}$$

$$= 0.0597 \quad (T_0 = 260 \text{ K})$$

or

$$k/\pi\alpha_0 = 162.6 \text{ (g}^{-1} \text{ cm}^2)$$

The values of a , b , a^1 , and b^1 were obtained by interpolation of the values given by Rodgers and Walshaw 1966 and are,

$$a = 0.0168 \text{ (K}^{-1}\text{)}$$

$$b = -3.63 \times 10^{-5} \text{ (K}^{-2}\text{)}$$

$$a^1 = 0.0172 \text{ (K}^{-1}\text{)}$$

$$b^1 = -4.68 \times 10^{-5} \text{ (K}^{-2}\text{)}$$

Subroutine "h2on2o590" of Appendix E performs the above calculation for T_{H2O} .

The value of T_{CO2} is calculated in subroutine "co2ir" by simply taking the band absorptance for CO_2 , A_{CO2} , before the water vapor correction and dividing it by the width of the CO_2 band 300 cm^{-1} to obtain the mean

absorptivity A , i.e.

$$T_{CO_2} = [1 - A_{CO_2}/300] \quad 3.4.13$$

The corrected band absorptance for N_2O is then obtained by multiplying the absorptance of N_2O calculated by equation 3.4.1 by $T_{H_2O} \times T_{CO_2}$.

3.5 Other Gases

We have included a subroutine "smallir" in Appendix E to calculate the band absorptances of some of the important greenhouse gases such as the chlorofluorocarbons which have atmospheric concentrations at the pptv level. Following Ramanathan 1975 in his analysis of the greenhouse effect due to chlorofluorocarbons, we use the weak line limit to calculate the band absorptance A , i.e.

$$A = S u \quad 3.5.1$$

Where S is the band strength in $\text{atm}^{-1} \text{cm}^{-2}$ and u is the absorber amount in atm-cm . Table 3.5 is reproduced from the WMO Report No. 16 (1985) and contains the band strength and band center for several low concentration atmospheric greenhouse gases. As noted by Ramanathan

(1975) the use of equation 3.5.1 should be limited to trace gases that have concentrations of 5 ppbv or less unless other justification can be given. Note the band center must be known to calculate the Planck function and hence the net atmospheric heating or cooling due to a particular gas as outlined in Appendix A.

Table 3.5. The band centers and band strengths (or intensities) of some of the CFCs as given in the WMO Report No. 16 (1985).

Molecule	Rough Spectral Range (cm ⁻¹)	Band Strength (atm ⁻¹ cm ⁻² 296K)
CFCs		
CFC13 (F11)	800-900	1828
	1050-1100	679
CF2Cl2 (F12)	875-950	1446
	1060-1125	1141
	1125-1175	767
CF3Cl (F13)	750-825	116
	1075-1125	1758
	1175-1240	2116
CF4 (F14)	600-650	39
	1250-1300	5472
CHClF2 (F22)	780-840	219
	1080-1140	637
	1280-1340	101
C2F6 (F116)	880-740	135
	1080-1150	975
	1220-1280	3374

Chapter 4

Solar Absorption

As can be seen from Figure 4.1, the solar spectrum extends from about $0.2 \mu\text{m}$ to $4 \mu\text{m}$ with significant absorption due to H_2O , O_3 , O_2 and CO_2 . In Figure 4.1 the top solid curve represents the solar spectral irradiance at the top of the atmosphere, the area between the top curve and the shaded region represents the energy reflected by the atmosphere, and the shaded region corresponds to the gaseous absorption by the atmosphere for clear sky conditions. The dashed line is the energy curve for a black body radiator at 5800K multiplied by the square of the ratio of the radius of the sun to the mean earth-sun distance.

Although the absorption of solar radiation due to water vapor is strong it occurs primarily for wavelengths greater than $0.8 \mu\text{m}$ and hence the atmosphere is still relatively transparent to solar radiation. From Figure 4.1 it is also evident that Rayleigh scattering is predominant at wavelengths less than 0.8

μm . This fact will be used in Sections 4.1 and 4.2 as a simplification for the calculation of solar absorption due to water vapor.

Solar Spectral Irradiance

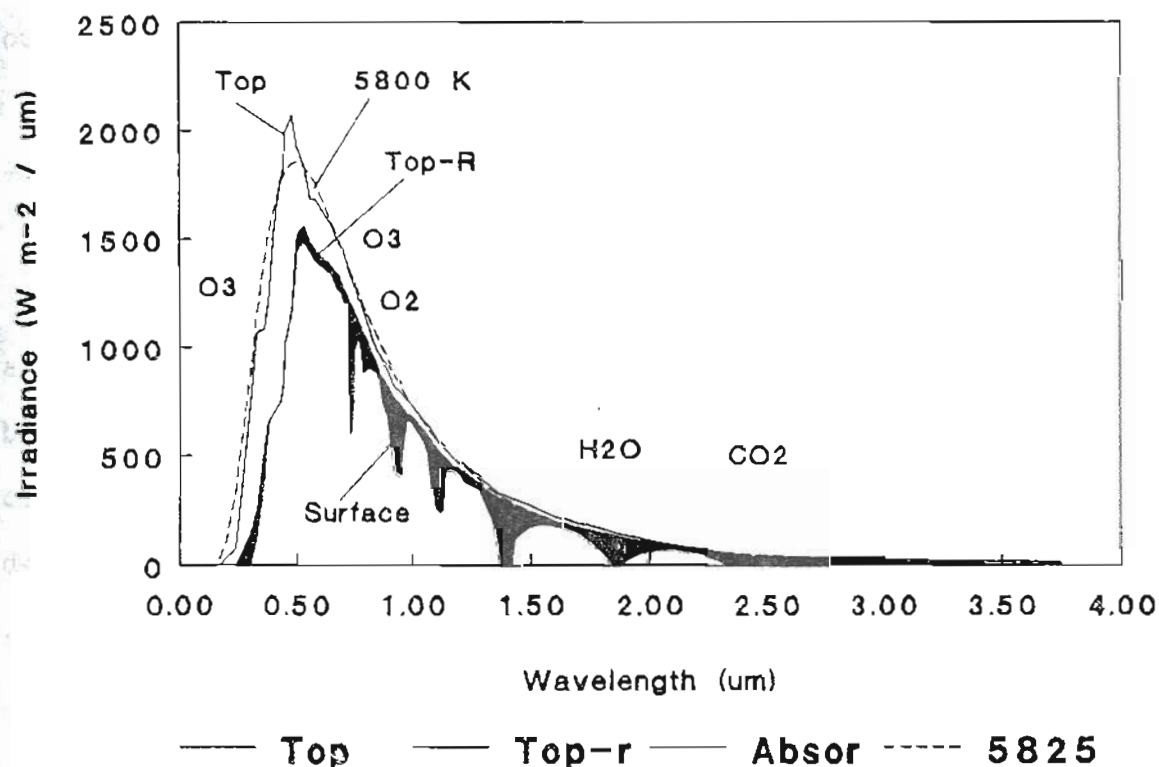


Figure 4.1. Spectral distribution solar radiation at the top of the atmosphere (a) and at sea level (b) for clear sky conditions. The shaded region represents the energy absorbed by atmospheric gases and the area between the shaded region and curve (a) represents the energy reflected by the atmosphere. The dashed curve (c) is the energy curve for a black body at 5800 K.

The OGI model uses the method developed by Lacis and Hansen (1974) for the calculation solar absorption due to water vapor and ozone. The absorption of solar radiation by CO₂ and O₂ is treated according to the parameterization of Sasamori et al (1972). Below we outline the specific details for each of the four gases.

4.1 Water Vapor

Following Lacis and Hansen (1974) we calculate the absorption of solar radiation due to water vapor for both clear sky and a cloudy sky. The model atmosphere contains a single cloud layer located in the model layer designated by the integer k and this cloud, covers a horizontal fraction A_c of that layer. The net fraction of incident solar radiation absorbed by water vapor in layer j is then calculated to be,

$$A_{H_2O}(j) = \{ (1 - A_c) A_{1H}(j) + A_c A_{2H}(j) \} \quad 4.1.1$$

where $A_{1H}(j)$ is the fraction of incident solar radiation absorbed by layer j under clear sky conditions, and $A_{2H}(j)$ is the counterpart of $A_{1H}(j)$ for cloudy skies. The total rate of energy absorption (w/m^2) by layer j is,

$$0.5 S_0 \mu_0 A_{H_2O}(j) \quad 4.1.2$$

where S_0 is the average solar constant (multiplied by .5 since there is an average of 12 hours in a day), and μ_0 is the cosine of the average zenith angle taken to be 60° . Although equations 4.1.1 and 4.1.2 are for water vapor, analogous equations are used for the calculation of total absorption due to ozone. That is, the clear sky absorption and cloudy sky absorptions are calculated separately and then combined using equations 4.1.1 and 4.1.2 with the appropriate absorptivities for ozone.

H₂O Clear Skies

Lacis and Hansen (1974) give,

$$A_{wv}(y) = \frac{2.9y}{(1 + 141.5y)^{.635} + 5.925y} \quad 4.1.3$$

for the fraction of incident solar radiation absorbed by a path length y (g/cm^2) of water vapor. For atmospheric calculations, y is taken to be the effective water vapor amount corrected for temperature T (K) and pressure P (atmospheres). For the direct solar beam,

$$y = \frac{M}{g} \int_0^P q \left(\frac{P}{P_0} \right)^n \left(\frac{T_0}{T} \right)^{1/2} dP \quad 4.1.4$$

where g is the acceleration of gravity, q is the specific humidity, $P_o = 1$ atm, and $T_o = 273$ K. The term M in equation 4.1.4 is the magnification factor accounting for slant path and refraction and is given by,

$$M = \frac{35}{\sqrt{(1224\mu_o^2 + 1)}} \quad 4.1.5$$

The effective water vapor path length for solar radiation reflected from the ground is obtained by,

$$y^* = \frac{M}{g} \int_0^{P_g} q\left(\frac{P}{P_o}\right) \left(\frac{T_o}{T}\right)^{1/2} dP \quad 4.1.6$$

$$+ \frac{5}{3g} \int_P^{P_g} q\left(\frac{P}{P_o}\right) \left(\frac{T_o}{T}\right)^{1/2} dP$$

where P_g is the pressure at the ground and $5/3$ is the magnification factor for the diffuse nature of the solar radiation reflected by the ground. The exponent n in both equations 4.1.4 and 4.1.6 is taken to be equal to unity.

The OGI model contains 18 layers (see Chapter 5). The pressure at the top of layer 1 is designated by $P_1 = 0.0$ and $P_{19} = 1$ atm is the pressure at the bottom of

layer 18. We can thus write the absorption of solar radiation by layer j as,

$$A_j = \mu_o \frac{s_o}{2} (A_{wv}(y_{j+1}) - A_{wv}(y_j) + R_g [A_{wv}(y_j^*) - A_{wv}(y_{j+1}^*)]) \quad 4.1.7$$

where R_g is the ground albedo. It should be noted that the above calculation assumes that Rayleigh scattering is negligible at the wavelengths associated with significant water vapor absorption for clear sky conditions.

The above clear sky calculations for water vapor solar absorption are performed by subroutine "h2Ovisclr" of Appendix E.

4.2 H₂O Cloudy Skies

Lacis and Hansen (1974) used a k distribution method (see Goody (1989) for further discussion) to calculate the absorptivity (fraction of incident solar radiation absorbed by path length y) of water vapor under cloudy conditions as

$$A_{wv}(y) = 1 - \sum_{n=1}^N p(k_n) e^{-k_n y} \quad 4.2.1$$

Equation 4.2.1 above is equivalent to assuming that water vapor is comprised of N absorbers with each having a mass absorption coefficient k_n and each having a

Table 4.1. Values of k_n and $p(k_n)$ given by Lacis and Hansen (1974) used in the calculation of water vapor absorptivity via the k distribution method described in the text.

n	k_n	$p(k_n)$
1	4×10^{-5}	0.6470
2	0.002	0.0698
3	0.035	0.1443
4	0.377	0.0584
5	1.95	0.0335
6	9.40	0.0225
7	44.6	0.0158
8	190.	0.0087

probability of absorbing equal to $p(k_n)$. The term $p(k_n)$ can also be thought of as the fraction of solar radiation absorbed by the n^{th} absorber. Lacis and Hansen (1974) perform a least squares fit of equation 4.1.9 to equation 4.1.3 to solve for $p(k_n)$ and k_n . These values are listed in Table 4.1.1. Notice that $p(k_1) = 0.6470$ for $k_1 = 4 \times 10^{-5}$. This implies that nearly 65% of the incident

solar radiation under goes very little absorption by water vapor.

To calculate the absorption in a cloudy atmosphere each layer j is assigned a total optical thickness and a single scattering albedo $w_{j,n}$ according to $\tau_{j,n}$

$$\begin{aligned}\tau_{j,n} &= \tau_j^c + k_n u_j \\ w_{j,n} &= \tau_j^c / \tau_{j,n}\end{aligned}\quad 4.2.2$$

where τ_j^c is the optical depth due to cloud particles in the j th layer and u_j is the effective water vapor amount in a vertical path through the j th layer.

The total reflection and transmission functions (due to direct and diffuse radiation) for each layer containing cloud are taken from Sagan and Pollack (1967) to be,

$$\begin{aligned}R_j &= \frac{(u+1)(u-1)(e^t - e^{-t})}{(u+1)^2 e^t - (u-1)^2 e^{-t}} \\ T_j &= \frac{4u}{(u+1)^2 e^t - (u-1)^2 e^{-t}}\end{aligned}\quad 4.2.3$$

$$u = \sqrt{\frac{1 - gw_{j,n}}{1 - w_{j,n}}}$$

$$t = \tau_{j,n} \sqrt{3(1 - w_{j,n})(1 - gw_{j,n})}$$

The asymmetry factor g , which is associated with the

relative amount of radiation scattered in the forward direction to that in the backward direction, is taken to be 0.85. [Note that $g=-1, 0, +1$ correspond to complete backward scattering, isotropic scattering, and complete forward scattering respectively]. We assume that each layer is homogeneous so that the reflection (transmission) for radiation incident from below R_j^* (T_j^*) equals the reflection (transmission) for radiation incident from above R_j (T_j).

The reflection and transmission functions for a "clear layer" are given by,

$$\begin{aligned} R_j &= R_j^* = 0 \\ T_j &= T_j^* = \exp\left(-\frac{5}{3}\tau_{j,n}\right) \end{aligned} \quad 4.2.4$$

except for a layer above the highest cloud which has a downward transmission function given by

$$T_j = \exp(-M\tau_{j,n}) \quad 4.2.5$$

where M is defined by 4.1.5 and $5/3$ is the magnification factor for diffuse radiation.

Figure 4.2 below shows two layers a and b with radiation S incident from above. The net effective transmission or reflectance for the composite layer are defined to be T_{ab} and R_{ab} respectively. From Figure 4.2

it is easy to see that,

$$R_{ab} = R_a + T_a R_b T_a^* / (1 - R_a^* R_b) \quad 4.2.6$$

and

$$T_{ab} = T_a T_b / (1 - R_a^* R_b)$$

Where we have used the fact that $\sum x^n = \frac{1}{(1-x)}$.

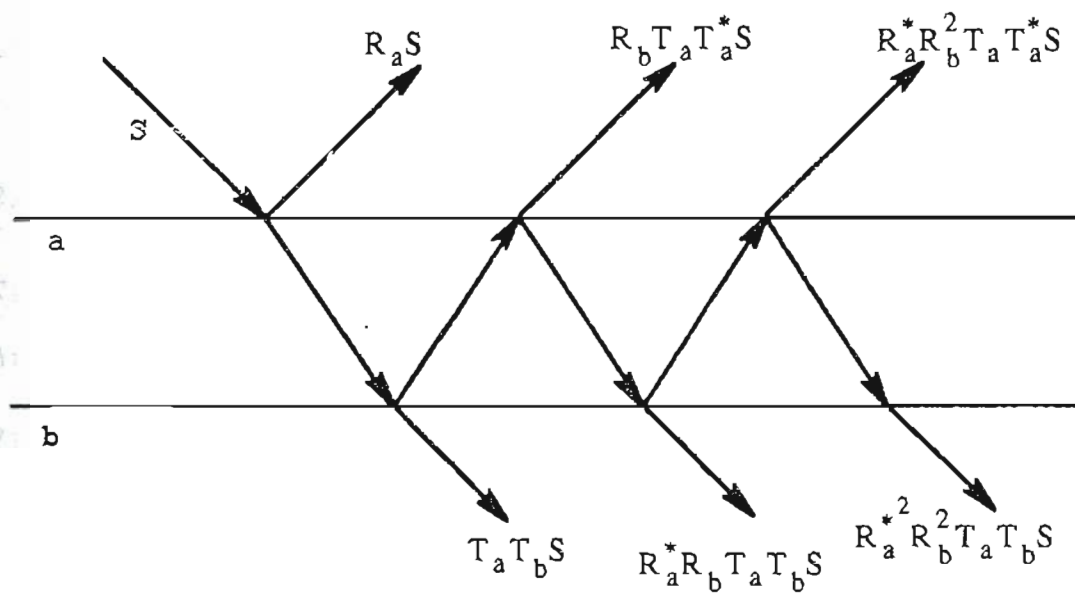


Figure 4.2. Schematic of the combined reflection and transmission of two atmospheric layers a and b.

Similarly,

$$R_{ab}^* = R_a^* + T_b^* R_b T_b^* / (1 - R_a^* R_b) \quad 4.2.7$$

and

$$T_{ab}^* = T_b^* T_a^* / (1 - R_a^* R_b)$$

Equipped with the above definitions, we follow the algorithm outlined by Lacis and Hansen (1974) for the cloudy sky absorption of solar radiation due to water vapor for each layer T.

For completeness we list below the steps given by Lacis and Hansen (1974).

- 1) R_j and T_j , $j=1, 18$ are computed for each layer using equations 4.2.3, 4.2.4, and 4.2.5.
- 2) The layers are added, going down, to obtain $R_{1,j}$ and $T_{1,j}$ for $j=2, 19$ and $R_{1,j}^*$ and $T_{1,j}$ for $j = 2, 18$.
- 3) Layers are added one at a time, going up, to obtain $R_{19-j,19}$, $j=1, 17$ starting with the ground layer $R_{19} = R_g$ and $T_{19}=0$.
- 4) As two composite layers, say layers l, j and $j+1, 19$ are added, the upward and downward fluxes at the boundary between the two layers are determined:

$$\begin{aligned} U_j &= T_{1,j} R_{j+1,19} / (1 - R_{1,j}^* R_{j+1,19}) \\ D_j &= T_{1,j} / (1 - R_{1,j}^* R_{j+1,19}) \end{aligned} \quad 4.2.8$$

The fraction of the total incident flux absorbed in the upper composite layer is

$$A_{1,j}(n) = p(k_n)[1 - R_{1,19}(n) + U_j(n) - D_j(n)] \quad 4.2.9$$

5) The absorption in each layer j due to the n^{th} absorber is then calculated by

$$A_j(n) = A_{1,j}(n) - A_{1,j-1}(n) \quad 4.2.10$$

6) Finally the total absorption for layer j is given by

$$A_j = \frac{S_0}{2} \mu_0 \sum_{n=2}^8 A_j(n) \quad 4.2.11$$

where S_0 and μ_0 are the solar constant and cosine of zenith angle respectively. The above calculations are performed in subroutine "h2ocloud" of Appendix Z.

4.3 Ozone

Absorption of solar radiation by ozone is the major source of heating in the stratosphere and hence is of primary importance. Ozone absorbs in two regions of the solar spectrum:

- 1) the strong absorption in the ultraviolet region-Hartley and Huggins bands and 2) the weak absorption in the visual region-Chappius band. Lacis and Hansen (1974) give the equation

$$A_{oz}^{vis}(x) = \frac{0.02118x}{1 + 0.042x + 0.000323x^2} \quad 4.3.1$$

for the fraction of incident solar energy absorbed by the Chappius band and state that this formula is very accurate for ozone amounts x between 10^{-4} cm and 10 cm (STP). They also give, for the ultraviolet absorption,

$$A_{oz}^{uv}(x) = \frac{1.082x}{(1 + 138.6x)^{0.805}} + \frac{0.0658x}{1 + (103.6x)^3} \quad 4.3.2$$

For atmospheric calculations, the ozone amount traversed by the direct solar beam in reaching the top of layer j is $x_j = U_j M$, where U_j is the total column of ozone above the top of layer j and M is the slant path magnification factor defined by equation 4.1.5. The effective path traversed by diffuse radiation from below reaching the top of layer j is given by,

$$x_j^* = U_t M + \bar{M}(U_t - U_j) \quad 4.3.3$$

where U_t is the total ozone column (cm-STP) above the main reflecting layer (the ground for clear skies or the cloud top for cloudy skies) and \bar{M} is the effective magnification factor for diffuse radiation which is taken to be 1.9 from empirical considerations given by Lacis and Hansen (1974).

Rayleigh scattering is modeled by assuming that scattering is negligible in the stratosphere and that the lower atmosphere has a reflectivity R_a' for the direct beam and R_a^{**} for the diffuse radiation reflected from the ground. Following an argument similar to that used to obtain equation 4.2.6 the effective albedo of the reflection region $R'(\mu_0)$ is given by

$$R'(\mu_0) = R_a'(\mu_0) + [1 - R_a'(\mu_0)](1 - R_a^{**})R_g / (1 - R_a^{**}R_g) \quad 4.3.4$$

Lacis and Hansen give the empirical estimates of R_a' and

$$R_a^{**} \quad R_a' = \frac{0.219}{1 + 0.816\mu_0} \quad \text{[clear skies]} \quad 4.3.5$$

$$R_a^{**} = 0.144$$

and

$$R_a' = R_a^{**} = \frac{\sqrt{3}(1-g)\tau^c}{2 + \sqrt{3}(1-g)\tau^c} \quad 4.3.6$$

[cloudy skies]

$$\approx \frac{0.13\tau^c}{1 + 0.13\tau^c}$$

for the asymmetry factor $g = 0.85$. In equation 4.3.6 τ^c is the optical depth of the cloud.

The total absorption of solar radiation due to ozone by layer j can now be calculated using equations 4.3.1 - 4.3.5 (or 4.3.6 for cloudy skies) and is

$$A_{j,oz} = \frac{s_o}{2} \mu_o \{A_{oz}(x_{j+1}) - A_{oz}(x_j) + R'(\mu_o) [A_{oz}(x_j^*) A_{oz}(x_{j+1}^*)]\} \quad 4.3.7$$

where

$$A_{oz}(x) = A_{oz}^{uv}(x) + A_{oz}^{vis}(x) \quad 4.3.8$$

The above calculations for clear skies are performed in subroutine "o3visclr" and those for cloudy skies in subroutine "o3cloud" of Appendix Z.

4.4 CO₂ and O₂

Carbon dioxide and oxygen are minor absorbers of solar radiation both together contributing about 9% to the total atmospheric absorption of solar radiation (Sasamori et al 1972). The parameterizations given by Sasamori et al (1972) for the fraction of incident solar radiation absorbed by carbon dioxide and molecular oxygen are used in the OGI model. These are based on an empirical fit and are:

for CO₂;

$$A_{co_2} = 2.35 \times 10^{-3} (u + 0.129)^{.26} - 7.5 \times 10^{-4} \quad 4.4.1$$

for O₂;

$$A_{O_2} = 7.5 \times 10^{-3} (M^*)^{.875} \quad 4.4.2$$

where u is the pressure corrected path length of CO_2 in cm-atm,

$$u = \int \frac{p}{p_0} du \quad 4.4.3$$

$$M^* = \frac{1}{\mu_0} \left(\frac{p}{p_0} \right) \quad 4.4.4$$

is the pressure corrected air mass, and μ_0 is the cosine of the zenith angle. The net energy absorbed in layer j is calculated as,

$$A_{CO_2, j} = A_{CO_2}(u_{j+1}) - A_{CO_2}(u_j) \quad 4.4.5$$

and

$$A_{O_2, j} = A_{O_2}(M_{j+1}^*) - A_{O_2}(M_j^*) \quad 4.4.6$$

for carbon dioxide and oxygen respectively. Here $U_{j+1}(M^*_{j+1})$ correspond to the net amount of CO_2 (or O_2) above the bottom of layer j , and $U_j(M^*_j)$ is the net amount above the top of layer j .

No effort has been made to distinguish between clear skies and cloudy skies for oxygen in this section since water vapor absorption occurs in a different part of the spectrum than oxygen absorption. Below the model

cloud the absorption by carbon dioxide as calculated by equation 4.4.5 is multiplied by $(1-A_c)$ where A_c is the cloud fraction. We do this since the absorption of solar radiation by carbon dioxide occurs in the same spectral region as that due to water vapor.

4.5 Surface Absorption

We use the method described by Lacis and Hansen (1974), with one modification, to calculate the absorption of solar radiation at the earth's surface. Since Lacis and Hansen only considered water vapor and ozone in their calculations, their net absorption of solar radiation will be slightly higher than it should be if molecular oxygen and carbon dioxide are also considered. Thus, we calculate the surface absorption for the part of the solar spectrum associated with water vapor absorption (35% from Table 4.1) and then the surface absorption due to the solar spectrum associated with ozone absorption (65%) following Lacis and Hansen (1974). The total surface absorption as calculated above is then reduced by an amount equal to the total atmospheric absorption due to carbon dioxide and oxygen, calculated according to the methods outlined in Section

4.4, times surface absorptance $(1-R_g)$. Below we outline the surface absorption parameterizations given by Lacis and Hansen (1974) for the water vapor and ozone regions of the solar spectrum.

Clear skies. For the spectral regions associated with significant water vapor absorption (35.3%) Rayleigh scattering is neglected and the fraction of the total flux of solar energy absorbed by the surface is taken to be

$$A_{g,wv} = \mu_o [0.353 - A_{wv}(y_t)](1 - R_g) \quad 4.5.1$$

where y_t is the effective water vapor amount in a vertical column above the surface and is calculated according to equation 4.1.4.

For the rest of the solar spectrum (64.7%) Rayleigh scattering is included as well as atmospheric absorption due to the ozone above the surface. The fraction of the total solar energy absorbed by the "ozone" region of the solar spectrum is given by,

$$A_{g,oz} = \mu_o [0.647 - R_r(\mu_o) - A_{oz}(u_t)](1 - R_g)/(1 - R_r^*R_g) \quad 4.5.2$$

where u_t is the ozone amount in a vertical path above the surface and $R_r(\mu_o)$ is the atmospheric albedo due to

Rayleigh scattering, $R_r^*(\mu_0)$ is the spherical albedo due to Rayleigh scattering of radiation reflected from the surface, and R_g is the surface albedo. Lacis and Hansen give the empirical values for R_r and R_r^* to be,

$$R_r(\mu_0) = \frac{0.28}{1 + 6.43\mu_0} \quad 4.5.3$$

$$R_r^* = 0.0685$$

Cloudy skies. For cloudy skies $A_{g,wv}$ is obtained by multiplying the total transmission to the ground $T_{1,19}$ for each value of k_n by the factor $p(k_n)(1-R_g)$ and summing from $n=2$ to $n=8$.

For cloudy skies, Rayleigh scattering is neglected below the cloud and hence $A_{g,oz}$ is calculated as,

$$A_{g,oz} = \mu_0 [0.647 - A_{oz}(\mu_0)] \times [1 - R_a'(\mu_0)](1 - R_g)/(1 - R_a''R_g) \quad 4.5.4$$

where u_t , and $R_a'(\mu_0)$ and $R_a''(\mu_0)$ are the ozone amount and atmospheric reflectivities given by equations 4.3.6.

Chapter 5

The OGI 1D Time Dependent RCM

5.1 Overview of Model Structure

The OGI model contains 18 atmospheric layers, extending from the surface to an altitude of approximately 40 km, and is shown schematically in Figure 5.1 below. We have used the constant σ coordinate system employed by Manabe and Strickler (1964) to designate the average pressure p_a of each layer and the pressure thickness dp of each layer.

$$p_{a_i} = \sigma_i^2 (3 - 2\sigma_i) \quad 5.1$$

$$dp_i = 6(\sigma_i - \sigma_i^2) d\sigma$$

$$d\sigma = \frac{1}{18}, \sigma_0 = 0, \sigma_1 = \frac{1}{36}, \sigma_2 = \frac{3}{36}, \dots, \sigma_{18} = \frac{35}{36}$$

The average pressure of each layer (p_{a_i}) and the pressure at the top (p_i) and bottom (p_{i+1}) of each layer are calculated once at the beginning of the main program by subroutine "presset" of Appendix E. The pressures at the bottom and top of each layer are calculated by

starting at $p_1=0$ (the top of the top layer is assumed to be at zero pressure) and adding the pressure thicknesses of each layer going down.

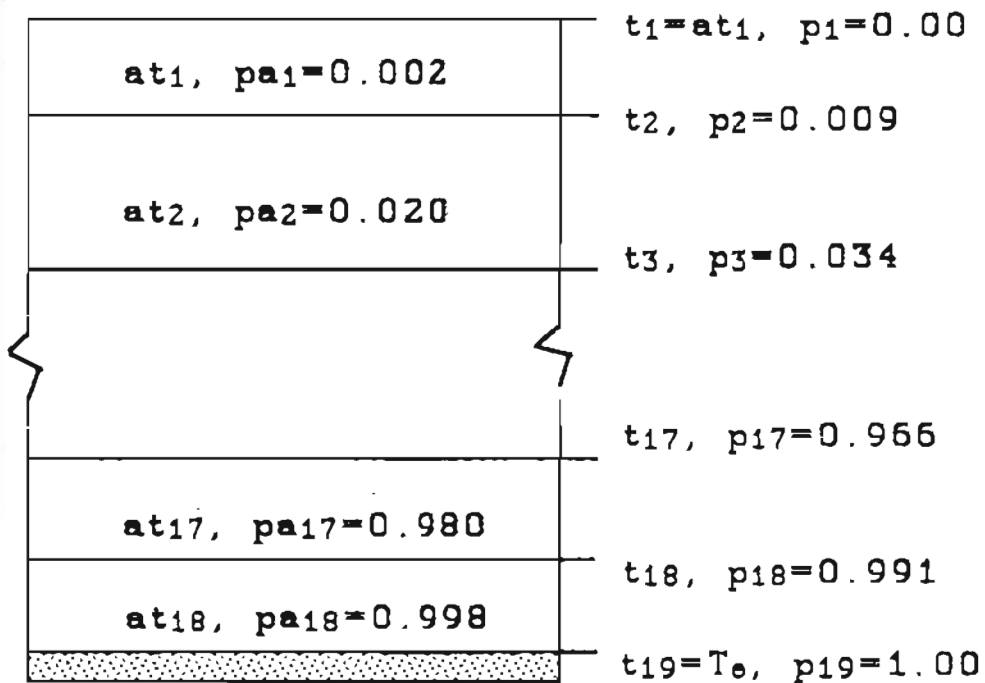


Figure 5.1. Schematic representation of the 18 layer OGI model of the earth-atmosphere system. The average pressure and temperature of each layer are labeled p_{ai} and at_i respectively. The pressure and temperature at the top (bottom) of each layer are labeled $p_i(p_{i+1})$ and $t_i(t_{i+1})$. The pressures (in atmospheres) of each layer are assigned as described in the text.

Thus, $p_2=p_1+dp_1$, $p_3=p_2+dp_2$, etc. The layers generated by using equation 5.1 have small pressure thicknesses at

the top of the atmosphere $\sigma=0$, where small pressure differences are needed to maintain adequate spatial resolution; and small pressure differences at the surface $\sigma=1$, where enhanced spatial resolution may be required when modeling the boundary layer.

The change in average temperature a_{i} of each layer is calculated using a numerical time stepping procedure. The IR heating rate in (K/day) is calculated by,

$$(\Delta a_{i}/\Delta t)_{IR}=(g/C_{pi}) (\Delta F_{i}/dP_{i}) \quad 5.1.2$$

where Δt is a time interval, and $F=(F^{+})-(F^{-})$ is the net upward flux of IR radiation (see Appendix A). The heating rate due to absorbed solar energy in layer i is calculated as,

$$(\Delta a_{i}/\Delta t)_{s}=(g/C_{pi}) (A_{i}/dP_{i}) \quad 5.1.3$$

where A_{i} is the net flux of solar energy (W/m²) absorbed by layer i and is calculated as explained in Chapter 4. In both equations 5.1.2 and 5.1.3, g is the acceleration due to gravity (9.81 m/s²) and C_{pi} is the effective specific heat capacity of each layer discussed below. The change in temperature, due to radiative heating, of layer i in a time equal to Δt_{0} is thus given by,

$$\Delta a_{tri} = [(\Delta a_{ti}/\Delta t)_s + (\Delta a_{ti}/\Delta t)_{IR}] \Delta t_o \quad 5.1.4$$

The change in surface temperature of the earth is calculated by taking the Earth's surface to be a thoroughly mixed layer of water of uniform depth h . The change in surface temperature Δa_{t19} is then calculated according to,

$$C_w \rho h (\Delta a_{t_{19}}) = [F_{19}^- + A_g - \sigma (a_{t_{19}})^4] \times \Delta t_o \quad 5.1.5$$

where C_w is the specific heat of water 4.186 J/(g K) , ρ is the density of water (1000 kg/m^3), Δt_o is the time step involved in the numerical time marching scheme, F_{19}^- is the downward flux of IR radiation calculated as outlined in Appendix A, and A_g is the absorbed flux of solar radiation at the surface calculated as described in Section 4.5. In the above description of the mixed layer the ocean dynamics have been greatly simplified. The inclusion of a non-zero heat capacity for the Earth's surface is our first attempt to estimate the time it takes the earth-atmosphere system to approach equilibrium after some atmospheric perturbation.

After the radiative temperature changes have been made, a convective adjustment is performed which may or may not change the temperature of a layer (and surface)

by and amount equal to Δatc_i . The details of the convective adjustment are outlined below in section 5.3.

The above time stepping procedure is repeated until equilibrium is reached. The equilibrium condition is met when:

$$\sum_{i=1}^{19} |\Delta atc_i + \Delta atr_i| < \text{low} \quad 5.1.6$$

where low is some preassigned small number usually taken to be 0.001 K and Δatr_i is the temperature change due to radiation as calculated by equation 5.1.4. When equilibrium is reached the net solar energy absorbed by the earth-atmosphere system is equal to the IR radiation given off by the earth atmosphere system back into space to within 0.01%.

The temperatures at the top and bottom of each layer are calculated by subroutine "tempset" (Appendix E) as pressure averaged temperatures. For example t_2 , the temperature at the bottom of layer 1 and the top of layer 2 is calculated according to,

$$t_2 = \frac{at_1[p_2 - pa_1] + at_2[pa_2 - p_2]}{pa_2 - pa_1} \quad 5.1.7$$

The temperatures (or pressures) at the bottom and top of each layer are used in estimating the derivatives of

functions with respect to temperature (or pressure) at the center of each layer. For example, the derivative of some function $F(T)$ with respect to temperature at the center of layer 2 is estimated by,

$$\frac{dF}{dT} \approx \frac{F(t_3) - F(t_2)}{t_3 - t_2} \quad 5.1.8$$

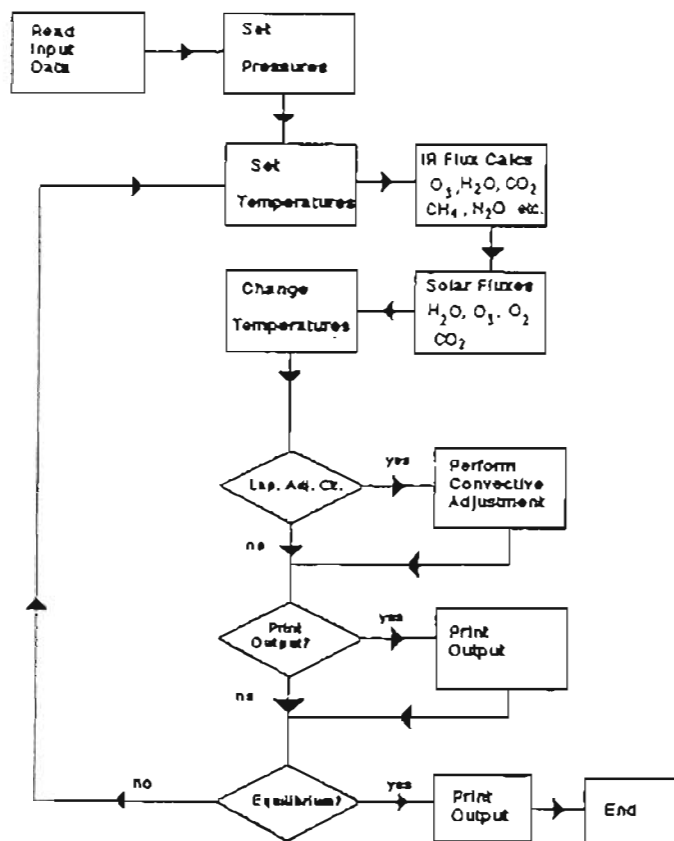


Figure 5.2. General flow diagram of the OGI model. As can be seen from the figure, the program is relatively simple in structure.

Figure 5.2 above gives a flow diagram for the calculations performed during a program run.

5.2 Atmospheric Gases (vertical profiles)

H₂O

Following Manabe and Wetherald (1967) we use,

$$C_p^* = C_p \left[1 + \frac{L}{C_p} \frac{\partial q}{\partial T} \right] \quad 5.2.1$$

for the effective specific heat of each layer. The first term in the brackets is just the specific heat of dry air while the second term is related to the change in latent heat energy with changing temperature. In equation 5.2.1, L is the latent heat of vaporization calculated as in Section 3.1 ($L=2510-2.38[T-273]$), C_p is the specific heat of dry air taken to be 1.005 J/(g K) , and $\partial q/\partial T$ is the partial derivative of absolute humidity q with respect to temperature.

The vertical profile of relative humidity h used in the OGI model is the same as that used by Manabe and Wetherald (1967) and is given by,

$$h = h^*(p_{ai} - .02 / .98) \quad 5.2.2$$

where h^* is the surface relative humidity taken to be 0.77. Equation 5.2.2 is used for each layer except the layer containing a cloud in which $h=1.0$. The specific humidity q is calculated by,

$$q = h^* e_{sat}(T) \quad q > 3 \times 10^{-6} \quad (\text{g H}_2\text{O} / \text{g air}) \quad 5.2.3$$

$$q = 3 \times 10^{-6} \quad \text{if } q = h^* e_{sat}(T) < 3 \times 10^{-6}$$

Thus the minimum value of q is taken as 3×10^{-6} (g H₂O/g air). The saturated vapor pressure $e_{sat}(T)$ is calculated using the Clausius Clapeyron equation given in Section 3.1. The value of $\partial q / \partial T$ is also calculated using the Clausius Clapeyron equation and is,

$$\partial q / \partial T = 0.622 h \partial(e_{sat}) / \partial T \quad 5.2.4$$

where,

$$\partial(e_{sat}) / \partial T = 0.622 L e_{sat} / (RT^2) \quad 5.2.5$$

and $R=0.287$ J/(g K) is the ideal gas law constant for air.

Other Gases

The vertical profile of CO₂ mixing ratio (ppmv)

is taken from Goody (1989) and is constant with altitude for all levels considered by the OGI model. The present day concentration is estimated from Hansen (1989) to be about 353 ppmv.

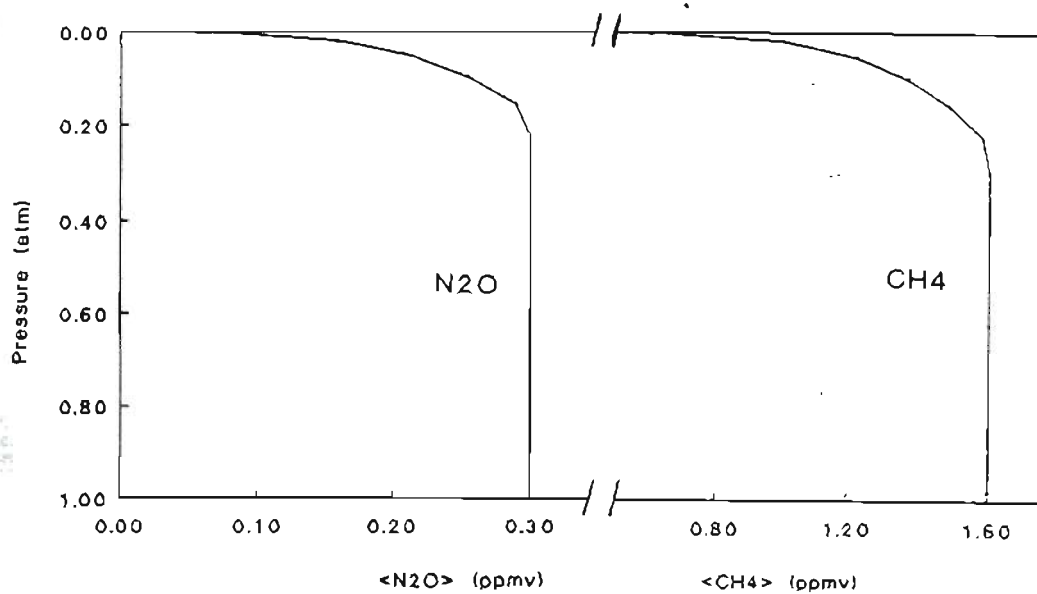


Figure 5.3. The vertical profiles of N₂O and CH₄ used in the OGI model. After Crutzen et al (1978).

The vertical profiles of N₂O and CH₄ are shown in Figure 5.3. These are analytical profiles that have been designed to fit the estimated values given by

Crutzen et al. (1978).

The vertical profile of ozone is shown in Figure 5.4. This profile is based on the 1962 standard atmosphere supplied in the AFGL LOWTRAN computer code by the National Climatic Center of NOAA, Digital Product Section, Federal Building, Asheville, NC 28801.

Ozone Profile (1962 Standard Atmosphere)

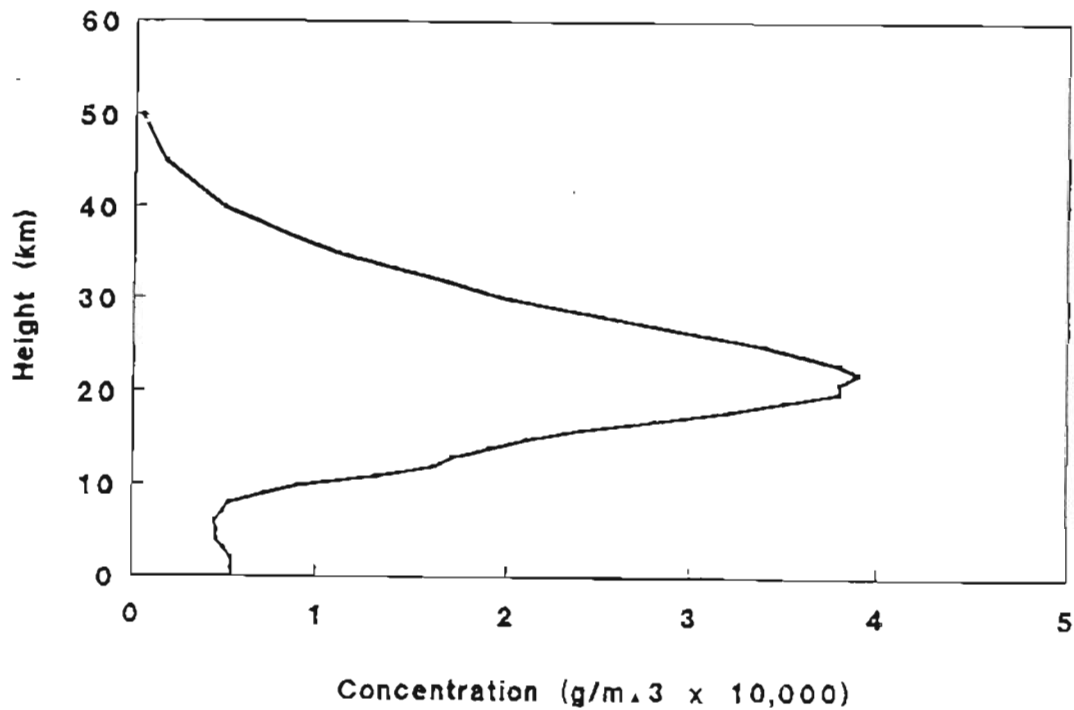


Figure 5.4. The vertical profile of ozone used in the OGI model (1962 standard atmosphere).

5.3 Convective Adjustment.

The OGI model uses a convective scheme that was first introduced by Manabe and Strickler (1964) in order to simulate the flux of latent and sensible heat from the Earth's surface. Manabe and Wetherald (1967) documented this scheme in more detail for their 1D RCM which assumed that the heat capacity of the Earth's surface was zero. Although the OGI model uses a non-zero heat capacity for the Earth's surface the essential features of the convective scheme are the same as that described by Manabe and Wetherald. The details of the convective scheme used in the OGI model are given below.

The temperature change Δt_i due to radiative heating (or cooling) for each layer and the surface is calculated during each time step as described in Section 5.1 above. After the new temperature is calculated, the lapse rate LAP_i between every two layers is checked starting at the surface moving upward. The lapse rate LAP_i between two layers is calculated according to,

$$LAP_i = - \frac{at_i - at_{i+1}}{za_i - za_{i+1}} \quad 5.3.1$$

where za_i is the vertical height to layer i . Notice

that the lapse rate is taken to be positive if the temperature decreases with increasing height. If the lapse rate between the surface and the lowest atmospheric layer (LAP_{18}) is greater than a preassigned critical lapse rate for layer 18 (LRC_{18}) then a convective adjustment is performed between the surface and layer 18.

The convective adjustment is accomplished by removing energy from the surface and increasing the temperature of layer 18. The increase in the temperature of layer 18 due to the convective adjustment is calculated using

$$C_{19}\Delta t_{19} = -(C_p^*_{18}) \Delta p_{18} \Delta t_{18} \quad 5.3.2$$

and

$$|\Delta t_{19}| + |\Delta t_{18}| = LAP_{18} - LRC \quad 5.3.3$$

where C_{19} is the heat capacity per unit area of the surface and $C_p^*_{18}$ is the effective specific heat capacity for layer 18 and is calculated according to equation 5.2.1. After this adjustment the lapse rate between layers 17 and 18 (LAP_{17}) is calculated and if $Lap_{17} > LRC_{17}$ a convective adjustment is performed between

layers 18 and 17. This adjustment removes energy from the lower layer (18) and puts it into the upper layer 17 according to,

$$(C_p^{*17}) \Delta p_{17} \Delta t_{17} = -(C_p^{*18}) \Delta p_{18} \Delta t_{18} \quad 5.3.4$$

and

$$|\Delta t_{18}| + |\Delta t_{17}| = L_{AP17-LRC} \quad 5.3.5$$

The adjustment between atmospheric layers is made so that the net content of energy in the atmosphere does not change during the convective adjustment between atmospheric layers.

After the above adjustment, the lapse rate between layers 17 and 16 is checked and if this exceeds the critical lapse rate assigned for this layer, equations similar to 5.3.4 and 5.3.5 are used to make the required convective adjustment. This process is continued going upwards for all atmospheric layers. The whole process is again repeated, from the ground up, until all calculated lapse rates are at or below the critical lapse rate for each level. At this time the energy account is balanced by removing an amount of energy from the surface equal to the net increase in energy of all atmospheric layers due to the adjustment process. That is,

$$\Delta at_{19} = \frac{\sum_{i=nt}^{18} C_{p_i} * (\Delta p_i / g) \Delta at c_i}{C_{19}} \quad 5.3.6$$

where C_{p_i} is the total specific heat capacity of each layer as calculated by equation 5.2.1. The integer nt in equation 5.3.6 is the upper most layer that experienced a temperature change due to a convective adjustment.

In the OGI model we take the tropopause to be at layer nt . For computational stability one half of the lapse rate adjustment is added to a semi-permanent account $ce(i)$ for each layer. That is the value of $ce(i)$ is replaced with its old value (initially 0.0 at the beginning of the simulation) plus $0.5 * \Delta at c_i$. The value of $ce(i)$ is used as an initial convective adjustment during each time step and the above procedure utilizing equations 5.3.1 through 5.3.6, is used as a fine tuning of the adjustment. This procedure of using the semipermanent convective adjustment $ce(i)$ results in a smoother less "steppy" convection and was found to give much more consistent results than using 5.3.1 through 5.3.6 alone. Because changes in atmospheric

composition can result in changes in required convective transport the value of $ce(i)$ is reduced by 0.1 percent each time step that layer i does not require a convective adjustment. In this way the semipermanent $ce(i)$ will not result in more convection than is needed.

Subroutine "lapadj" of Appendix E performs the convective adjustment. The critical lapse rate is set by subroutine "lap1" to be 6.5 K/km since this is standard in many 1D RCMs (see Ramanathan et al. 1987 or Vupputuri 1985) and hence makes for easy comparison between the OGI model and others. The critical lapse rate may also be set to the moist adiabatic lapse rate at each layer by using subroutine "lap2" of Appendix E.

Lindzen (1982) did a comparison of different lapse rate adjustment schemes for 1D RCMs and found that setting the critical lapse rate equal to the moist adiabatic lapse rate at each level gave a more realistic vertical temperature profile. Lindzen also noted that the constant 6.5 K/km critical lapse rate convective scheme yielded an earth-atmosphere system that was more sensitive to variations in greenhouse gas concentrations. We will explore some of these differences in the next chapter.

5.4 IR Flux for Cloudy Skies

In the OGI model we have followed the work of Schneider et al. (1978) and Cess (1974) and included a single cloud layer in an attempt to model the average cloudiness of the atmosphere. The cloud fully occupies one model layer (denoted by the integer k) in the vertical direction and covers a fraction A_c of the layer in the horizontal direction. The cloud is assumed to be a perfect blackbody for infrared radiation as suggested by Stephens (1984). The treatment of the cloud for solar radiation was completely described in Chapter 4 and hence will not be discussed here.

The calculation of the net upward flux of IR radiation F^+ in the cloudy atmosphere is performed by following a method outlined by Stephens (1984) which we briefly describe here. We write the net upward flux of IR radiation F^+ as,

$$F^+ = A_c F^+_{\text{cloud}} + (1 - A_c) F^+_{\text{clear}} \quad 5.4.1$$

where F^+_{clear} is the clear sky flux calculated according to the method described in Appendix A, and F^+_{cloud} is

calculated according to,

$$F_{\text{cloud}}^+ = F_{\text{clear}}^+ \quad (Z \leq Z_{\text{kap}+1}) \quad 5.4.2$$

and

$$F_{\text{cloud}}^+ = \sigma T(\text{kap})^4 + \int_{z_{\text{kap}}}^z \epsilon'_{\text{H}_2\text{O}} d[\sigma T^4(z')] \quad 5.4.3$$

$$+ \sum_{i=1}^N \int_{z_{\text{kap}}}^z A_{\text{vi}} \Delta v_i d[\pi B_{\text{vi}}(z')] \quad (Z \geq Z_{\text{kap}})$$

where $T(\text{kap})$ is the temperature of the cloud top $\epsilon'_{\text{H}_2\text{O}}$ is the modified emissivity of water vapor, $A_{\text{vi}} \Delta v_i$ is the band absorptance of the i th atmospheric species (CO_2 , CH_4 , N_2O , O_3 , ...), B_{vi} is the value of the Planck function at the center of the spectral band for the i th species, and Z_{kap} and $Z_{\text{kap}+1}$ correspond to the top and bottom of the cloud layer. Notice that the upward flux is the same below the cloud bottom for both clear and cloudy skies.

Similarly the net downward flux of IR radiation is calculated as,

$$F^- = A_c F_{\text{cloud}}^- + (1 - A_c) F_{\text{clear}}^- \quad 5.4.4$$

$$F_{\text{cloud}}^- = F_{\text{clear}}^- \quad (Z \geq Z_{\text{kap}}) \quad 5.4.5$$

and

$$F_{\text{cloud}}^- = \sigma T(\text{kap} + 1)^4 + \int_{z_{\text{kap} + 1}}^z \epsilon'_{\text{H}_2\text{O}} d[\sigma T^4(z')] \quad 5.4.6$$

$$+ \sum_{i=1}^N \int_{z_{\text{kap} + 1}}^z A_{\nu_i} \Delta \nu_i d[\pi B_{\nu_i}(z')] \quad (Z \leq Z_{\text{kap} + 1})$$

The above calculations are performed by the subroutines "water" for the water portion of the calculations and "acool" for all other gases. Here again notice that the downward flux for clear skies is the same as that for cloudy skies above the cloud top.

Chapter 6

The OGI 1DRCM Performance and Sensitivity

In this chapter we will explore the mechanics of the OGI 1D RCM. In particular, in the first section the vertical equilibrium temperature profiles predicted by the model, using different convective schemes, are presented. Also in Section 6.1 the time development of the approach to equilibrium, for various ocean mixed layer depths, is analyzed. In Section 6.2 the sensitivity of the model's stability to choice of time step is explored. We end this chapter with Section 6.3, which investigates the sensitivity of the equilibrium surface temperature predicted by the model to changes in initial conditions. A comparison of the model's sensitivity, to variations in trace gas concentrations, with those predicted by other equivalent models is made in the next chapter.

6.1 Equilibrium Temperature Profile

The vertical equilibrium temperature profiles

predicted by the OGI 1D RCM for various assumed convective schemes are shown in Figure 6.1.

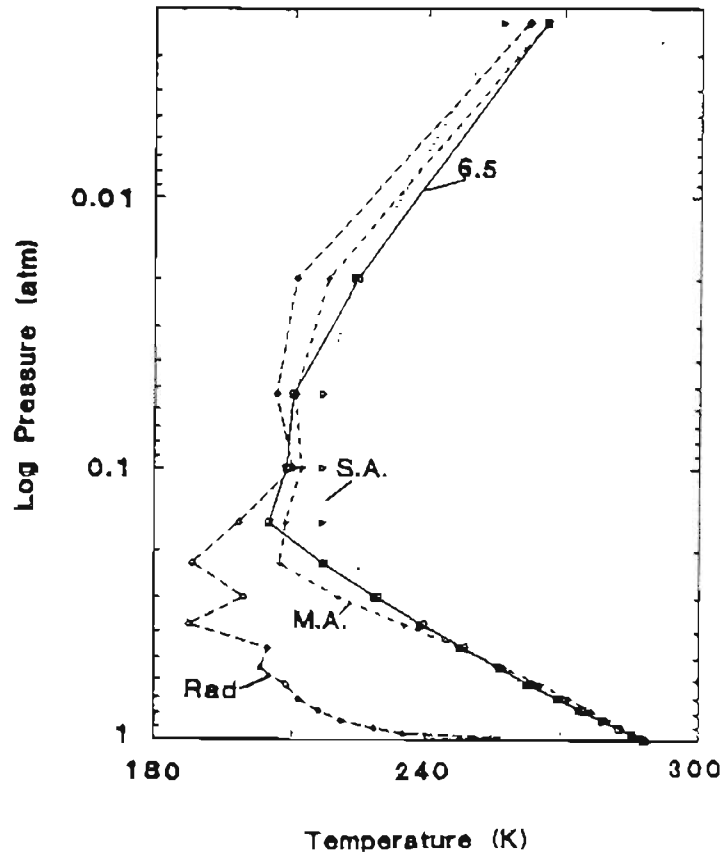


Figure 6.1. A comparison of vertical temperature profiles obtained from: using 6.5 K/km as the critical lapse rate for the convective adjustment (6.5); using the moist adiabatic lapse rate (M.A.); no convective adjustment (Rad); the 1976 standard atmosphere (S.A.).

Figure 6.1 shows the vertical profiles, at all 18 model layers, for: the 1976 standard atmosphere; pure radiative equilibrium (no convection); the moist adiabatic lapse rate convective adjustment; and the 6.5

K/km convective adjustment schemes.

The pure radiative (Rad) equilibrium profile fails to agree with the standard atmospheric (S.A.) profile in two important ways. First in the troposphere, where convection is predominate, the predicted lapse rate of the Rad profile is much larger than the S.A. profile. This is especially obvious from a careful inspection of Figure 6.1. Secondly the location of the tropopause predicted by the Rad profile is at a pressure of 0.55 atm (approx. 4.2 km) and that of the S.A. profile is at 0.22 atm (approx. 10.5 km). Both of these discrepancies are attributable to the rapid decrease in temperature of the near surface layers due to the lack of convective energy transport from the surface. The Rad profile is obviously an unrealistic equilibrium profile in that the lapse rate predicted is highly unstable. It should be noted the Rad profile does generally agree with the S.A. profile at higher altitudes where convective transport in the real atmosphere is minimal.

Both the moist adiabatic (M.A.) and 6.5 K/km (6.5) lapse rate adjustment schemes result in predicted vertical profiles that are in good agreement with the S.A. profile. The excellent agreement between the 6.5 profile and the S.A. profile in the troposphere should

not be construed as meaning that the 6.5 lapse rate scheme is the best representation of reality. In fact the only reason the agreement between the two is so good is because both the S.A. and the 6.5 profiles were designed to give a lapse rate of 6.5 K/km in the troposphere. Stone and Carlson (1979) note that the 6.5 K/km vertical lapse rate is not representative of the global average lapse rate and that the annual tropospheric average lapse rate is closer to 5.2 K/km. Lal and Ramanathan (1984) note that a better representation of the mean annual lapse rate, especially in the tropics, can be obtained by using the moist adiabatic lapse rate as the critical lapse rate for the convective adjustment. As can be seen from Figure 6.1 the M.A. lapse rate is less than 6.5 K/km in the lower troposphere and greater than 6.5 K/km in the upper troposphere. In addition the tropopause height of the M.A. profile is one layer lower than the 6.5 profile. Table 6.1 summarizes the sensitivity of the model to a doubling of CO₂ for the various lapse rate schemes.

As can be seen the moist adiabatic lapse rate scheme predicts a lower sensitivity to doubled CO₂ than all of the other convective schemes which generally

Table 6.1. Comparison of model sensitivity for doubled CO₂ using different convective schemes.

Lapse Rate scheme	ΔT 2xCO ₂ (K)	T _e
None (Radiative Eq.)	3.10	326.7
6.5 K/km	1.97	289.5
5.1 K/Km	1.89	285.1
Moist Adiabatic	1.37	288.3
6.5 K/km	2.02	292.5

agree. This is similar to the results reported by Lindzen et al (1982) where they obtain a 25 percent reduction in surface temperature change due to doubled CO₂ using the M.A. scheme as opposed to the 6.5 scheme.

6.2 Time Constants

Figure 6.2 shows the time development of the surface temperature T_s after the model was started from an isothermal earth atmosphere of 280 K using different ocean depths. Two features of importance appear in Figure 6.2. First, it can be seen that the final equilibrium surface temperature does not depend on the heat capacity of the surface. This result is the same

as would be expected for pure radiative equilibrium, and can be explained intuitively as follows.

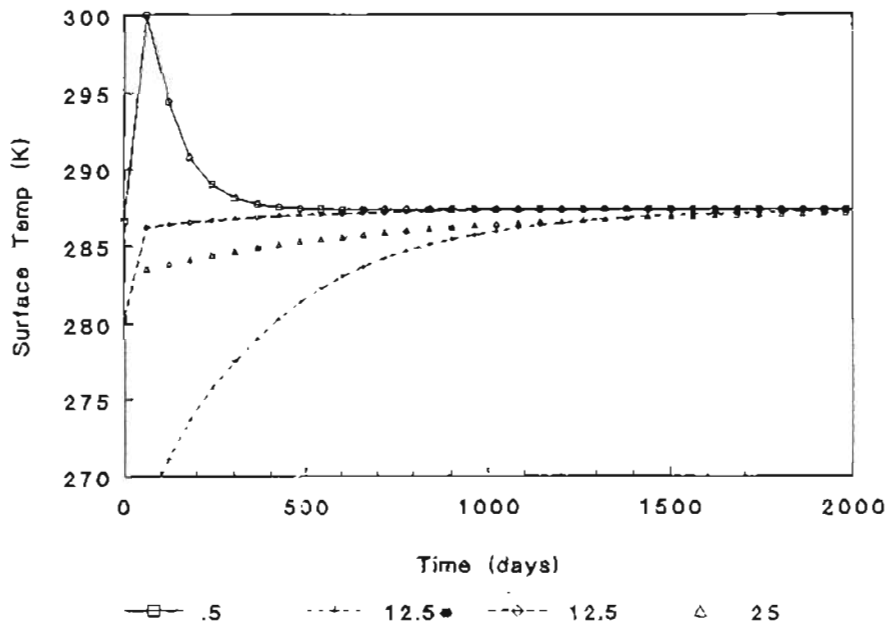


Figure 6.2. Model's approach to equilibrium for assumed ocean mixed layer depths of 0.5, 12.5, and 25.0 meters. Assumed initial thermal structure was an isothermal 280 K Earth-atmosphere except for 12.5* which indicates initial isothermal Earth-atmosphere of 260 K.

Since the convective adjustment only mixes the energy internally in the system, from surface to atmosphere, it does not constitute an external source or sink. Hence, as with the zero dimensional model of Chapter 1, the equilibrium value of T_s does not depend on the depth of the ocean. This is an important feature of the model since, if we are not interested in the model's time development, we can quickly ascertain the

change in T_s due to some perturbation (such as $2\times\text{CO}_2$) by using a shallow ocean depth. Figure 6.2 also shows that the equilibrium surface temperature is independent of assumed initial thermal structure of the atmosphere. Thus the equilibrium achieved by the model is very stable.

Figure 6.3a shows the time constant, τ , of the model for ocean mixed layer depths of 0.5, 1.2, 2.4, 12.5, 25.0, and 50.0 meters. Because of the initial discontinuous jumps in surface temperature seen in Figure 6.2, the time constants were obtained by graphing the natural log of the absolute value of ΔT (Temp - Temp at equilibrium) on the ordinate and time on the abscissa for times greater than 150 days. Such a graph is shown in Figure 6.3b for a 0.5 meter ocean mixed layer depth. The slope of this graph is taken to be $-1/\tau$ (assuming that $\Delta T = \Delta T_0 \exp[-t/\tau]$, which from Figure 6.3b appears to be valid). As can be seen from Figure 6.3a there is a strong linear relation between the response time of the model and the depth of the ocean. A linear regression was made on the data presented in Figure 6.3a resulting in a slope of 24.5 Days/(meter of ocean) and an intercept of 65 days. The intercept can be identified

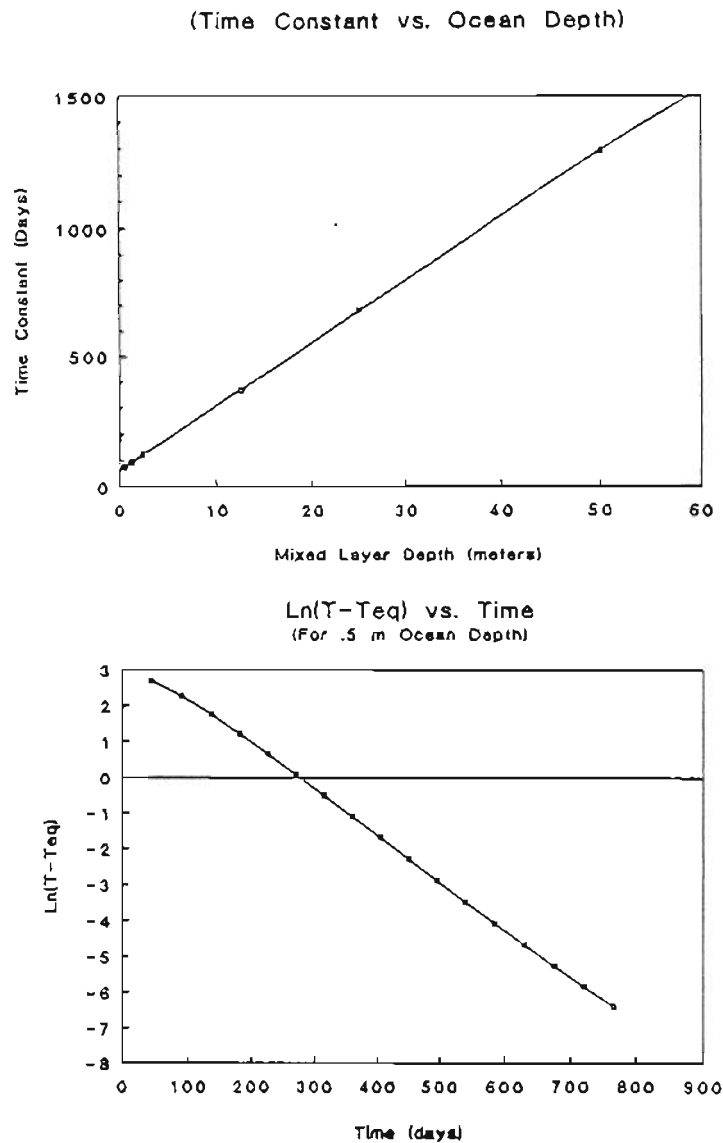


Figure 6.3. (a) time constant τ as a function of ocean mixed-layer depth, and (b) an example of a $\ln(\Delta T)$ versus time graph for 0.5 meter mixed-layer depth.

as the response time of the model atmosphere. It should be noted that the time constant as calculated above is not the time it takes to reach equilibrium, but the time

it takes ΔT to be reduced to $1/e$ of its starting value. The actual time to reach a stable equilibrium (so that the outward flux of IR radiation is within 0.02 W/m^2 of the absorbed solar radiation) typically requires approximately ten time constants.

6.3 Time Step Sensitivity

In this section the sensitivity of the model's output to the value of the time step used in the numerical calculations is explored. An ocean mixed layer depth of 2.5 meters and an initial isothermal 280 K Earth-atmosphere are used for all calculations so that the results of this section can be considered conservative estimates of the maximum allowable time step that can be used and still obtain reliable results.

Figure 6.4a and 6.4b show the equilibrium temperature (T at 1000 days) and outward flux of IR radiation at the top of the atmosphere (F_{out}) for various time steps. From these figures it can be seen that a time step of 0.9 days is very safe in that it gives results consistent with much shorter time steps and that possibly a step of 2 days will still give good results. All results of this thesis have been performed

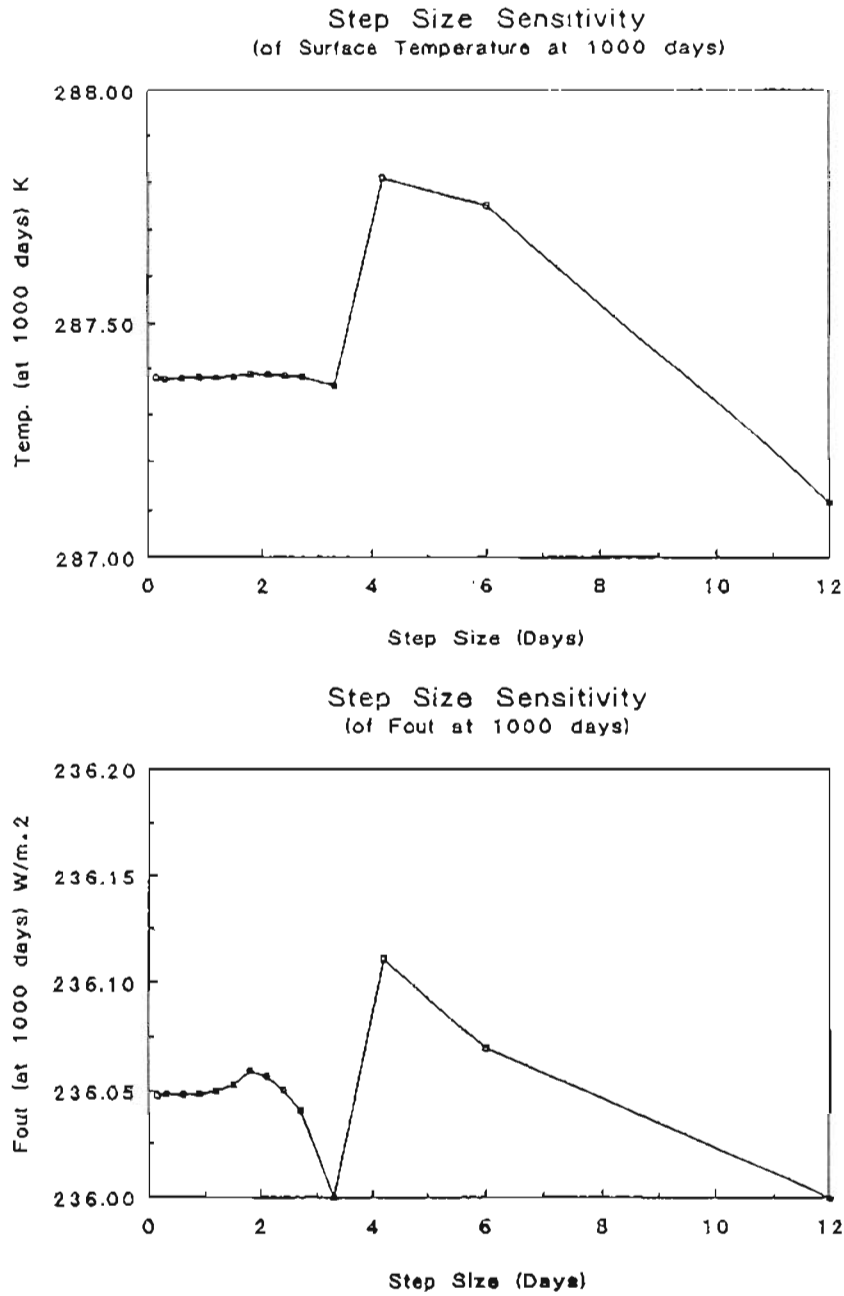


Figure 6.4. (a) Equilibrium temperature (Temp. at 1000 days) versus time step, and (b) outward flux of IR radiation (Fout) versus time step.

with a time step less than or equal to .9 days unless otherwise stated. The real computer time (on a Del 386 25 MHz microcomputer) for each step is approximately 10 seconds per step. Thus at 0.9 days per step it takes about 1 hour to simulate 1 year of climate. It should be stressed that for the above conditions (2.5 meter ocean and 280 K isothermal structure) a time step of 12 days still gave a stable equilibrium and that only at a time step of 15 days was the surface temperature output from the model erratic. Thus, the model could be used for pedagogical purposes at a 10 day time step requiring about 6.0 minutes per year of simulation on a computer equivalent to the Del 386.

6.4 Model Sensitivity Studies

In this section we study the effects of various perturbations in models boundary conditions on the equilibrium surface temperature. Table 6.2 lists the results of the experiments performed for this section. The first entry in Table 6.2 is for the standard run and all other experiments are compared to the standard by looking at the change in surface temperature, from the

standard, due to the specified perturbation.

A 2 percent increase in solar constant is often cited in the literature as being equivalent to a doubling of CO₂ from (320 to 640 ppmv); see for example Cess and Potter (1989). In the next chapter we show that for a doubling of CO₂ our model predicts a change in surface temperature of about 1.9 K, and from Table 6.2 we see that the surface temperature changes by 2.4 K for a 2 percent increase in solar constant. Chylek and Kiehl (1981) compare four 1D RCMs and show that all four predict a surface temperature change of between 2.0 and 2.2 K for a 2 percent increase in solar radiation where the model described by Cess and Potter (1989) predicted a surface temperature change of 1.7 K. The 2.4 K change predicted by the OGI model is generally consistent with these results.

Decreasing the cloud fraction a_c from 0.5 to 0.4 has the obvious effect of decreasing the planetary albedo. In the OGI model this change results in a surface temperature increase of 4.7 K. The decrease of cloud optical depth from 9.0 to 8.0 also decreases the albedo resulting in a 2.3 K surface temperature increase, and increasing the surface albedo from 0.10 to

Table 6.2. Results of experiments performed with the OGI 1DRCM to test the sensitivity of the model to various perturbations in input parameters. The standard run was performed with the trace gas concentration profiles described in chapter 5; cloud fraction, $a_c=0.5$; cloud layer, $k_{ap}=11$ (4.0 km); surface albedo, $r_g=0.10$; cloud optical depth, $depth=9.0$; solar constant divided by 2, $S_0=680$ W/m²; average cosine of zenith angle, $\mu=0.50$, mean ocean mixed layer depth of 2.5 m; and computational time step of 0.30 days.

Perturbation	ΔT (K)
Standard	0.0
1.02 * solar constant	+2.1
$a_c=0.4$	+3.1
$depth=8.0$	+1.8
$k_{ap}=10$ (5.1 km)	+2.6
$r_g=0.12$	-1.4
w/o CO ₂	-12.2
w/o CH ₄	-.7
w/o N ₂ O	-.6
w/o Tropospheric O ₃	-.8
w/o any O ₃	+12.8

0.12 results in a 1.7 K surface temperature decrease. A change in cloud height from 4.0 km to 5.1 km results in

a surface temperature increase since the lower cloud is warmer and hence emits more radiation upward. Thus when the cloud layer is lifted and cools the surface temperature must increase to compensate for the decrease in outward IR flux to space associated with a cooler cloud. This potential feedback was first described by Manabe and Wetherald (1967) when they investigated a fixed cloud top temperature (FCT) scheme in their RCM and showed that the surface temperature sensitivity to doubled CO₂ was essentially doubled for this type of cloud height specification. The OGI model assumes that the cloud altitude is fixed (FCA) which is consistent with most other 1D RCMs and makes for an easier more direct comparison between the OGI model and other RCMs. It should be noted that this type of feedback is a potentially very strong feedback and a similar feedback is most likely partially responsible for the greater sensitivities (for doubled CO₂) seen in three dimensional general circulation models.

The last five experiments summarized in Table 6.2 shows the effect of individually removing each of the greenhouse gases CO₂, CH₄, N₂O, tropospheric O₃, and all of the O₃. An inspection of these results can give us

an idea of the relative importance of each gas to the natural greenhouse warming of approximately 33 K discussed in Chapter 1. Note that the OGI model predicts a temperature decrease of 12.6 K if the CO₂ were to be completely removed from the atmosphere. Kondratyev and Moskalenko (1982) state that CO₂ contributes 7.2 K to the greenhouse warming. The actual warming due to CO₂ is somewhat complicated though since in the OGI model, as with the real earth, as the surface temperature decreases the amount of water vapor in the atmosphere also decreases resulting in an enhanced reduction in surface temperature. This is the well known and studied positive water vapor feedback, recently experimentally quantified by Raval and Ramanathan (1989) to amplify changes in surface temperature by roughly 60 percent. The 12.6 K warming due to CO₂ stated in Table 6.2 includes this water vapor feedback and if we divide this value by 1.6 we obtain a value of 7.9 K without feedback which is agreeable with Kondratyev's and Moskalenko's value of 7.2 K. For CH₄, N₂O, and tropospheric O₃ we obtain a combine surface warming of 1.8 K and thus we infer that the rest of the

33 K (18.6 K) warming is due solely to water vapor. It is interesting, but after some thought it is not surprising to see that the complete removal of all ozone results in a surface temperature increase of 13.8 K. The removal of all ozone increases the transparency of the atmosphere allowing more energy to reach the Earth's surface.

In the next chapter the sensitivity of the OGI model to changes in trace gas concentrations is explored and our results are compared to the results of other equivalent 1D RCMs.

Chapter 7

Trace Gas Perturbations and Climate Sensitivity

In this chapter the sensitivity of the OGI 1DRCM to variations in trace gas concentrations is assessed and compared to previously published results from other similar 1D RCMs. Also in this chapter we use the OGI model to simulate the climate of the past century in an attempt to explore the relation between man's activities and climate.

7.1 Surface Temperature Sensitivity to Trace Gas Perturbations.

Figure 7.1 gives the predicted values of the change in surface temperature ΔT_s due to a doubling of CO_2 (from 320 to 640 ppmv) for the OGI model and ten other similar 1D RCMs. For comparison all model results are for the case of fixed cloud top altitude and the inclusion of the positive water vapor feedback discussed

Comparison of Eleven 1D RCMs (Change in Ts for 2xCO₂)

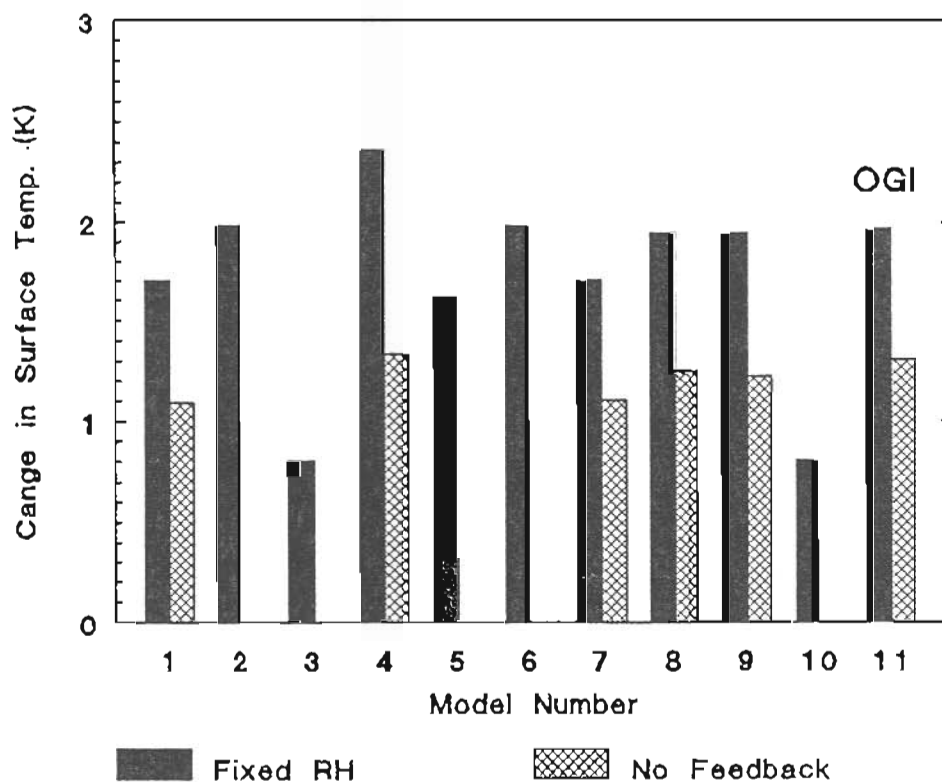


Figure 7.1. Comparison of the predicted change in surface temperature ΔT_s by ten 1D RCMs with the OGI model. The numbers in the square brackets correspond to ΔT_s with water vapor feedback, ΔT_s with no feedbacks, and the ratio of ΔT_s with water vapor feedback to that with no feedback.

Legend

1. Cess and Potter (1989) [1.7, 1.09, 1.56]
2. Lindzen et al (1982) [1.98, ***, ***]
3. Hummel and Kuhn (1981) [0.8, ***, ***]
4. Manabe and Wetherald (1967) [2.36, 1.33, 1.77]
5. Vupputuri (1988) [1.62, ***, ***]
6. Augustsson and Ramanathan (1977) [1.98, ***, ***]
7. Mitchell (1989) [1.7, 1.1, 1.55]
8. Ramanathan et al (1987) [1.94, 1.25, 1.55]
9. Hansen et al (1981) [1.94, 1.22, 1.59]
10. Rasool and Schnieder (1971) [0.8, ***, ***]
11. MacKay, OGI (1990) [1.97, 1.32, 1.49]

in the last chapter. Also where data were available, the results for constant water vapor mixing ratio (no water vapor feedback) are given.

The range of ΔT s values given in Figure 7.1 span from a minimum of 0.8 K to a maximum of 2.4 K. The two extreme low values of 0.8 K were reported respectively by Rasool and Schneider (1971), and Hummel and Kuhn (1981). If these extreme values were omitted, the range of values would narrow to between 1.62 and 2.4 K; with five of the ten values being between 1.90 and 2.00 K. The value of 1.98 K predicted by the OGI model is very consistent with the majority of the other model predictions. This good agreement between the 1D RCMs can be attributed to three points. First, the radiative parameterizations used are all designed to fit the same well known absorption profiles of carbon dioxide and water vapor. Secondly, the water vapor feedback is similarly parameterized in most of the 1D RCMs by assuming a constant relative humidity profile as first suggested by Manabe and Wetherald (1967); see Chapter 5. As pointed out in the last chapter, the observational results of Raval and Ramanathan (1989) tend to give support to this method of dealing with the temperature dependency of the water vapor mixing ratio. Their

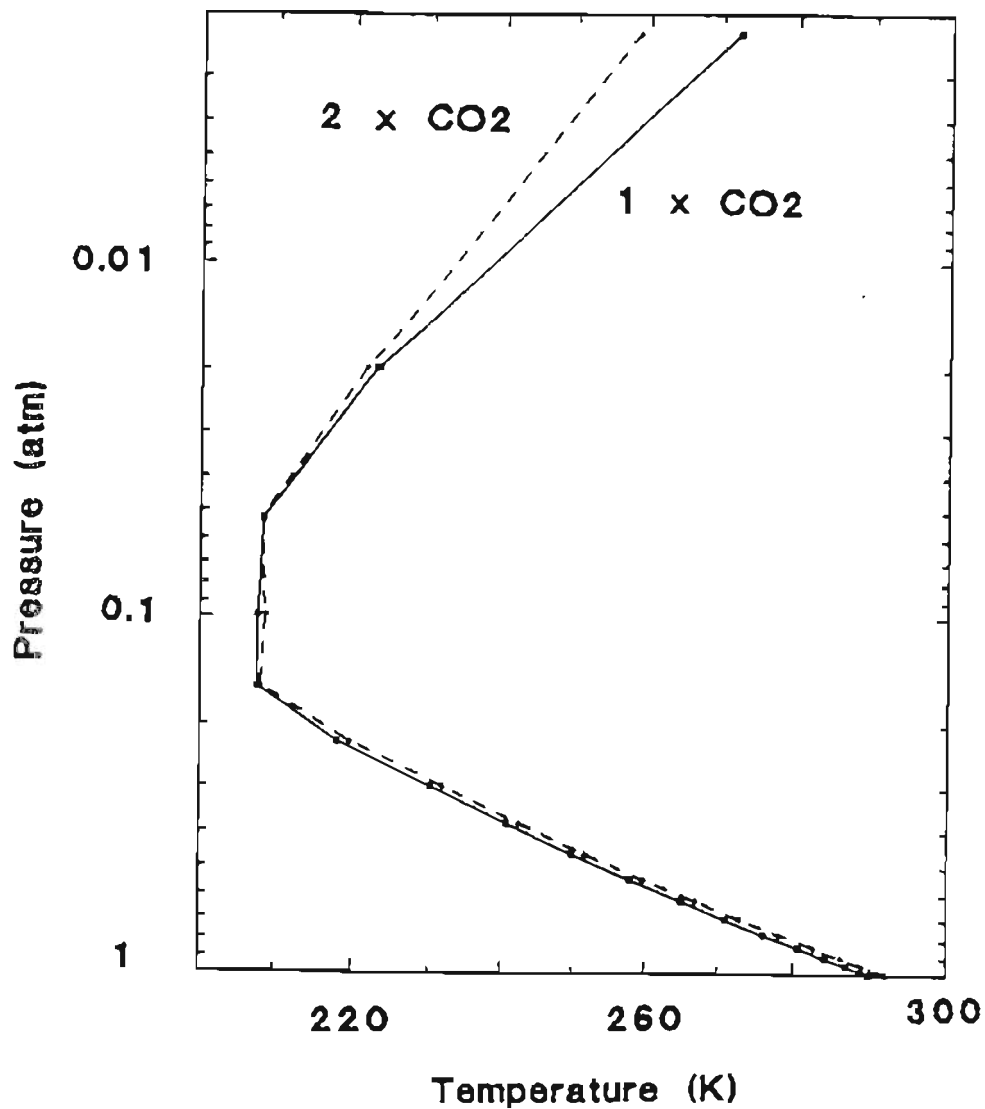


Figure 7.2. Vertical thermal structure predicted by the OGI model for CO₂ concentrations of 320 ppmv (1xCO₂) and 640 ppmv (2xCO₂).

observations support a feedback amplification of the surface temperature of about 1.6 and the models shown give an amplification of 1.6 to 1.8. Finally, most 1D RCMs simulate convective heat transfer in a way similar to that used in the OGI model. With all the

similarities between the 1D RCMs, especially before additional feedbacks are included, it would be surprising if they did not all agree. However, it should be emphasized that the inclusion of additional feedback processes, such as the ice albedo feedback or cloud cover feedback, tend to cause larger discrepancies between the 1D RCMs.

Figure 7.2 compares the vertical thermal structure predicted by the OGI model for uniform CO₂ concentrations of 320 ppmv and 640 ppmv. Aside from the increase in surface temperature, the most notable feature is the large amount of cooling that takes place in the stratosphere upon a doubling of CO₂. This stratospheric cooling has been noted by many others; see for example Manabe and Wetherald (1967). Other investigators such as Vupputuri (1988) have incorporated stratospheric chemical dynamics into their 1D RCM to investigate the influence of the above stratospheric cooling to the chemical mass balance of ozone.

Figure 7.3 compares the OGI model predictions for ΔT s due to changes in atmospheric concentrations of CO₂, CH₄, N₂O, and Tropospheric ozone with the ΔT s predicted by a similar 1D RCM and Published by Ramanathan and

others in the 1985 WMO report No.16; see WMO (1985) in references. The OGI model compares very well with the

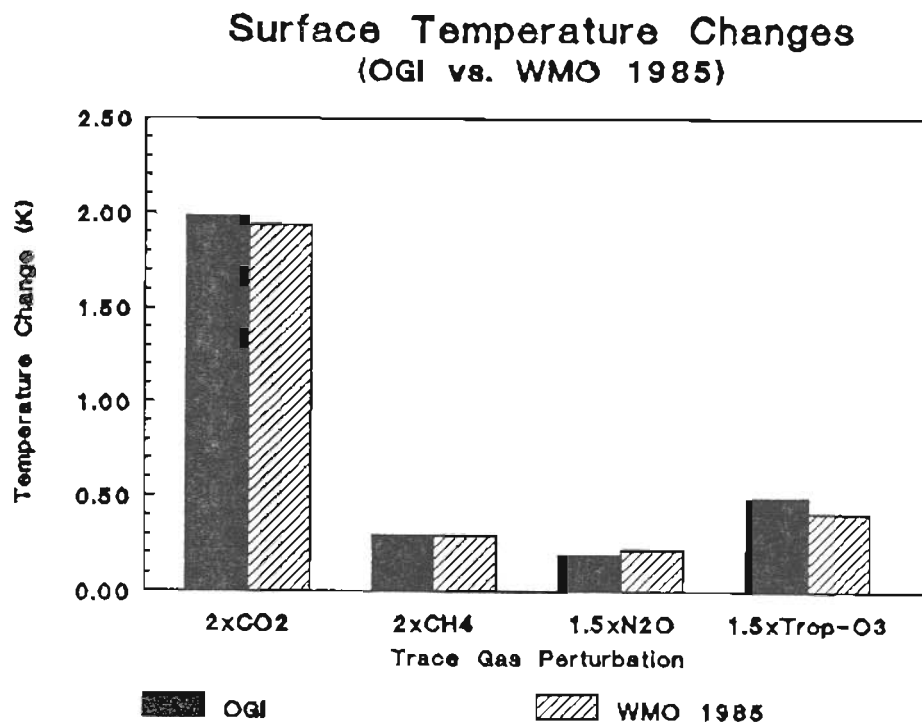


Figure 7.3. Comparison of OGI model's predicted change in surface temperature for various trace gas perturbations with those given by WMO (1985).

WMO values primarily because both models have been influenced substantially by the work of Manabe and Wetherald (1967), Lacis and Hansen (1974), Ramanathan (1976), Donner and Ramanathan (1982), and Kiehl and

Ramanathan (1983).

7.2 Modeled Trends in Temperature of the Past Century

In recent years, especially with the warm decade of the 1980's, the public as well as scientists came to believe that there may be a relation between increased concentrations of greenhouse gases and rising global temperatures since the industrial revolution (mid-nineteenth century. Schnieder (1989) gives an excellent overview of this problem from scientific, political, and sociological perspectives. We address the problem briefly in this section.

Throughout the history of modern science, scientists have been notorious skeptics. It seems that whenever scientists embrace a theory too whole heartedly as fact, someone comes along and demonstrates an exception to the rule. This was the case with the mechanics of Aristotle, Galileo, and Newton, and will undoubtedly be true of the Mechanics of Einstein, Schrodinger, Heisenberg, and Bohr. This skepticism of science is one of the pillars of the scientific method which enables it to be so successful at describing and

understanding nature. It is with just this sort of caution that many climatologists approach the question as to the relationship between trace gas concentration increases of the past century and a rise in global temperature.

Although most scientists agree that the theoretical basis of the greenhouse effect, as discussed in Chapter 1 is very sound, there are questions as to how the real Earth will respond to increases in atmospheric trace gas concentrations. By how much will the positive feedbacks such as the water vapor feedback enhance global warming, or are there some large negative feedbacks in the climate system that will dampen out the effects of increased trace gas concentrations? Will it take 3 years or 3,000 years for the predicted equilibrium temperature to be achieved? If it is 3 years then future predictions are much easier to make. If it is 3,000 years, then unforeseen alterations in the Earth's dynamical system could make future predictions meaningless. What are the social, political, and economic influences on the climate?

One method that can be used to explore the relation between man's activities and climate is to obtain the global temperature record of the past century and

compare it with model predictions of temperature change due to increases in anthropogenic trace gas emissions. Hansen and Lebedeff (1987) and Jones et al (1987) have independently reconstructed the mean global temperature record for the past 110 and 130 years respectively. Care was taken with both records to address the impact of the urban heat island effect, where increases in temperature at a particular station would be attributable to increases in human activity around the station. The two reconstructions are very similar in that they both show an increase in mean global temperature over the past 100 years of about 0.5 K and have the same major qualitative features.

Hansen et al (1981) have also used a 1D RCM to simulate expected changes in mean global surface temperatures due to the changes in trace gas concentrations that have taken place between 1880 and 1980 and have shown that there are large similarities between the actual temperature increase and the temperature increase predicted by their model. We have used the OGI model for a similar comparison.

In Figure 7.4 the OGI model predictions for the change in surface temperature due to changes in the

atmospheric concentrations of CO₂, CH₄, N₂O, and chlorofluorocarbons F-11 and F-12 from 1850 to 1990 are

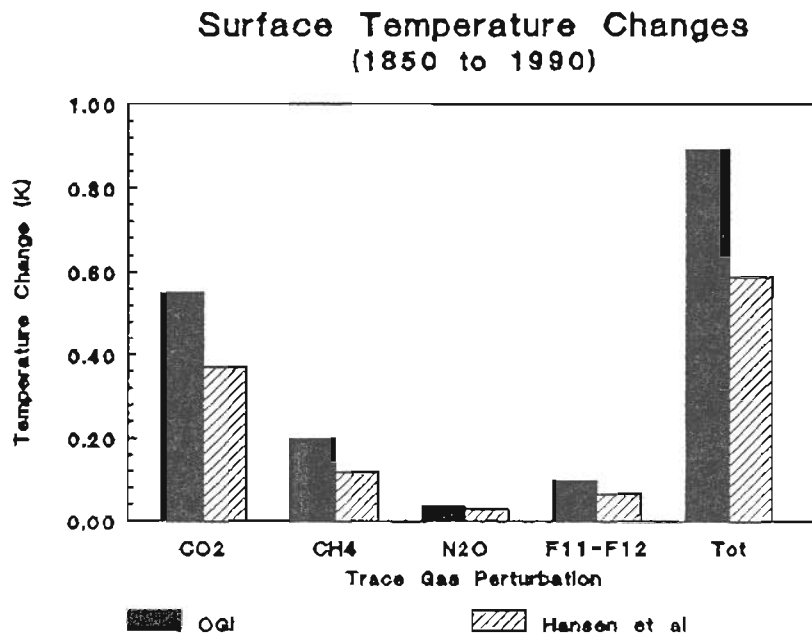


Figure 7.4. Predicted changes in surface temperature due to changes in the atmospheric concentrations of five greenhouse gases over the period from 1850-1990. Trace gas concentration estimates were obtained from Hansen et al (1989).

compared with the published results of Hansen et al. (1989). This comparison is not direct in that Hansen et al. have considered the case of no feedbacks at all and the OGI model results all include the water vapor feedback which amplifies ΔT s. Hansen et al. note that

to obtain the values presently predicted by the three dimensional GCMs it would be necessary to multiply their

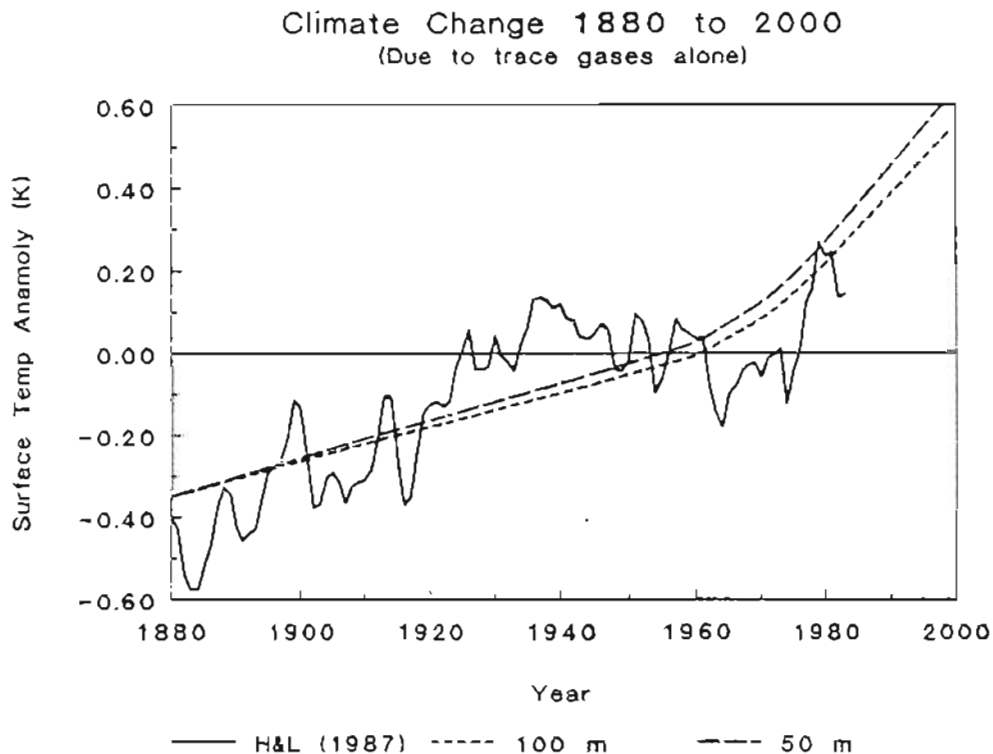


Figure 7.5. Comparison of the actual reconstructed temperature anomalies from Hansen and Lebedeff (1987) with those predicted by the OGI model due to changes in the concentrations of the green house gases CO₂, CH₄, N₂O, F-11, and F-12 from 1880 to 2000. Note: The reconstructed record has been filtered by taking a three year running average.

predictions by a factor of 2 to 4. Considering the above differences between the two models, they are in good agreement with each other. We present the OGI

values of ΔT s including the water vapor feedback to make these results consistent with the continuous run presented in Figure 7.5.

In Figure 7.5 the OGI model prediction for the temperature of the last 110 years plus ten years into the future (1880-2000) is shown with the reconstructed temperature record of Hansen and Lebedeff (1987). The reconstructed record has been filtered by taking a three year running average of the record. The OGI model assumed an ocean mixed layer depth of both 50 and 100 meters in an attempt to model the time response of the Earth's climate system. The greenhouse gases included were CO₂, CH₄, N₂O, F-11, and F-12. The trace gas concentration estimates were obtained from Hansen et al (1989) for the years 1880-1990. For years 1990 to 2000 we have assumed the same linear growth rate of the trace gases that was observed from 1980 to 1990. A linear regression of the model simulations on the reconstructed record was performed for the two curves of Figure 7.5. The square of the correlation coefficient R^2 is taken as the goodness of fit. The values of R^2 were 0.51 and 0.55 for ocean depths of 100 and 50 meters respectively. The trend in the reconstructed record (slope of linear

regression of T on year) was .55 K/century while the trends of the simulations were 0.51 and 0.55 K/century for the 100 and 50 meter deep oceans respectively. Table 7.1 summarizes these results. The X-coef in Table 7.1 is equal to the value of m (slope) in the equation

$$y_i^* = m \cdot x_i + b \quad 7.2.1$$

that gives the best fit between y_i^* and the reconstructed record y_i , according to minimizing

$$\sum (y_i^* - y_i)^2$$

where x_i in equation 7.2.1 is the value of the simulated record for the i^{th} year.

It should be noted that obtaining the model trend using linear regression over the full 100 or 110 years is an underestimate of the actual temperature change predicted by the model for the last century. The reason for this is that the temperature change is not linear but accelerates with the greatest change per decade occurring over the last decade of the simulation.

The model temperature record in general agrees well with the reconstructed record in that both records have

an increase of about 0.5 or 0.6 K over the last century. The reconstructed record has several distinct features that are not explained by our simple model. First the reconstructed record has many fluctuations that are typical of natural variability. Second there is a distinct warm period or "hump" in the reconstructed record centered around 1930 or 1940 that is not present in the model simulation of Figure 7.5. Hansen et al (1981) showed that their 1D RCM was able to fit the actual record much better if they included sharp cooling episodes due to volcanic eruptions. They also discussed the possibility that variations in solar luminosity may have influenced the actual climate record of the past century.

Following the work of Hansen et al (1981), we have included an estimation of the effect on the atmospheric albedo of the major volcanic eruptions that have taken place since 1880. The results of this simulation using an ocean mixed layer depth of 80 meters is shown in Figure 7.6 and in Table 7.1. The variations in the atmospheric concentrations of trace CO₂, CH₄, N₂O, F-11, and F-12 are the same as for Figure 7.5. To simulate the increased atmospheric albedo due to the injection of

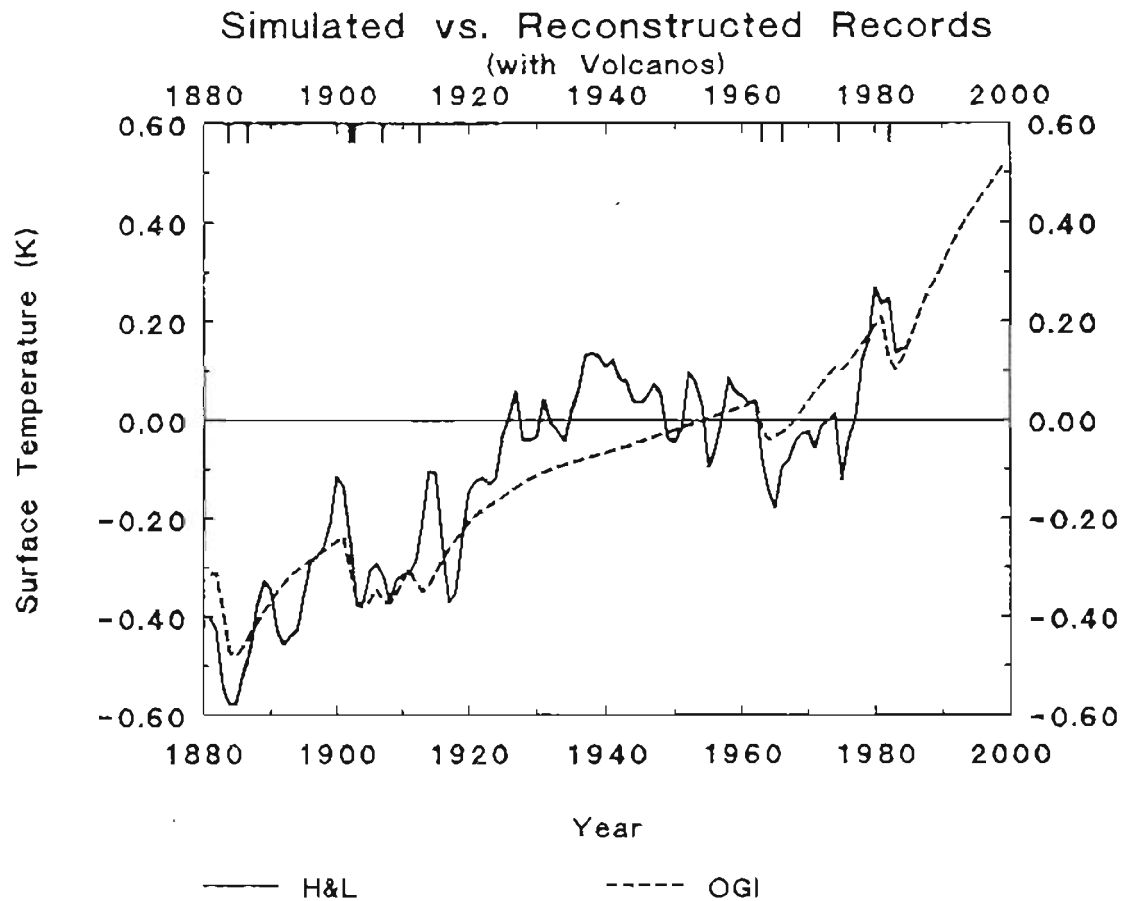


Figure 7.6. Same as in Figure 7.5 but with the addition of volcanic aerosol loading of the stratosphere.

volcanic debris into the stratosphere we have used the volcano energy index (VEI) and the dust veil index (DVI) given for the eleven volcanic eruptions discussed by Mass and Portman (1989). Of the many volcanic eruptions of the past century they believed that eleven were energetic enough to have potentially influenced the climate. These eruptions are summarized in Table 7.2.

Table 7.1. Comparison of the OGI model simulations with the reconstructed mean annual global surface temperature record of Hansen and Lebedeff (1987). The trend is obtained from the slope of the linear regression of each time series on the year while the goodness of fit R2 and the x-coefficient refer to the regression of the record simulated by the model on the reconstructed record. Note: all values are rounded to the nearest 0.01.

Record	trend (K/century)	R2	X-coef
Reconstructed	0.55	1.00	1.00
50 m	0.55	0.61	0.91
100 m	0.51	0.61	1.00
100 m (+ Volc.)	0.55	0.76	1.00

The albedo α_1 of the upper atmospheric layer (layer 1) due to this aerosol loading is calculated according to,

$$\alpha_1 = \sum_{i=1}^{10} \alpha_i$$

where

$$\alpha_i = \alpha_o \exp[-(t - t_{oi})] \quad \text{if } t > t_{oi}$$

$$\alpha_i = 0.0 \quad \text{if } t < t_{oi}$$

$$\alpha_o = a[\text{DVI}][\text{VEI}]/6000$$

7.2.2

The value of 6000 is used in the denominator of α_o so

that the maximum albedo of the upper layer due to

Table 7.2. The eleven volcanic eruptions cited by Mass and Portman (1990) as having the potential to impact the climate of the last century. * the values of α_0 are rounded off to the nearest 0.001. ** These values of DVI and VEI were not cited by Mass and Portman but were estimated by the author of this thesis.

Name	Date	DVI	VEI	α_0 *
Krakatau	8/1883	1000	6	0.013
Tarawera	6/1886	800	5	0.000
Mount Pelee	5/1902	100	4	0.001
Soufriere	5/1902	300	4	0.003
Santa Maria	10/1902	600	6	0.008
Ksudach	3/1907	500	5	0.005
Katmai	6/1912	500	6	0.007
Agung	3/1963	800	4	0.007
Awu	8/1966	200	4	0.002
Fuego	10/1974	250	4	0.002
El Chichon**	4/1982	1000	6	0.013

Krakatoa (1883) is equal to the adjustable parameter a . In equation 7.2.2 t is the time in years and t_{oi} is the eruption time of the i th volcano. Notice that the time constant for the decay of the stratospheric albedo due to each volcano is implicitly assumed to be one year. To produce Figure 7.6 we empirically set the constant a equal to 0.013 and the eruption of 1886 was omitted based on qualitative disagreement between the simulation

and reconstructed records.

As can be seen from Table 7.1 the inclusion of volcanos into the OGI model significantly improves the fit between the model and the reconstructed record; R^2 increased from 0.61 to 0.76. However, it should be emphasized that agreement between model output and the reconstructed temperature record should be viewed with caution. Even though the model may offer a plausible explanation, chances are there undoubtedly exist other possible explanations.

Future investigations using the OGI 1D-RCM on the climatic influences of trace gas concentration changes, volcanic activity, solar luminosity variations, and atmospheric/ocean dynamics are justified. Properly modeling the atmospheric and/or ocean dynamics will require the extra spatial resolution obtainable with a 2-dimensional (or 3-dimensional) model since the inclusion of horizontal transport is essential for the physical description of the ocean and atmosphere seasonal variability.

An interesting question comes to mind when looking at the results of the OGI model displayed in Figure 7.6. Since the OGI model results are due solely to the

greenhouse gas fluctuations and water vapor feedback, we would have to multiply our values by 1.5 to 2.5 to agree with most GCMs which presently predict surface temperature changes of between 2.8 and 5.2 K for doubled CO₂, see Mitchell (1989). As can be seen from Figure 7.6 the temperature trend predicted by the OGI model agrees well with the changes in surface temperature observed over the past century. Why then do the GCMs predict substantially higher values of surface temperature changes for doubled CO₂ than the 1D RCMs, when the 1D RCMs appear to agree so well with the temperature changes of the past century?

Two plausible explanations for this overestimation are as follows. First, the thermal inertia of the climate system may be underestimated (in some instances ignored all together) in the GCMs causing the model temperature response to be faster than the actual response of the climate system. Second, assuming that the response time associated with a 100 meter deep mixed layer is realistic, then there may be negative feedbacks that have not been included that will, to some degree, cancel the positive feedbacks. In fact it can argued that since there are many aspects of nature that are not

well understood at present, then chances are there are just as many positive feedbacks as negative. Thus including no feedbacks at all might be a more realistic representation of the real world than including several obvious positive feedbacks.

If the first explanation is valid, then global warming due to atmospheric increases in greenhouse gases will be delayed, resulting in greater uncertainties as to what the actual results of these increases will be since there will be more time for other changes to take place before the full effect can be realized. If the second explanation is valid then most all climate models have been overestimating the influence of greenhouse gas fluctuations on global surface temperature. It should be stressed that other equally plausible explanations surely exist.

Chapter 8

Conclusions

In this paper the theory and the development of a time-dependent one dimensional radiative convective model has been presented in detail in Chapters 1 through 5 and a listing of the actual source code is given in Appendix E. This work should prove to be extremely useful to others wanting to employ a 1 dimensional radiative convective climate model to study the response of the earth-atmosphere system to external and internal perturbations.

In Chapters 6 and 7 the response of the model was examined revealing several important features of the model. First, it was found that the equilibrium temperature profile predicted by the model was very stable in that it was independent of: the assumed initial temperature structure of the Earth-atmosphere ; the depth of the ocean mixed layer; and computational step size less than 0.9 days. Secondly, the predicted changes in surface temperature due to a doubling of CO₂

and CH₄ and an increase of N₂O and tropospheric O₃ increase of 50 % is in good agreement with changes previously published by others in the last decade. This good agreement between the OGI model and other recent models gives credibility to the OGI model since as noted by Cess (1989), the agreement between 1D RCMs is good since the problem of radiative transfer is now well understood.

The OGI 1D RCM can thus be considered a valid research tool that can be used by others to explore problems in atmospheric sciences related to the climate response of the Earth-atmosphere system. Most importantly though is that the OGI 1DRCM is very amenable to further improvements and developments. For example, the future incorporation of an aerosol absorption and scattering model, an interactive sea ice growth model, or various cloud parameterization schemes, could all be helpful in exploring current topics of interest to the scientific community. These additions can now be made with confidence since the basic structure of the model has been shown to be solid.

However, as noted in both chapters 1 and 7 the one dimensional nature of the model has limited spatial

resolution. To simulate the seasonal variations in climate a 2-dimensional (or 3-dimensional) model should be used. The addition of the horizontal transport of energy in the 2-D model will allow the model to more realistically simulate convection, ice albedo feedback, latitudinal dependency of surface temperature change due to double CO₂, as well as other physical processes. In addition the use of a 2-D model can be used to explore the possibility of internal oscillations of the climate system that may be responsible for some of the natural climate variability.

The next phase of this work has two main objectives. First, modifications will be made on the OGI 1D RCM to improve its flexibility as a research tool. Second, a 2-D model will be developed to be used to explore the climate system in more detail.

References

- Arrhenius, Svante, 1896. On the Influence of Carbonic Acid in the Air upon the Temperature of the Ground. Phil. Mag. S. 5. Vol.41.No.251, 237-276
- Augustsson, T. and V. Ramanathan, 1977. A Radiative-Convective Model Study of the CO₂ Climate Problem. Journal of Atmospheric Sciences, Vol. 43, 448-451.
- Cess, R.D., and V. Ramanathan, 1972. Radiative Transfer in the Atmosphere of Mars and That of Venus Above the Cloud Deck. Journal of Quantitative Spectroscopy and Radiative Transfer, Vol. 12, 933-945.
- Cess, R.D., 1974. Radiative Transfer Due to Atmospheric Water Vapor: Global considerations of the Earth's Energy Balance. Journal of Quantitative Spectroscopy and Radiative Transfer, Vol. 14, 861-871.
- Cess, R.D. 1989. Gauging water-vapour feedback. Nature Vol 342 736-737.
- Crutzen, P.J., I.S.A. Isaksen, and J.R. McAfee, 1978. The Impact of the Chlorocarbon Industry on the Ozone Layer. Journal of Geophysical Research, Vol. 83, 345-353.
- Donner, L., and V. Ramanathan, 1980. Methane and Nitrous Oxide: Their effects on the Terrestrial Climate. Journal Of Atmospheric Sciences, Vol. 37, 119-124.
- Goody, R.M., 1964. Atmospheric Radiation I Theoretical Basis. Oxford at the Clarendon Press.
- Goody, R.M. and Y.L.Yung, 1989. Atmospheric Radiation Theoretical Basis Second Edition. Oxford University Press.

- Green, A.E.S., C.S. Lindenmeyer and M. Griggs, 1964. Molecular Absorption in Planetary Atmospheres. *Journal of Geophysical Research*, Vol. 69, 493-504.
- Hansen, J., D. Johnson, A Lacis, S. Lebedeff, P. Lee, D. Rind, and G. Russell, 1981. Climate Impact of Increasing Atmospheric Carbon Dioxide. *Science* Vol. 213, No. 4511. 957-962.
- Hansen, J. and S. Lebedeff, 1987. Global Trends of Measured Surface Air Temperature. *Journal of Geophysical Research*, Vol. 92, No. D11, 13345-13372.
- Hansen, J., A.Lacis, and M.Prather, 1989. Greenhouse Effect of Chlorofluorocarbons and Other Trace Gases. *Journal of Geophysical Research*, Vol. 94, No. D13, 16417-16421.
- Hummel, J.R. and W.R.Kuhn, 1981. Comparison of Radiative-Convective Models With Constant and Pressure-Dependent Lapse Rates. *Tellus* Vol. 33 254-261.
- Kiehl, J.T. and V. Ramanathan, 1983. CO₂ Radiative Parameterization Used in Climate Models: Comparison With Narrow Band Models and With Laboratory Data. *Journal of Geophysical Research*, Vol 88, No. C9, 5191-5202
- K.Ya Kondratyev and N.I.Moskalenko, 1984. in *The Global Climate Chapter 13*, John T. Houghton editor. Cambridge University Press.
- Kuo, H.L., 1977. Analytic Infared Transmissivities of the Atmosphere. *Beitr. Phys. Atmos.*, Vol. 50, 331-349.
- Lacis, A.A., and J.E. Hansen, 1974. A Parameterization for the absorption of Solar Radiation in the Earth's Atmosphere. *Journal Of Atmospheric sciences*, Vol. 31, 118-133.
- Lal, M., and V. Ramanathan, 1984. The Effects of Moist Convection and Water Vapor Radiative Processes On Climate Sensitivity. *Journal Of Atmospheric sciences*, Vol. 41, 2238-2249.

Lindzen, R.S., A.Y.Hou, and B.F. Farrell, 1982. The Role of Convective Model Choice in Calculating the Climate Impact of Doubling CO₂. Journal Of Atmospheric sciences, Vol. 39, 1189-1205.

Liou, Kuo-Nan. 1980. An Introduction to Atmospheric Radiation. Academic Press.

Manabe, S. and R.F. Strickler, 1964. Thermal Equilibrium of the Atmosphere with a Convective Adjustment. Journal Of Atmospheric sciences, Vol. 21, 361-385

Manabe, S. and R.T. Wetherald, 1967. Thermal Equilibrium of the Atmosphere with a given Distribution of Relative Humidity. Journal of Atmospheric Sciences, Vol. 24, No.3, 241-259

Mass, C.F. and D.A. Portman, 1989. Major Volcanic Eruptions and Climate: A Critical Evaluation. Journal of Climate, Vol. 2, 566-593

McCartney E.J., 1983. Absorption and Emission by Atmospheric Gases, The Physical Processes. John Wiley and Sons.

Mitchell, John F.B., 1989. The "Greenhouse" Effect and Climate Change. Reviews of Geophysics Vol. 27 No. 1 115-139.

North G.R., R.F. Cahalan, and J.A. Coakley Jr., 1981. Energy Balance Climate Models, Rev. of Geophysics and Space Physics, 19, 91-121.

Ramanathan, V. 1975. Greenhouse Effect Due to Chlorofluorocarbons: Climatic Implications. Science Vol. 190 50-51.

Ramanathan, V., 1976. Radiative Transfer Within the Earth's Troposphere and Stratosphere: A simplified Radiative-Convective Model. Journal of Atmospheric Sciences, Vol. 33, 1330-1346.

Ramanathan, V., and J.A. Coakley Jr., 1978. Climate Modeling Through Radiative Convective Models. Rev. of Geophysics and Space Physics, **6**, 465-489.

Ramanathan, V., E.J.Pitcher, R.C. Malone, and M.L. Blackmon, 1983. The Response of a Spectral General Circulation Model to refinements in Radiative Processes. Journal of Atmospheric sciences, Vol. 40, 605-631.

Raval, A. and V. Ramanathan, 1989. Observational Determination of the Greenhouse Effect. Nature Vol. 342 758-761

Roberts, R.E., J.E.A. Selby, and L.M. Biberman, 1976. Infrared Continuum Absorption by Atmospheric Water Vapor in the 8-12 μm Window. Applied Optics, Vol.15, No. 9, 2085-2090.

Rodgers, C.D. and C.D. Walshaw, 1966. The Computation of Infrared Cooling Rate in Planetary Atmospheres. Quarterly Journal of the Royal Meteorological Society, Vol. 92, 67-92.

Rodgers, C.D., 1967. The Use of Emissivity in Atmospheric Radiation Calculations. Quarterly Journal of the Royal Meteorological Society, Vol. 93, 43-54.

Schneider, S.H., W.M. Washington, and R.M. Chervin, 1978. Cloudiness as a Climate Feedback Mechanism: Effects on Cloud Amounts of Prescribed Global and Regional Surface Temperature Changes in the NCAR GCM. Journal of Atmospheric sciences, Vol. 35, 2207-2221.

Stephens, G.L., 1984. The Parameterization of Radiation for Numerical Weather Prediction and Climate Models. Monthly Weather Review, Vol. 112, 826-867.

Stone, P.H., and J.H. Carlson, 1979. Atmospheric Lapse Rate Regimes and Their Parameterization. Journal of Atmospheric sciences, Vol. 36, 415-423.

Tyndall, J., 1863. On Radiation Through the Earth's Atmosphere. London, Edinburgh, and Dublin Philosophical Magazine 4:200

Vupputuri R.K.R., 1985. The Effect of Ozone Photochemistry on Atmospheric and Surface Temperature Changes due to Increased CO₂, N₂O, CH₄ and Volcanic Aerosols in the Atmosphere. Atmosphere-Ocean, Vol. 23, 359-374.

Washington, W.M., and C.L. Parkinson, 1986. An Introduction to Three-Dimensional Climate Modeling. University Science Books.

WMO Report No. 16, 1985. Atmospheric Ozone: Assessment of Our Understanding of the Processes Controlling its Present Distribution and Change.

emissivity at thermal equilibrium, the source function J_ν equals the Planck function $B_\nu(T)$. It should be noted here that, $B_\nu(T) = b_\nu(T) / \pi$ where $b_\nu(T)$ is the Planck radiation formula discussed in Chapter 1. If the radiation is isotropic then integrating $B_\nu(T) \cos(\theta)$ over the solid angle $\sin(\theta) d\theta d\phi$ gives $b_\nu(T)$ which is the intensity of radiation having wavenumber between ν and $\nu + d\nu$ leaving the blackbody in a direction normal to the surface. The angle θ is the angle measured from the normal to the plane and ϕ is the azimuthal angle.

Using $J_\nu = B_\nu(T)$ we can rewrite equation A.1.1 as,

$$\frac{dI_\nu}{k_\nu \rho ds} = -I_\nu + B_\nu(T) \quad \text{A.1.2}$$

This is called Schwarzschild's equation. In a plane parallel atmosphere distances are typically measured in a direction normal to the plane of stratification (x-y plane in Figure A.1).

Noting that $s = z / \cos\theta$ and assuming I_ν to be a function of θ and z only (azimuthal symmetry) we can rewrite equation A.1.2 as,

$$\cos\theta \frac{dI_V(z, \phi)}{k_V \rho ds} = - I_V(z, \phi) + B_V(T) \quad \text{A.1.3}$$

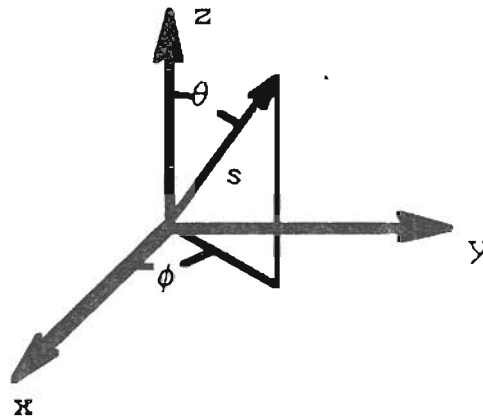


Figure A.1. The coordinate system used to describe a plane parallel atmosphere.

The Normal optical thickness τ of a layer is defined to be,

$$\tau = \int_z^{\infty} k \rho ds \quad \text{A.1.4}$$

where τ is maximum at the surface where $z=0$ and τ approaches zero as z approaches infinity.

With this definition for the normal optical thickness equation A.1.3 becomes,

$$\mu \frac{dI_V(z, \phi)}{d\tau} = I_V(\tau, \mu) - B_V(T) \quad \text{A.1.5}$$

for the upward flux of radiation and

$$-\mu \frac{dI_V(z, \phi)}{d\tau} = -I_V(\tau, -\mu) - B_V(T) \quad \text{A.1.6}$$

for the downward flux, where $\mu = \cos \theta$. (note that $1 \geq \mu \geq 0$ for both A.1.5 and A.1.6). Multiplying A.1.5 by $(d\tau/\mu)\exp(-\tau/\mu)$ and integrating both sides of the equation (using integration by parts on the first term on the right hand side) from $\tau' = \tau$ to τ_1 gives,

$$I_V(\tau, \mu) \approx I_V(\tau_1, \mu) e^{-(\tau_1 - \tau)/\mu} + \int_{\tau}^{\tau_1} \frac{d\tau'}{\mu} B_V(T(\tau')) e^{-(\tau - \tau')/\mu} \quad \text{A.1.7}$$

for the upward flux. The downward flux can be obtained by multiplying both sides of A.1.6 by $(d\tau/ -\mu)\exp(\tau/\mu)$ and integrating from $\tau' = 0$ to τ . Doing this gives,

$$I_V(\tau, -\mu) = I_V(0, -\mu) e^{-\tau/\mu} + \int_0^{\tau} \frac{d\tau'}{\mu} B_V(T(\tau')) e^{-(\tau - \tau')/\mu} \quad \text{A.1.8}$$

To find the monochromatic upward and downward fluxes of radiation at the level τ we note that $I_V(0, -\mu) = 0$ (no

downward flux from outer space) and $I_\nu(\tau_1, \mu) = B_\nu(T_s)$ (the flux of radiation from the surface is assumed to be due to a blackbody radiator). We can now integrate A.1.7 and A.1.8 over the solid angle from $\mu=0$ to 1 and $\phi=0$ to 2π to obtain, for the monochromatic upward and downward fluxes of IR radiation,

$$F_\nu^+(\tau) = 2\pi B_\nu(T_s) \int_0^1 \mu d\mu \exp(-(\tau_1 - \tau)/\mu) + 2 \int_0^1 d\mu \int_\tau^{\tau_1} d\tau' \pi B_\nu[T(\tau')] \exp(-(\tau' - \tau)/\mu) \quad \text{A.1.9}$$

$$F_\nu^-(\tau) = 2 \int_0^1 d\mu \int_0^\tau d\tau' \pi B_\nu[T(\tau')] \exp(-(\tau - \tau')/\mu) \quad \text{A.1.10}$$

We now consider a wavenumber interval $\Delta\nu$ which is sufficiently small to allow the use of the mean Planck function $B_\nu(T)$ over the interval. The transmission function is defined to be

$$T_\nu(\tau) = \frac{1}{\Delta\nu} \int_{\Delta\nu} k_\nu du \quad \text{A.1.11}$$

where

$$\tau = \int_u^{u_1} k_\nu du \quad \left(\tau_1 = \int_0^{u_1} k_\nu du \right) \quad \text{A.1.12}$$

is the monochromatic optical depth and

$$u = \int_0^z \rho dz \quad \left(u_1 = \int_0^{\infty} \rho dz \right) \quad \text{A.1.13}$$

is the normal path length.

The upward flux of radiation passing through level τ due to radiation in the wavenumber interval $\Delta\nu$ is from equation A.1.9,

$$\begin{aligned} F_{\nu}^{+}(\tau) &= \frac{1}{\Delta\nu} \int_{\Delta\nu} d\nu F_{\nu}^{+}(\tau) \\ &= 2\pi B_{\nu}(T_s) \int_0^1 \mu d\mu T_{\nu} \left[\frac{(\tau_1 - \tau)}{\mu} \right] \\ &\quad + 2 \int_0^1 d\mu \int_{\tau}^{\tau_1} d\tau' \pi B_{\nu}(T_s) T_{\nu} \left[\frac{(\tau' - \tau)}{\mu} \right] \end{aligned} \quad \text{A.1.14}$$

The diffuse transmission function for flux density is defined to be,

$$T_{\nu}^{*} = 2 \int_0^1 T_{\nu}(\tau/\mu) \mu d\mu \quad \text{A.1.15}$$

From equations A.1.11 and A.1.15 it is easy to see that

$$\frac{dT_{\nu}^{*}}{d\tau} = -2 \int_0^1 T_{\nu}(\tau/\mu) d\mu \quad \text{A.1.16}$$

Inserting equations A.1.16 and A.1.15 into equation A.1.14 we obtain,

$$F_{\nu}^{+}(\tau) = \pi B_{\nu}(T_s) T_{\nu}^{*}(\tau_1 - \tau) - \int_{\tau}^{\tau_1} \pi B_{\nu}(\tau') \frac{dT_{\nu}^{*}(\tau' - \tau)}{d\tau'} d\tau' \quad \text{A.1.17}$$

for the upward flux of radiation through level τ , having wavenumbers in the interval $\Delta\nu$.

The point of all of this is to be able to write the upward flux of radiant energy in a form that has already implicitly taken the angular integration into account. We can similarly write for the downward flux of energy over the wavenumber interval $\Delta\nu$,

$$F_{\nu}^{-}(\tau) = - \int_0^{\tau} \pi B_{\nu}(\tau') \frac{dT_{\nu}^{*}(\tau - \tau')}{d\tau'} d\tau' \quad \text{A.1.18}$$

Using equations A.1.12 and A.1.13 equations A.1.17 and A.1.18 may be written in terms of the normal optical path length u as,

$$F_{\nu}^{+}(u) = \pi B_{\nu}(T_s) T_{\nu}^{*}(u) + \int_0^u \pi B_{\nu}(u') \frac{dT_{\nu}^{*}(u - u')}{du'} du' \quad \text{A.1.19}$$

$$F_{\nu}^{-}(u) = \int_{u_1}^u \pi B_{\nu}(u') \frac{dT_{\nu}^{*}(u' - u)}{du'} du' \quad \text{A.1.20}$$

and equation A.1.15 can be written as,

$$T_{\nu}^* = 2 \int_0^1 T_{\nu}(u/\mu) \mu d\mu \quad \text{A.1:21}$$

The integration over $\mu = \cos\theta$ is seldom performed for flux calculations. Instead it is standard practice to assume that,

$$T_{\nu}^* = T_{\nu}(1.66u) \quad \text{A.1.22}$$

where 1.66 is called the diffusivity factor.

A.2 Theory of Working Equations

The model atmosphere is depicted in Figure A.2 below where, z is the vertical coordinate measured from the surface of the earth ($z=0$). The top atmospheric layer is assumed to be isothermal and its bottom is located at $z=z_t$. We designate the upward and downward flux of IR radiation at level z by $F^+(z)$ and $F^-(z)$ respectively.

The monochromatic transmission function between layers z and z' is now taken to be,

$$T_v(z, z') = \exp\left[-\int_z^{z'} k\rho' dz''\right] \quad \text{A.2.1}$$

where k is the mass absorption coefficient and

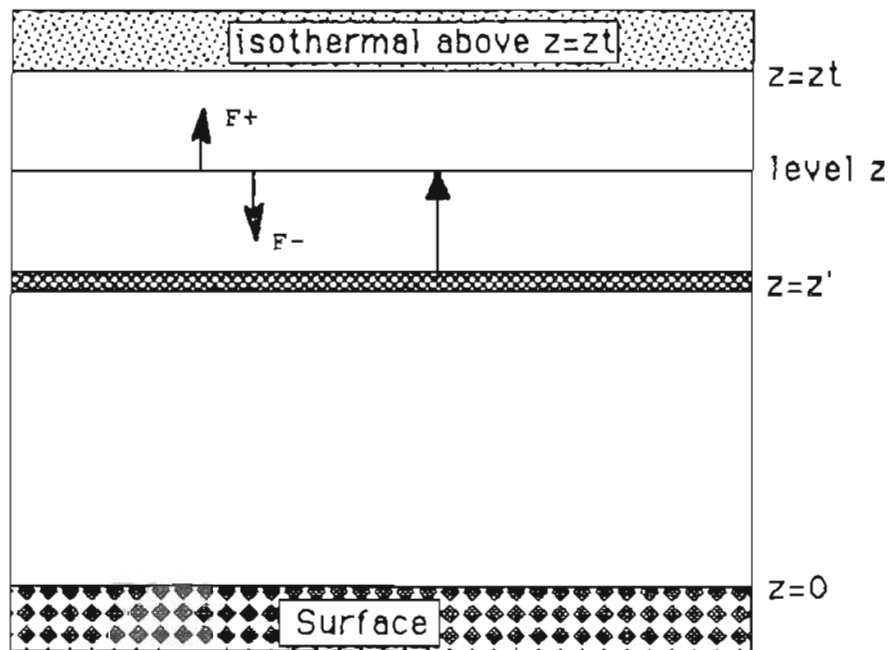


Figure A.2. The model atmosphere. The IR flux is calculated at level z due to the layer at level z' .

$\rho' = 1.66 \times \text{density}$, and the factor 1.66 is the diffusivity factor. Following the argument developed in the last section we have for the net downward flux of radiation at level z

$$F^-(z) = - \int_0^{\infty} dV \int_z^{\infty} \pi B_v(z') \frac{dT_v(z, z')}{dz'} dz' \quad \text{A.2.2}$$

where $B_\nu(z')$ is the plank function for the temperature at level z' and wavenumber ν . The monochromatic absorption function is defined as, $A_\nu = 1 - T_\nu$. Thus equation A.2.2 can be rewritten in terms of the absorption function as,

$$F^-(z) = \int_0^\infty d\nu \int_z^\infty \pi B_\nu(z') \frac{dA_\nu(z, z')}{dz'} dz' \quad \text{A.2.3}$$

$$= \int_0^\infty d\nu \left\{ \int_{z_t}^\infty dz' \pi B_\nu(z') \frac{dA_\nu(z, z')}{dz'} + \int_z^{z_t} dz' \pi B_\nu(z') \frac{dA_\nu(z, z')}{dz'} \right\}$$

Assuming that the temperature T is constant above $z=z_t$, integrating the second integral by parts, and noting that $A_\nu(z, z) = 0$ yields,

$$F^-(z) = \int_0^\infty d\nu \left\{ \pi B_\nu(z_t) A_\nu(z, \infty) + \int_{z_t}^z A_\nu(z, z') d[\pi B_\nu(z')] \right\} \quad \text{A.2.4}$$

The broadband emissivity ϵ and the modified emissivity α are defined to be

$$\epsilon(z, z') = \int_0^\infty A_\nu(z, z') \frac{\pi B_\nu(z')}{\sigma T(z')^4} \quad \text{A.2.5}$$

$$\alpha(z, z') = \int_0^\infty A_\nu(z, z') \frac{d[\pi B_\nu(z')]}{d[\sigma T(z')^4]}$$

Rewriting equation A.2.4 in terms of the broadband emissivities gives

$$F^-(z) = \sigma T_{zt}^4 \epsilon(z, \infty) + \int_{z_t}^z \alpha(z, z') \frac{d[\sigma T_z^4]}{dz'} dz' \quad \text{A.2.6}$$

For the upward flux $F^+(z)$, we can start with the equation

$$F^+(z) = \int_0^\infty d\nu \left[\pi B_\nu(0) T_\nu(z, 0) + \int_0^z \pi B_\nu(z') d[T_\nu(z', z)] \right] \quad \text{A.2.7}$$

This equation is a slightly modified version of A.1.17 with the diffuse transmission function being replaced by equation A.2.1. Following similar steps to the ones used in deriving equation A.2.6 we arrive at

$$F^+(z) = \int_0^\infty d\nu \left[\pi B_\nu(0) + \int_0^z \pi A_\nu(z, z') d[\pi B_\nu(z')] \right] \quad \text{A.2.8}$$

$$= \sigma T^4(0) + \int_0^z \alpha(z, z') d[\sigma T^4(z')] \quad \text{A.2.9}$$

for the net upward flux F^+ at level z .

Equations A.2.8 and A.2.4 are used in the calculation of the upward and downward flux of IR radiation for the spectral interval for which the band absorptance $\int A_\nu d\nu$ is given. This is the case for the involving calculations of CO_2 , CH_4 , N_2O , and O_3 . These spectral intervals are assumed to be narrow enough so

that B_{ν} can be estimated by the value of B_{ν} at the center of the band.

Equations A.2.6 and A.2.9 are used for IR flux calculations involving water vapor which has readily available emissivity data. Combining equations A.2.8 and A.2.9 the upward flux of IR radiation at level z due to water vapor and N other atmospheric gases is calculated according to,

$$F^+(z) = \sigma T^4(0) + \int_0^z \alpha_{H_2O}(z, z') d[\sigma T^4(z')] \quad A.2.10$$

$$+ \sum_{i=1}^N \int_0^z \pi A_{\nu_i}(z, z') \Delta V_i d[\pi B_{\nu_i}(z')]$$

The downward flux is calculated by combining equations A.2.4 and A.2.6 to give

$$F^-(z) = \sigma T_{zt}^4 \epsilon_{H_2O}(z, \infty) + \int_{z_t}^z \alpha_{H_2O}(z, z') d[\sigma T_z^4]$$

$$+ \sum_{i=1}^N \left\{ \pi B_{\nu_i}(z_t) A_{\nu_i}(z, \infty) \Delta V_i + \int_{z_t}^z A_{\nu_i}(z, z') \Delta V_i d[\pi B_{\nu_i}(z')] \right\} \quad A.2.11$$

The net heating rate (K/sec) of a layer of thickness Δz can be obtained from an inspection of Figure A.3 below.

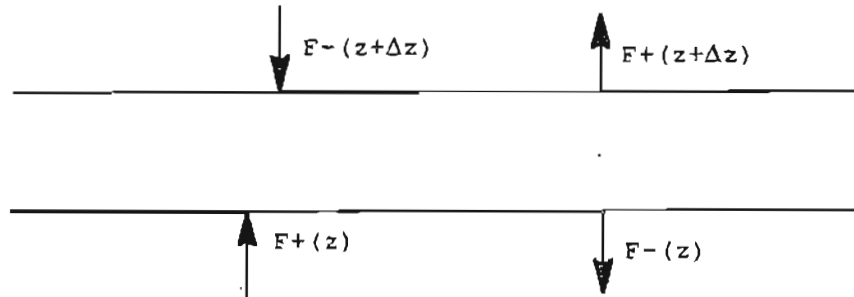


Figure A.3. Calculation of net heating rate in terms of fluxes of radiation.

As can be seen from Figure A.3,

$$\rho C_p \frac{\Delta T}{\Delta t} \Delta z = F^-(z + \Delta z) + F^+(z) - F^+(z + \Delta z) - F^-(z) \quad \text{A.2.12}$$

where ρ is the density of air in Kg/m³, C_p is the specific heat of air in J/(Kg K), Δz is in meters and F is in W/m². Defining the net flux to be $F = (F^+) - (F^-)$ then,

$$\frac{\Delta T}{\Delta t} = - \frac{1}{\rho C_p} \frac{\Delta F}{\Delta z} = \frac{g}{C_p} \frac{\Delta F}{\Delta p} \quad \text{A.2.13}$$

where $\Delta p = -\rho g \Delta z$ is the pressure difference between the bottom and top of the layer and g is the acceleration due to gravity.

In the OGI model subroutines "h2oir" and "acool"

are used to calculate the upward and downward fluxes of IR radiation according to A.2.10 and A.2.11 and then the cooling rate is calculated utilizing equation A.2.13.

Appendix B
Physical Constants and Conversions

B.1 Physical Constants

General

Na- Avragadro number $6.02 \times 10^{23} \text{ mol}^{-1}$

k- Boltzmann constant $1.38 \times 10^{-23} \text{ J/K}$

R- ideal gas constant 8.31 J/(K-mol)

L- Loschmidt number $2.69 \times 10^{19} \text{ cm}^{-3}$ (at STP)

h- Planck constant $6.63 \times 10^{-34} \text{ J-s}$

σ - Stefan-Boltzman's constant $5.67 \times 10^{-8} \text{ W/(m}^2\text{K}^4)$

c- Speed of light in vacuum $2.998 \times 10^8 \text{ m/s}$

Earth

Re- Mean Radius $6.37 \times 10^6 \text{ m}$

res- Mean Earth-Sun distance $1.50 \times 10^{11} \text{ m}$

g- acceleration og gravity 9.81 m/s^2

Do- Approximate mean depth of ocean 4000 m

Ao- Approximate areal extent of oceans 71%

Po- Standard surface pressure $1.013 \times 10^5 \text{ N/m}^2$

Ra- Specific gas constant for dry air .287 J/(K-g)

Cp- Specific heat of air at constant pressure 1.005
J/(K-g)

Cv- Specific heat of air at constant volume .718 J/(K-
g)

γ - Cp/Cv 1.40

Ma- Molecular mass of air 28.96 g/mol

Sun

Rs- mean solar radius 6.96×10^8 m

Ts- effective radiating temperature 5783 K

Water

ρ - density 1000 kg/m³ (fresh water)

Cw- specific heat 4.186 J/(K-g)

Lv- Latent heat of vaporization (at 373 K) 2256 J/g

Lf- Latent heat of fusion (at 273 K) 335 J/g

Mw- Molecular mass of water 18.0 g/mol

ϵ - Ratio of molecular mass of water to dry air .622

B.2 Conversion of Units

Pressure

$$1 \text{ atm} = 1.013 \times 10^5 \text{ N/m}^2 = 760 \text{ mmHg} = 1013 \text{ mbar} = 14.7 \text{ psi}$$

Absorber amounts U

$$U \text{ (atm-cm)} = C \times 0.8 \times \Delta P$$

$$U \text{ (g/cm}^2\text{)} = 3.56 \times 10^{-5} \times \Delta P \times C \times M_g$$

$$U \text{ (g/cm}^2\text{)} = 4.45 \times 10^{-5} \times M_g \times U \text{ (atm-cm)}$$

$$U \text{ (molecule/cm}^2\text{)} = L \times U \text{ (atm-cm)}$$

Note: C- is the concentration of the gas in ppmv
 ΔP - is the pressure difference between the top and bottom of the vertical path in atm
 M_g is the molecular mass of the gas in g/mol
L is the Loschmidt number $2.69 \times 10^{19} \text{ cm}^{-3}$

Appendix C Explanation of input file 'cdatc'

1,1,1 Line 1 are values of out1,out2,out3
253.30370 for output options
211.20200
207.28810
206.22660 Lines 2 through 20 are the initial values
203.29860 of the temperature of each layer at(i) (K).
217.45990 The values are read in from 1 to 19 (top
229.59090 of the atmosphere down).
240.10870
249.28610
257.30890
264.30650
270.36870
275.55600
279.90560
283.43410
286.13850
287.99610
288.96040
288.99650

-Lines 21,22: The initial ozone profile (uo(i)) total column
thickness(cm at STP) from the top of the atmosphere down.
-Lines 23,24: A new ozone profile after some prearranged time
tm3
-Line 25: The time tm3(days) when the ozone profile changes
tm3 is set to a value so the atmosphere has time to reach
equilibrium before the ozone profile changes. This allows for
a simple test to see what affect the ozone profile has on the
equilibrium temperature profile
0.00, .041, .210, .290, .328, .349, .359, .365, .367, .370
.373, .375, .377, .379, .381, .382, .383, .3833, .3836
0.0, .041, .210, .290, .328, .357, .372, .3795, .384, .3885
.3925, .3955, .399, .4015, .4045, .406, .4075, .4082, .4088
3

-Lines 26 & 27: The respective k & p values used in the
k-distribution for the calculation of solar absorption due to
water vapor in a cloudy atmosphere.(see text on water vapor

absorption in cloudy skies) The k and p values are not adjustable parameters.

.00004, .002, .035, .377, 1.95, 9.40, 44.6, 190.
.647, .0698, .1443, .0584, .0335, .0225, .0158, .0087

-Line 28: The solar constant divided by 2 (W/m^2); the zenith angle (degrees); the albedo at the top of the atmosphere; the time step (days); the equilibrium check condition (K); and the total number of days in program run

685, 60.0, .00, .300, .0001, 5

-Line 29: The critical lapse rate and the heat capacity of the earth's surface ($10^7 (J/(m^2 K))$). 2.09 corresponds to an ocean mixed layer depth of about 5.0 meters.

6.5, 2.0

-Line 30: Initial concentration of CO_2 (ppmv); the new concentration of CO_2 after some time tm_4 ; tm_4 (days); and the rate (1/yr) of growth of CO_2 ($c=c_0 \exp(\text{rate} \cdot \text{time})$).

Allowing equilibrium to be reached with the initial CO_2 concentration and then changing the CO_2 concentration at tm_4 (usually 1400 days) and letting the system reach equilibrium offers a method to check the influence of a change in CO_2 concentration on the equilibrium temperature profile. By setting tm_4 very large (greater than the duration of run to be made) and using a value of rate that simulates the growth of CO_2 allows for a study of the continuous change in temperature profile with time as the $\langle CO_2 \rangle$ increases.

320, 640, 4, 0.00

-Line 31: Same as for CO_2 except for CH_4 and without the rate option

1.6, 3.2, 2

-Line 32: Same as for CH_4 except for N_2O

.30, .45, 1

-Line 33: Amount of Cloud cover and layer in which the cloud resides

0.5, 11

-Line 34: Surface albedo and cloud optical depth

.10, 9.

-Line 35: Initial starting time usually just taken as 0.0

0.0

-line 36: The number of time steps (pout) before sending output to the screen or output files.

5

-line 37: If this value (dlast) is greater than day in line 28 above then the output files are closed, new output files are opened, a new input file cdat2 is read, and execution of the program is repeated

0

Appendix D Explanation of Output Options

D.1 Output When out1 Equals 1

```

*****
*   output of IR fluxes and heating/cooling rates(which are optional
*   in this output section
19  if(out1.eq.1) then
    if (tme.le.step.or.tme.gt.day) then
*   optional remove * at the beginning of each line to obtain output
*   write(20,*)
*   write (20,1019)
*   write (20,1010)
*   do 120 i=1,19
*       write(20,1000) pa(i),za(i),at(i),do(i),dw(i),dc(i),d4(i),
*   1 d5(i),ds(i),df(i)/(1.0+c(i))
*120  continue
*       write(20,*)
*25  write(20,1018)
*   write(20,1009)
*   do 30 i=1,18
*       write(20,1005) (ce(i)+ch(i))/step,dg(i)/(1+c(i))
*   x,shoc(i)+sho(i),shwc(i)+shw(i),sho2(i),shco2(i)
*30  continue
*       write(20,*)
*
*
*   write (20,1050)
*   write (20,1041)
*   write (20,1042) c20,c40,n20
*   write(20,1051)
*   write (20,1043) ac
*   write (20,1048) rg
*   write (20,1049) theta
*   write(20,1052) z(nt)
*   write (20,1050)
*   write (20,1051)
*   write(20,1020)
*   end if
*   write(20,1022) tme,f(19),g(19),f(1),f(nt),abtot,step,
*   x (sun-f(1))/sun,s1
*   end if
*****

```

The above section of the main program sends output to file oc3 if out1=1 (out1 is read in from the input file cdat1). The cooling rates and heating rates below were obtained by removing the asterisks in the above program section and are output only at the beginning and end of each run. Usually only the concentrations of the various gases, cloud fraction, ground albedo, average solar zenith (radians), and tropopause height are sent as output to the file oc3 at the beginning and end of each run. During the main run Time, F19, g19, F1, Fnt, abtot,step, and albedo are sent to oc3 after every pout time steps (where pout is read in from the input file usually cdat1). Definitions of output variables are:

```

*   press- the pressure at the middle of each layer
*   hght-  the height at the middle of each layer
*   temp-  the average temperature of each layer
*   do-   is the IR cooling due to Ozone (K/day)
*   dw-   "           water vapor

```

dc- " carbon dioxide
 d4- " methane
 d5- " Nitrous oxide
 ds- " all small concentration gases (< 5ppbv)
 dtot- is the total IR cooling
 Convect- total convective heating (K/day)
 tot het- Total heating due to solar absorption by all gases
 het o3- " ozone
 het wat- " water vapor
 het O2- " molecular oxygen
 het CO2- " carbon dioxide
 Time- time in days after the beginning of the run
 F19- downward IR flux at the surface (W/m²)
 g19- Solar radiative absorbed by the surface (W/m²)
 F1- Outward IR flux from the top of the atmosphere (W/m²)
 Fnt- Downward IR flux at the tropopause (W/m²)
 abtot- Total flux of solar radiation absorbed by the Earth-Atm.
 step- time step used
 albedo- Fraction of total incident solar radiation not absorbed

cooling rates in K/day

press	hght	temp	do	dw	dc	d4	d5	ds	dtot
.002	40.186	270.26	.978	.566	2.266	.030	.019	.000	3.857
.020	25.847	224.08	.135	.464	1.426	.017	.014	-.002	2.052
.053	19.754	206.89	-.364	.377	.498	.003	.001	-.002	.513
.099	15.956	208.13	-.279	.325	.199	-.004	-.006	-.002	.233
.156	13.193	204.85	-.179	.258	.092	-.010	-.011	-.002	.147
.223	11.007	217.22	-.077	.789	.986	-.012	-.010	-.002	.771
.297	9.143	229.34	-.033	1.515	.117	-.009	-.004	-.001	1.562
.376	7.526	239.85	-.006	1.735	.107	-.007	.000	.000	1.757
.458	6.116	249.02	-.001	1.683	.054	-.007	.003	.001	1.588
.542	4.883	257.03	.006	1.682	-.024	-.002	.004	.002	1.424
.624	3.808	264.02	-.130	6.105	-1.525	-.018	-.040	-.003	3.412
.703	2.876	270.08	-.002	.901	-.223	-.005	-.007	.001	.464
.777	2.079	275.26	.001	1.420	-.332	.001	-.007	.001	.674
.844	1.411	279.60	.002	1.907	-.434	.005	-.008	.002	.822
.901	.868	283.13	-.004	2.263	-.487	.007	-.009	.003	.896
.947	.453	285.83	-.003	2.513	-.494	.008	-.010	.003	.940
.980	.167	287.68	-.013	2.708	-.499	.008	-.009	.004	.967
.998	.019	288.65	.003	2.893	-.492	.009	-.009	.004	1.028
1.000	.000	288.77	.000	.000	.000	.000	.000	.000	.000

heating rates in K/day

Convect	tot het	het o3	het wat	het O2	het CO2
.000	3.858	3.733	.032	.070	.025
.000	2.054	1.933	.001	.055	.066
.000	.516	.414	.003	.049	.050
.000	.234	.145	-.006	.045	.037
.000	.148	.066	.009	.043	.030
.631	.141	.028	.047	.041	.025
1.276	.286	.015	.214	.040	.022
1.276	.482	.005	.439	.038	.020
1.043	.546	.007	.533	.038	.018
.869	.556	.007	.591	.037	.016
2.881	.529	.005	.625	.036	.015
.156	.309	.005	.387	.036	.014
.387	.289	.006	.410	.035	.014
.558	.266	.006	.423	.035	.013
.654	.243	.004	.431	.035	.013
.714	.228	.005	.437	.034	.013

.753	.217	.002	.444	.034	.012
.814	.215	.008	.449	.034	.012

```

*****
concentration of (ppmv)      CO2      CH4      N2O
                           320.0000   1.6000   .3000

cloud fraction      .50000
ground albedo      .10000
average solar zenith (radians)      1.04720
tropopause height(km)      10.04019
*****

```

Time	F19	g19	F1	FNT	abtot	step	albedo
.900	347.333	172.102	234.242	.000	234.414	.900	.311
6.300	347.358	172.101	234.251	-218.757	234.415	.900	.311
11.700	347.378	172.099	234.260	-218.766	234.415	.900	.311
17.100	347.401	172.098	234.267	-218.770	234.416	.900	.311
22.500	347.420	172.096	234.274	-218.776	234.417	.900	.311
27.900	347.441	172.095	234.280	-218.780	234.417	.900	.311

```

cooling rates in K/day
press  hght  temp  do  dw  dc  d4  d5  ds  dtot
.002  40.189  270.25  .978  .566  2.267  .030  .019  .000  3.858
.020  25.850  224.11  .135  .464  1.428  .017  .014  -.002  2.054
.053  19.755  206.96  -.364  .377  .499  .003  .001  -.002  .514
.099  15.957  208.15  -.279  .325  .199  -.004  -.006  -.002  .233
.156  13.194  204.86  -.179  .258  .092  -.010  -.011  -.002  .147
.223  11.008  217.24  -.077  .789  .086  -.012  -.010  -.002  .772
.297  9.143  229.35  -.033  1.515  .117  -.009  -.004  -.001  1.562
.376  7.527  239.86  -.006  1.736  .107  -.007  .000  .000  1.757
.458  6.116  249.03  -.001  1.683  .054  -.007  .003  .001  1.588
.542  4.883  257.04  .006  1.682  -.024  -.002  .004  .002  1.424
.624  3.808  264.03  -.130  6.107  -1.525  -.018  -.040  -.003  3.412
.703  2.876  270.09  -.002  .902  -.223  -.005  -.007  .001  .464
.777  2.079  275.27  .001  1.421  -.332  .001  -.007  .001  .675
.844  1.411  279.62  .002  1.908  -.434  .005  -.008  .002  .822
.901  .868  283.14  -.004  2.264  -.487  .007  -.009  .003  .896
.947  .453  285.84  -.003  2.513  -.494  .008  -.010  .003  .940
.980  .167  287.70  -.013  2.709  -.499  .008  -.009  .004  .967
.998  .019  288.66  .003  2.893  -.491  .009  -.009  .004  1.027
1.000  .000  288.79  .000  .000  .000  .000  .000  .000  .000

```

```

heating rates in K/day
Convect tot het het o3  het wat het O2  het CO2
.000  3.858  3.733  .032  .070  .025
.000  2.054  1.933  .001  .055  .066
.000  .516  .414  .003  .049  .050
.000  .234  .145  .006  .045  .037
.000  .148  .066  .009  .043  .030
.631  .141  .028  .048  .041  .025
1.276  .287  .015  .214  .040  .022
1.276  .482  .005  .439  .038  .020
1.042  .546  .007  .533  .038  .018
.868  .556  .007  .591  .037  .016
2.883  .529  .005  .625  .036  .015
.155  .309  .005  .388  .036  .014
.386  .289  .006  .410  .035  .014
.557  .266  .006  .423  .035  .013
.653  .243  .004  .431  .035  .013

```

.713	.228	.005	.437	.034	.013
.751	.217	.002	.444	.034	.012
.813	.215	.008	.449	.034	.012

```

*****
concentration of (ppmv)   CO2      CH4      N2O
                        320.0000   1.6000   .3000

cloud fraction          .50000
ground albedo          .10000
average solar zenith    1.04720
tropopause height(km)  12.05581
*****

```

Time	F19	q19	F1	FNT	abtot	step	albedo
30.600	347.448	172.094	234.284	-218.784	234.418	.900	.311

D.2 Output When out2 Equals 1

```

*****
*   output of vertical temperature profile and convective adjustment
*   in K/step
*   if(out2.eq.1) then
*       write (30,1011)
*       do 45 i=1,19
*           write(30,1035)  at(i),ch(i),ce(i)
45      continue
*       write(30,1036) tme
*   end if
*****

```

The above section of the main program sends output to file oc8 if out2=1 (out2 is read from the input file usually cdat1). For changes in the vertical temperature profile resulting from variations in input parameters this is the most useful output file. Con ch and Con ce are included because the format of this file is such that it can be pasted into the input file cdat1 for consecutive runs.

Definitions of output variables are:

Temp- temperature at each layer (270.26 is the temperature of the top layer, layer1)
 Con ch- convective adjustment during the last time step in K.
 Con ce- accumulated convective adjustment in K.

Temp (K)	Con ch	Con ce
270.25980	.00000	.00000
224.07530	.00000	.00000
206.89490	.00000	.00000
208.13070	.00000	.00000
204.84520	.00000	.00000
217.22480	.00000	.56829
229.34160	.00080	1.14770
239.84800	.00065	1.14805
249.01540	.00122	.93779
257.02950	.00208	.78033
264.01950	-.00136	2.59393
270.07510	.00095	.13929
275.25680	.00190	.34680
279.60170	.00229	.49974
283.12620	.00189	.58649
285.82780	.00200	.64046
287.68330	.00261	.67480
288.64650	.00206	.73068
288.77250	-.00147	-.97129
Time=	.90days	
Temp (K)	Con ch	Con ce
270.26040	.00000	.00000
224.08540	.00000	.00000
206.90880	.00000	.00000
208.13580	.00000	.00000
204.84750	.00000	.00000
217.22610	.00035	.56704
229.34390	.00006	1.14807
239.85040	.00012	1.14816

249.01800	.00009	.93845
257.03210	.00008	.78135
264.02230	.00038	2.59417
270.07800	.00010	.13990
275.25970	.00021	.34749
279.60460	.00011	.50077
283.12930	.00013	.58760
285.83090	.00043	.64144
287.68640	.00006	.67621
288.64960	.00003	.73189
288.77550	-.00021	-.97253
Time= 6.30days		
Temp (K)	Con ch	Con ce
270.25860	.00000	.00000
224.09290	.00000	.00000
206.92130	.00000	.00000
208.11970	.00000	.00000
204.85020	.00000	.00000
217.22830	.00005	.56778
229.34620	.00013	1.14821
239.85280	.00001	1.14817
249.02050	.00053	.93816
257.03480	.00006	.78130
264.02490	.00038	2.59420
270.08060	.00011	.13986
275.26250	.00022	.34749
279.60740	.00036	.50062
283.13200	.00028	.58747
285.83360	.00043	.64129
287.68920	.00011	.67613
288.65250	.00007	.73176
288.77840	-.00027	-.97251
Time= 11.70days		
Temp (K)	Con ch	Con ce
270.25600	.00000	.00000
224.09850	.00000	.00000
206.93250	.00000	.00000
208.14270	.00000	.00000
204.85320	.00000	.00000
217.23030	.00012	.56780
229.34840	.00007	1.14817
239.85510	.00003	1.14814
249.02290	.00016	.93832
257.03730	.00004	.78135
264.02750	.00004	2.59438
270.08330	.00001	.13996
275.26520	.00002	.34762
279.61020	.00022	.50066
283.13490	.00000	.58723
285.83650	.00004	.64143
287.69210	.00026	.67594
288.65530	.00002	.73176
288.78130	-.00009	-.97272
Time= 17.10days		
Temp (K)	Con ch	Con ce
270.25340	.00000	.00000
224.10260	.00000	.00000
206.94280	.00000	.00000
208.14500	.00000	.00000
204.85650	.00000	.00000

217.23240	.00015	.56779
229.35060	.00011	1.14812
239.85740	.00033	1.14797
249.02520	.00012	.93822
257.03970	.00028	.78116
264.03000	.00028	2.59426
270.08580	-.00007	.13986
275.26780	-.00005	.34747
279.61290	.00022	.50081
283.13760	.00004	.58765
285.83930	.00005	.64158
287.69490	-.00003	.67580
288.65810	.00042	.73163
288.78390	-.00014	-.97272
Time= 22.50days		
Temp (K)	Con ch	Con ce
270.25130	.00000	.00000
224.10550	.00000	.00000
206.95220	.00000	.00000
208.14690	.00000	.00000
204.86000	.00000	.00000
217.23430	.00031	.56784
229.35270	.00025	1.14807
239.85950	.00057	1.14781
249.02750	.00055	.93801
257.04200	.00027	.78103
264.03240	-.00008	2.59309
270.08830	.00010	.14007
275.27030	.00019	.34759
279.61540	.00005	.50090
283.14020	.00002	.58759
285.84190	.00015	.64158
287.69750	.00011	.67609
288.66070	.00005	.73172
288.78660	-.00023	-.97269
Time= 27.90days		
Temp (K)	Con ch	Con ce
270.25020	.00000	.00000
224.10670	.00000	.00000
206.95650	.00000	.00000
208.14760	.00000	.00000
204.86180	.00000	.00000
217.23530	.00008	.56801
229.35370	.00006	1.14824
239.86060	.00008	1.14809
249.02860	.00000	.93781
257.04320	-.00002	.78087
264.03350	.00030	2.59425
270.08940	.00000	.13990
275.27140	-.00006	.34749
279.61650	.00012	.50080
283.14130	.00017	.58742
285.84300	.00011	.64132
287.69860	.00017	.67595
288.66180	.00019	.73156
288.78790	-.00010	-.97280
Time= 30.60days		

D.3 Output When out3 Equals 1

```

*****
.*  output of surface time, temperature, ir flux leaving the
*   top of the atmosphere and total absorbed solar energy
    if (tme.le.step) then
      write(25,1060)
    end if
    if (out3.eq.1) then
      write(25,1038)  tme,at(19),f(1),abtot
    end if
*****

```

The above section of the main program sends output to file oc4 if out3=1 (out3 is read from the input file usually cdat1). For surface temperature changes resulting from variations in input parameters this is the most useful output file.
 Definitions of output variables are:

time- time in days after the start of the run
 Surface T- surface temperature after time days.
 Fout- the outward flux of IR radiation from the top of the atmosphere (W/m²)
 abtot- The total absorbed solar radiation (W/m²) by the Earth-Atmosphere system.

time	Surface T	Fout	abtot
.90000	288.77250	234.24210	234.41420
6.30000	288.77550	234.25080	234.41480
11.70000	288.77840	234.25960	234.41550
17.10000	288.78130	234.26670	234.41610
22.49999	288.78390	234.27420	234.41670
27.89999	288.78660	234.28040	234.41730
30.59999	288.78790	234.28420	234.41760

D.4 Output Sent to Screen Every pout Time steps.

```

*****
      prt=prt+1.
      if (prt.gt.pout.or.tme.lt.02*step) then
      prt=0.0
*   output to screen
      print*,s1-low,tme,at(19),at(18),sun-sout,f(1)
      goto 19
      end if
*****

```

The above section of the main program sends output to the screen every pout time steps. This helps keep track of how the run is doing.

s1-low is the difference between the sum of the absolute values of the temperature changes for all layers during the last step and the value low. (If s1-low < 0.00 execution of program stops since equilibrium has been reached.) It is useful at to monitor this to determine how close the program is to equilibrium. Typically the s1-low is not used as a condition to determine if the program has reached equilibrium. The equilibrium conditions is usually met when the absolute value of $f(1)-(sun-sout)$ is less than 0.02 W/m², where $f(1)$ is the IR flux leaving the top of the atmosphere and $(sun-sout)$ is the total absorbed solar flux.

at(19) and at(18) are the average surface temperature and temperature of the lowest atmospheric layer respectively.

Below is a sample of what the screen looks like after the sample 30 day run.

```

C:\MAC>lhb
  2.147695E-02   9.000000E-01   288.772500   288.646500
  234.414100    234.242100
  1.160050E-02   6.300000   288.775500   288.649600
  234.414800    234.250800
  9.689319E-03  11.700000   288.778400   288.652500
  234.415400    234.259600
  9.622664E-03  17.100000   288.781300   288.655300
  234.416100    234.266700
  1.045937E-02  22.499990   288.783900   288.658100
  234.416700    234.274200
  7.804778E-03  27.899990   288.786600   288.660700
  234.417300    234.280400
done

```

Appendix E
Program Source Code

```

program rcm
*****
*   This program is an 18 layer one-dimensional
*   time-dependent radiative convective model of the
*   Earth-atmosphere system.
*   It was developed by Robert M. MacKay and M.A.K.
*   Khalil at the Oregon Graduate Institute of Science
*   and Technology, Center of Atmospheric Studies,
*   Beaverton, Oregon 97006-1999 USA.
*   Disk copies of this program may be obtained from
*   the authors at any time.
*****
*   *****Description of variables*****
*****
*   t, z, p, b, uo, and ul are the temperature, height,
*   pressure, planck function, first ozone profile,
*   optional ozone profile associated with the top and
*   bottom of each atmospheric layer respectively.
*   sg is the sigma variable used for identifying
*   the pressure of each layer.
*****
*   at, pa, za, uoa, cp are the temp., press., height,
*   ozone amt, and total heat capacity for each layer.
*   c is the ratio of the total heat capacity, moist +
*   dry, to the dry heat capacity of each layer.
*****
*   ta is the average temperature for a path between
*   layer i and j ut is the transferred from subroutines
*   n2o5cool and n2o6cool.
*****
*   gam is the critical lapse rate for convective
*   adjustment at each layer. ce+ch the net convective
*   heating at each layer in K/step
*****
*   tr2 is the H2O CO2 overlap transmission
*   tco2n2 is the n2o CO2 overlap transmission
*   tnc4 is the N2O CH4 overlap transmission
*   tr5 is the H2O N2O (1285 cm-1) overlap transmission
*   tr3 is the H2O Ozone overlap transmission
*   tr4 is the H2O CH4 overlap transmission
*   tr6 is the H2O N2O (580 cm-1) overlap transmission
*****

```

```

*      dg is the total solar heating of each layer in
*      K/day
*      sho,shw,shoc,shwc,shco2,sho2 are the solar heating
*      terms
*      due to ozone, water, ozone cloudy portion, water
*      cloudy
*      portin, CO2, and oxygen respectively in K/day.
*      Note: these calculations assume that the layer is
*      dry and hence a term (1+c) is use in the actual
*      calculations of temperature change in subroutine
*      tempchg.
*      g(19) is the total flux of solar radiation absorbed
*      by the surface and g(1) is the solar energy into
*      the top of the atmosphere. gw,go,gwc, and goc are
*      the above for the subroutines for water and ozone
*      clear and cloudy skies.
*      xk, and pk are k and probability values for k
*      distribution method for calculation of solar
*      absorpition by water vapor in cloudy skies.
*****
*      df is the total ir cooling (assuming a dry layer)
*      in K/day
*      dc,dw,do,d4,d5,ds are the corresponding cooling
*      rates for CO2, water, ozone methane, nitrous oxide
*      1285 cm-1 and nitrous oxide 580 cm-1, and small
*      conc trace gases (F11,F12,...)
*      respectively. As with solar absorpition
*      the effective heat capacity due to moisture changes
*      is accounted for in subroutine tempchg
*      f(19) is the total downward flux of ir radiation at
*      the earth's surface, f(1) is the total upward flux
*      of ir radiation at the top of the atmosphere, and
*      f(nt) is the total downward flux of
*      ir radiation at the tropopause. fw,fc,fo,f4,f5,
*      and fs are the corresponding values returned from
*      the subroutines water, co2,
*      ch4cool, o3cool, n2o5cool, and small
*****
*
      real t(20),z(20),p(20),sg(20),b(20),uo(20),u1(20)
      real at(20),pa(20),za(20),uoa(20),cp(20),c(20)
      real ta(20,20),ut(20,20),ca(20,20)
      real gam(20),ch(20),ce(20)
      real tr2(20,20),tco2n2(20,20)
      real tnc4(20,20), tr5(20,20)
      real tr3(20,20),tr4(20,20),tr6(20,20)
      real dg(20),sho(20),shw(20),shoc(20)
      real shwc(20), shco2(20),sho2(20)
      real g(20),gw(20),go(20),gwc(20),goc(20)

```

```

real xk(10),pk(10)
real qc(4),dq(4,14),ec(14),vc(14),sc(14)
real dc(20),dw(20),do(20),d4(20),d5(20),ds(20)
real df(20),f(20),fo(20),fw(20),fc(20),f4(20)
real f5(20),fs(20)
*****
*   s0-solar constant / 2.0
*   theta- average solar Zenith angle
*   step- time step between calculations (days)
*   albedo - reflectivity of the top atmospheric layer
*   ( usually=0.0)
*   s1- sum of abs(delta T) for each layer during each
*   step
*   low- if s1 is less than low then equilibrium has
*   been reached
*   tme- time (days)
*   day- if tme if greater than day then program
*   execution stops
*   sout- the outward flux of solar radiation from the
*   top of atm
*   lap-lapse rate for fixed lapse rate adjustment
*   (usually 6.5)
*   sun- s0*cos(theta)
*   abw-total solar absorption by water vapor (clear
*   skies)
*   abwc-total solar absorption by water vapor (cloudy
*   skies)
*   abo-total solar absorption by ozone (clear skies)
*   aboc-total solar absorption by ozone (cloudy skies)
*   abo2-total solar absorption by oxygen
*   abco2-total solar absorption by carbon dioxide
*   abtot-total solar absorption by all gases
*   c20-initial concentration of carbon dioxide
*   rate- growth rate (1/yr) of CO2
*   c40-initial concentration of methane
*   n20-initial concentration of nitrous oxide
*   c21- concentration of CO2 after time = tm1
*   c41-concentration of CH4 after time = tm2
*   N21-concentration of N2O after time = tm4
*   tm3-time after wich ozone profile changes
*   con2-time dependent concentration of CO2
*   depth- optical depth of the cloud
*   rg- surface albedo
*   ac- horizontal cloud extent
*   pout- output sent to files every (step*pout days)
*   dlast-for multiple runs if dlast is greater than
*   day
*   then then program resets with input from cdat2 and
*   reruns automatically

```

```

*      kap- cloud layer
*      nt- tropopause layer
*      out1,out2,out3- controls output of data see below
*****
      real s0,theta,step,albedo,s1,low,tme,day,sout,lap
      real sun,abw,abo,abwc,aboc,abo2,abco2,abtot
      real c20,rate,c40,n20,c21,c41,n21,tm1,tm2,tm3,tm4
      real con2,depth,rg,ac,pout,dlast
      integer kap,nt,out1,out2,out3,gp,nr
*****
*      The data qc,vc,sc,and ec are for the CO2 15 micron
*      band calcs following Kiehl and Ramanathan (1983).  qc
*      are the isotopic abundances relative to C-16 O2-18;
*      vc is the wavenumber at the center
*      of each band; sc is the band strength; and ec is the
*      energy of the lower state for each transition.
      data qc(1),qc(2),qc(3),qc(4)/1.0,.0112,.00408,
      x .000742/
      data vc(1),vc(2),vc(3),vc(4),vc(5),vc(6),vc(7)
      x ,vc(8),vc(9),vc(10),vc(11),vc(12),vc(13),vc(14)
      x /667.38, 618.029,720.805,667.751,647.063,791.446
      x,597.34,741.72,668.11,544.29,668.67, 652.52,720.29,
      x 615.89/
      data sc(1),sc(2),sc(3),sc(4),sc(5),sc(6), sc(7),
      x sc(8),sc(9),sc(10),sc(11),sc(12),sc(13),sc(14)
      x /194.0,4.27,5.0,15.0,.6,.022,.14,.144, .85,.01,.3,
      x .045, .005,.015/
      data ec(1),ec(2),ec(3),ec(4),ec(5),ec(6),ec(7)
      x ,ec(8), ec(9),ec(10),ec(11),ec(12),ec(13), ec(14)
      x /0.00,667.38,667.38,667.38,1285.41,1285.41,
      x 1335.13, 1335.13,1335.13,1388.185,1388.185,
      x 1932.473,2076.855,1932.473/
*      dq is the mean spacing between lines for each band
*      of CO2 15 micron region
      do 2 i=1,4
      do 1 j=1,14
      if (i.ge.3) then
      dq(i,j)=0.78
      else
      if(j.eq.4.or.j.eq.7.or.j.eq.8.or.j.eq.9.or.
x j.eq.12) then
      dq(i,j)=.78
      else
      dq(i,j)=1.56
      endif
      endif
1      continue
2      continue
*      open input/output files

```

```

      open(unit=10,file='cdat1',status='old')
*   qp is a toggle for multiple program runs using
*   different input files.
*   the first time through oc3,oc4, and oc8 are output
*   files. The next time through the ouput files are
*   assigned at the end of the main program
*   to be oc2,oc5, and oc7 and execution is redirected to
*   line 3 so that the output format can be read from the
*   new input file cdat2.
      qp=0
*   nr is a counter used in subroutine co2. it is
*   incremented by 1 each time co2 is called and when
*   nr=10 new absorbtivities for co2 are
*   calculated based on the new temperature structure.
*   Since the temperature dependence of the absorptivities
*   is weak and the computations are time consuming this
*   save time without introducing errors.
      nr=0
*   out1,out2,out3 =0 no output to oc3,oc8,oc4 =1 yes
*   output. This helps easily control the amount of
*   output sent to files.
3     read(10,*) out1,out2,out3
      if(qp.eq.0)then
        if(out1.eq.1) then
          open(unit=20,file='oc3' )
          end if
        if (out3.eq.1) then
          open(unit=25,file='oc4' )
          end if
        if(out2.eq.1) then
          open(unit=30,file='oc8' )
          end if
        end if
      qp=1.0
*****
*     read input data
      read(10,1034) (at(i),i=1,19)
      read(10,*) (uo(i),i=1,19)
      read(10,*) (u1(i),i=1,19)
      read(10,*) tm3
      read(10,*) (xk(i),i=1,8)
      read(10,*) (pk(i),i=1,8)
      read(10,*) s0,theta,albedo,step,low,day
      read(10,*) lap,cp(19)
      read(10,*) c20,c21,tm4,rate
      read(10,*) c40,c41,tm2
      read(10,*) n20,n21,tml
      read(10,*) ac,kap
      read (10,*) rg,depth

```

```

        read(10,*)tme
        read(10,*)pout
        read(10,*)dlast
* calculate ozone amounts from top of atm to center of
* each layer
        do 4 i=1,18
            uoa(i)=(uo(i)+uo(i+1))/2
4        continue
* use heat capacity units of Watts-Day/(m^2 K)
        cp(19)=cp(19)*1e7/86400
        nt=6.0
            sun=s0
            s0=s0*(1.0-albedo)
            theta=theta*3.1415926/180.0
            sun=sun*cos(theta)
            g(1)=s0*cos(theta)
*
* set initial pressures,temperature,height, and
* reference lapse
* rate of each layer.
        call presset(sg,p,pa)
        call tempset(t,at,p,kap)
        call height(z,za,p,pa,at)
* lap1 assigns a fixed lapse rate adjustment
        call lap1(gam,lap)
*
* main iterative part of the program
* calculate pressure weighted average temperature
* btwn layer i and j
10 call tempave (at,sg,ta)
* calculate the n2o (1285 cm-1) ch4 overlap
        call n2c41285 (tnc4,p,pa,at,c40)
* moist adiabatic lapse rate calculation (used
* instead of lap1 above)
        call lap2 (gam,at,pa)
* recalc temps at top and bottom of each layer
        call tempset (t,at,p,kap)
* optional used to continuously change the
* concentrations
* of trace gases for extra long runs
* call conchg(tme,n20,c20,c40)
        if ((tme.gt.tm1.and.tme.le.tm1+step).or.
x(tme.gt.tm2.and.tme.le.tm2+step).or.(tme
x .gt.tm3.and.tme.le.tm3+step).or.(tme.gt.tm4.and
x .tme.le.tm4+step))then
* conchk checks tme with tm1,tm2,tm3,tm4 to see if the
* concentration of a gas is to change by a discrete
* amount
        call conchk(tme,n20,c20,c40,n21,c21,c41

```



```

x ,tm1,tm2,tm3,tm4,uo,u1,uoa,cp,at,step)
endif
*
* Calculate h2o IR absorption and transmissions
  call h2oir (pa,at,p,t,ta,dw,fw,tr2,ac,kap,tr3,
x tr4,tr5,tr6,nt)
*
* update co2 concentration and calculate IR absorption
* transmission
  con2=c20*exp(rate*tme/365.)
  call co2ir (t,p,pa,dc,fc,ta,tr2,tr3,con2
x ,ac,kap,tco2n2,nt,qc,dq,ec,vc,sc,ca,nr)
*
* Calculate clear sky solar absorption due to water
* vapor
  call h2ovisclr(s0,theta,pa,p,at,shw,gw,abw
x ,ac,rg,kap)
*
* Calculate cloudy sky solar absorption due to water
* vapor
  call h2ocloud (p,pa,at,xk,pk,depth,theta,s0,rg,kap
x,ac,shwc,abwc,gwc)
*
* Methane IR absorption
  call ch4ir (ta,p,pa,t,d4,f4,tr4,c40,ac,kap,nt)
*
* N2O (1285 cm-1) IR absorption
  call n2o1285 (ta,p,pa,t,d5,f5,tr5,tnc4,
x n20,ac,kap,nt,ut)
*
* N2O (590 cm-1) IR absorption
  call n2o590 (p,pa,ta,t,d5,f5,tr6,tco2n2,
x n20,ac,kap,nt,ut)
*
* set ds and fs to zero each time before
* recalculation
  do 15 i=1,19
    ds(i)=0.0
    fs(i)=0.0
15 continue
* calculate contribution to ds and fs for a trace gas
of small
* concentration (less than 5 ppbv). 275 is the
* concentration in ppt
* 850 is the band center, and 1828 is the band
* strength. The first
* two calls to small below are for F11 and the next
* three are for F12.
* the transmission of the H2O continuum at 1000 cm-1 is

```

```

*   used for the
*   overlap correction for each band in the window region
*   800-1200 cm-1.
      call smallir (ta,p,pa,t,ds,fs,275.,ac,kap,
        x nt,850.0, 1828.0,tr3)
*
      call smallir (ta,p,pa,t,ds,fs,275.,ac,kap,
        x nt,1075.0,679.0,tr3)
*
      call smallir (ta,p,pa,t,ds,fs,468.,ac,kap,
        x nt,912.0,1446.0,tr3)
*
      call smallir (ta,p,pa,t,ds,fs,468.,ac,kap,
        x nt,1090.0,1140.0,tr3)
*
      call smallir (ta,p,pa,t,ds,fs,468.,ac,kap,nt,
        x 1150.0,767.0,tr3)
*
      call smallir (ta,p,pa,t,ds,fs,.00028,ac,kap,nt,
        x 1150.0,767.0,tr3)
*
      call smallir (ta,p,pa,t,ds,fs,.00028,ac,kap,nt,
        x 1150.0,767.0,tr3)
*
*   Ozone planck function and IR absorption
      call plank(b,t,1042.)
*
*   IR cooling due to O3.
      call o3ir (at,b,p,pa,uo,uoa,do,fo,ac,kap,nt,tr3)
*
*   ozone clear and cloudy skies solar absorption
*   Clear
      call o3visclr (s0,theta,uo,p,sho,go,abo,ac,rg)
*
*   Cloudy
      call o3cloud (s0,theta,uo,p,shoc,goc,aboc,
        x ac,rg,kap,depth)
*
*   solar absorption for CO2
      call co2vis (p,pa,shco2,abco2,c20,s0,theta,kap,ac)
*
*   solar absorption for molecular oxygen
      call oxyvis (p,sho2,abo2,s0,theta,kap,ac)
*
*   combine IR and Solar heating rates and fluxes
      call combine(dw,dc,do,d4,d5,ds,shw,shwc,shoc
        x      ,sho2,shco2,sho,dg,df)
      f(19)=fw(19)+fc(19)+fo(19)+f4(19)+f5(19)+fs(19)
      f(18)=fw(18)+fc(18)+fo(18)+f4(18)+f5(18)+fs(18)

```

```

    f(nt)=fw(nt)+fc(nt)+fo(nt)+f4(nt)+f5(nt)+fs(nt)
    g(19)=goc(19)+gwc(19)+go(19)+gw(19)-
x(1-rg)*(abo2+abco2)
    abtot=abw+abo+aboc+abwc+rg*(abo2+abco2)
    f(1)=fw(1)+fc(1)+fo(1)+f4(1)+f5(1)+fs(1)
    sout=albedo*sun+(g(1)-abtot)
*   change the average temperature of each layer
    call tempchg(pa,p,cp,at,dg,df,g,step,s1,f
x,ch,ce,kap,ft,c)
*   recalculate the height of each layer
    call height(z,za,p,pa,at)
*   perform the lapse rate adjustment
    call lapadj (at,gam,za,cp,ch,nt,ce)
*   update time
    tme=tme+step
*   update printer count
    prt=prt+1.
    if (prt.gt.pout.or.tme.lt.02*step) then
        prt=0.0
*   output to screen
    print*,s1-low,tme,at(19),at(18),sun-sout,f(1)
        goto 19
    end if
*
    if (tme.gt.day) then
        goto 19
    end if
*
    if (s1.gt.low) then
        goto 10
    end if
*****
*   output of IR fluxes and heating/cooling
*   rates(which are optional
*   in this output section
19   if(out1.eq.1) then
        if (tme.le.step.or.tme.gt.day) then
*   optional remove * at the beginning of each line to
*   obtain output
*   write (20,1010)
*   do 120 i=1,19
*   write(20,1000) pa(i),za(i),at(i),do(i),dw(i)
x,dc(i),d4(i), d5(i),ds(i),df(i)/(1.0+c(i))
*120 continue
*25 write(20,1018)
*   write(20,1009)
*   do 30 i=1,18
*   write(20,1005) (ce(i)+ch(i))/step,dg(i)/(1+c(i))
*   x,shoc(i)+sho(i),shwc(i)+shw(i),sho2(i),shco2(i)

```

```

*30   continue
*
*
      write (20,1050)
      write (20,1041)
      write (20,1042) c20,c40,n20
      write(20,1051)
      write (20,1043) ac
      write (20,1048) rg
      write (20,1049) theta
      write(20,1052) z(nt)
      write (20,1050)
      write (20,1051)
      write(20,1020)
      end if
      write(20,1022) tme,f(19),g(19),f(1),f(nt),abtot
x,step, (sun-f(1))/sun,s1
      end if
*****
*   output of vertical temperature profile and
*   convective adjustment in K/step
      if(out2.eq.1) then
      write (30,1011)
      do 45 i=1,19
      write(30,1035) at(i),ch(i),ce(i)
45   continue
      write(30,1036) tme
      end if
*****
*   output of surface time, temperature, ir flux leaving
*   the top of the atmosphere and total absorbed solar
*   energy
      if (tme.le.step) then
      write(25,1060)
      end if
      if (out3.eq.1) then
      write(25,1038) tme,at(19),f(1),abtot
      end if
*****
      if (tme.gt.day) then
      goto 100
      end if
*
      if (s1.gt.low) then
      goto 10
      end if
*
*   then next 15 lines allows the program to be reset
*   automatically to new initial conditions found in

```

```

*   'cdat2' provided "dlast" from cdat1 is larger than
*   the length of the first run
*   " day" from cdat1
100  if (tme.lt.dlast) then
      close(unit=10)
      open(unit=10,file='cdat2',status='old')
      if (out1.eq.1) then
        close(unit=20 )
        open(unit=20,file='oc2' )
      end if
      if (out3.eq.1) then
        close(unit=25)
        open(unit=25,file='oc5' )
      end if
      if (out2.eq.1) then
        close(unit=30)
        open(unit=30,file='oc7' )
      end if
      goto 3
    end if
    print*, 'done'
*****
1000  format(10(f6.3,2x))
1005  format (2x,6(f7.3,1x))
1009  format (2x,'Convect',1x,'tot het',1x,
2'het o3',2x,'het wat',1x,'het O2',2x,'het CO2')
1010  format('press',3x,'hght',4x,'temp',4x,'do',6x,'dw'
1,6x,'dc', 6x,'d4',6x,'d5',6x,'ds',6x,'dtot')
1011  format ('Temp (K)',6x,'Con ch',8x,'Con ce')
1019  format ('cooling rates in K/day')
1018  format ('heating rates in K/day')

1020  format('Time',6x,'F19',7x,'g19',7x,'F1',8x,'FNT'
x,7x,'abtot',5x,'step',6x,'albedo',4x,'S1',6x)
1022  format(9(f8.3,2x))
1034  format (f10.5)
1035  format (3(f10.5,4x))
1036  format ('Time=',f8.2,'days')
1038  format (4(f10.5,4x))
1042  format (25x,3(f8.4,2x))
1041  format (1x,'concentration of (ppmv)      CO2
x CH4      N2O')
1043  format (2x,'cloud fraction',1x,f10.5)
1048  format (2x,'ground albedo',1x,f10.5)
1049  format (2x,'average solar zenith',1x,f10.5)
1050  format (80('*'))
1051  format (' ')
1052  format(2x,'tropopause height(km)',1x,f10.5)
1060  format(1x,'time',10x,'Surface T',5x,'Fout',10x,

```

```

      x'abtot')
      end
*****
* use for long runs from pre 1860 to 1990 using a linear
* interpolation method to calculate the concentration
* of CO2,CH4, F11, and
* F12 according to the values given by Hansen et al 1989
* at the times 1860, 1960, 1970,1980, and 1980.
      subroutine conchg(tme,n20,c20,c40)
      real tme,n20,c40,c20
      if (tme.gt.1860.and.tme.lt.1960) then
      c20=285+.317*(tme-1860)
      c40=.8+.005*(tme-1860)
      end if
      if (tme.gt.1960.and.tme.lt.1970) then
      c20=316.7+.810*(tme-1960)
      c40=1.3+.01*(tme-1960)
      end if
      if (tme.gt.1970.and.tme.lt.1980) then
      c20=324.8+1.28*(tme-1970)
      c40=1.4+.015*(tme-1970)
      end if
      if (tme.gt.1980) then
      c20=337.6+1.59*(tme-1980)
      c40=1.55+.0175*(tme-1980)
      end if
      if (tme.gt.1940) then
      n20=.285+.0005*(tme-1940)
      end if
      return
      end
*****
* used for step wise concentration changes ie 2xCO2 etc.
* if tme is greater than tm1,tm2,tm3,tm4 the the
* concentration of N2O changes from n20 to N21, .....
      subroutine conchk(tme,n20,c20,c40,n21,c21,c41
      x ,tm1,tm2,tm3,tm4,u0,u1,uoa,cp,at,step)
      real u0(20),u1(20),uoa(20),cp(20),at(20)
      real c20,c21,n20,n21,c40,c41,tme,tm1,tm2,tm3,tm4
      real step
      if (tme.gt.tm1.and.tme.le.tm1+step) then
      n20=n21
*       cp(19)=20.0*1e7/86400
*       do 200 i=1,19
*         at(i)=290.0
*200    continue
      end if
      if (tme.gt.tm2.and.tme.le.tm2+step) then
      c40=c41

```

```

end if
if (tme.gt.tm3.and.tme.le.tm3+step) then
do 201 i=1,19
  uo(i)=u1(i)
  uo(i+1)=u1(i+1)
  if (i.le.18)then
    uoa(i)=(uo(i+1)+uo(i))/2.0
  end if
201 continue
end if
if (tme.gt.tm4.and.tme.le.tm4+step) then
c20=c21
end if
  write(20,1041)
  write (20,1042) c20,c40,n20,uo(19)
  write(20,1045)
write (20,1030) tme
write(30,1041)
  write (30,1042) c20,c40,n20,uo(19)
write(30,1045)
write (30,1030) tme
1030 format (f10.5)
1045 format ('time in days')
1042 format (25x,4(f8.4,2x))
1041 format ('concentration of (ppmv)      CO2      CH4
x N2O      O3tot')
return
end
*****
* Used to calculate the temperature change of each layer
* and the surface after each time step.
  subroutine tempchnng(pa,p,cp,at,dg,df,g,step,s1,f,
x ch,ce,kap,abt,c)
  real pa(20),at(20),dg(20),df(20),f(20),g(20),ch(19)
  real p(20),cp(20),ce(20),c(20)
  real dt,s1,dr,step,e1,e,q,l
  integer kap
  abt=0.0
  et=0.0
  s1=0.0
  do 3400 j=1,18
*   if (j.eq.kap) then
*     h=1.0
*   end if
    e1=esat(at(j)+1)
    e=esat(at(j))
*   calculate modified heat capacity Manabe & Wetherald
*   1967?
*   dr is the derivative of absolute humidity wrt

```

```

* temperature
  dr=rwat(pa(j),e1,j,kap)-rwat(pa(j),e,j,kap)
  l=2510-2.38*(at(j)-273)
  c(j)=.622*1*1*rwat(pa(j),e,j,kap)
  x/(1.005*.287*at(j)**2)
* Heat capacity units are Watt-day/(K m^2). when cp(i)
* is multiplied by the heating or cooling in K/day then
* the result is the heating or cooling in Watts/m^2
  cp(j)=(1.0+c(j))*1.038165e7*(p(j+1)-p(j))/86400
* Note dg and df are in units of K/day assuming a dry
* atmosphere.
* Hence we divide by 1.0+c(j) to get the moist atmosphere
* results.
  dt=step*(dg(j)+((ce(j))*(1.0+c(j))/step)-df(j))
  x/(1.0+c(j))
* et is the total energy in W/m^2 given to the
* atmosphere by the surface
* during convection.
  et=et+cp(j)*(ce(j))
  sl=sl+abs(dt+ch(j))
  at(j)=at(j)+dt
3400 continue
  et=et/step
  ce(19)=-et*step/cp(19)
  q=(g(19)-et+f(19)-5.67e-8*(at(19))**4)
  q=step*q/(cp(19))
  at(19)=at(19)+q
  return
end
*****
* Combines heating and cooling rates from all
* atmospheric gases considered
  subroutine combine (dw,dc,do,d4,d5,ds,shw,shwc
  x,shoc, sho2,shco2,sho,dg,df)
  realdw(20),dc(20),do(20),shw(20),sho(20),shwc(20)
  real shoc(20),shco2(20)
  real dg(20),df(20),d4(20),d5(20),d6(20),sho2(20)
  do 3500 i=1,18
  df(i)=dw(i)+do(i)+dc(i)+d4(i)+d5(i)+d6(i)
  dg(i)=shw(i)+sho(i)+shwc(i)
  x+shoc(i)+shco2(i)+sho2(i)
3500 continue
  return
end
*
*****
* Calculates IR cooling due to all bands of water vapor.
* Also calls h20trans which calculates the transmission
* of water vapor for various spectral regions to be used

```



```

*   in overlap corrections.
      subroutine h2oir (pa,at,p,t,ta,dw,fw,tr2,ac,kap,
        x tr3,tr4,tr5,tr6,nt)
*   em and am are the water vapor emissivities and
*   modified emissivities for rotation and vibration
*   -rotation bands using and empirical
*   fit given by Ramanathan 1976 see chapter 3 of text
      dimension pa(20),p(20),dw(20),t(20),fw(20),at(20)
      dimension ta(20,20),em(20,20),am(20,20)
      dimension tr1(20,20),tr2(20,20),tr3(20,20)
      real fu(20),fd(20),ftot(20),b(20),drl(20),fr(20)
      real tr4(20,20),tr5(20,20),tr6(20,20),trc(20,20)
      real sig,cf,eml,u1,e,ac
      integer kap,nt
*   sig is the Stefan-Boltzman constant
      sig=5.67e-8
      call h2otrans (pa,at,p,tr1,tr2,tr3,tr4,tr5,tr6,trc
        x,kap)
*   tr1 is the water vapor continuum transmission from 480
*   to 800 cm-1
*   and tcool calculates the cooling rate due to it. trc
*   is the emissivity of the water vapor continuum between
*   800 and 1200 cm-1 and is calculate in
*   h2otrans and then added to em.
      call bpl (b,t,730.0)
      call tcool (140.,tr1,b,p,drl,fr,ac,kap,nt)
*
      do 740 i=2,19
      do 739 j=1,i-1
          e=esat(at(j))
*   r is the absolute humidity of water vapor gH2O/g Air.
*   u1 is the temperature and pressure corrected path
*   length of water vapor in g/cm^2
          r=rwat(pa(j),e,j,kap)
          if (j.eq.1) then
              u1=((p(j+1))/2)*sqrt(273/at(j))*r*1033*(p(j+1))
          else
              u1=((pa(j)+p(j+1))/2)*sqrt(273/at(j))
x*r*1033*(p(j+1)-pa(j))
          end if
          do 735 k=j+1,i-1
              e=esat(at(k))
              r=rwat(pa(k),e,k,kap)
              u1=u1+pa(k)*sqrt(273/at(k))*r*1033*
x(p(k+1)-p(k))
735      continue
          eml=(1-.5*((1/(1+19*sqrt(u1))))+
x(1/(1+3.5*sqrt(u1))))
          eml=eml*.59*((273/ta(j,i))**.25)

```

```

        em(j,i)=eml+trc(j,i)
        am(j,i)=.847*(u1**.022)*em(j,i)
739    continue
740    continue
        do 760 i=1,19
        do 759 j=1,i
            e=esat(at(i))
            r=rwat(pa(i),e,i,kap)
            u1=((pa(i)+p(i))/2)*sqrt(273/at(i))*r*1033
            x*(pa(i)-p(i))
            do 755 k=j,i-1
                e=esat(at(k))
                r=rwat(pa(k),e,k,kap)
                u1=u1+pa(k)*sqrt(273/at(k))*r*1033*
            x*(p(k+1)-p(k))
755    continue
            eml=(1-.5*((1/(1+19*sqrt(u1)))+
            x(1/(1+3.5*sqrt(u1))))))
            eml=eml*.59*((273/ta(j,i))**.25)
            em(i,j)=eml+trc(i,j)
            am(i,j)=.847*(u1**.022)*em(i,j)
759    continue
760    continue
* fd and fu are the downward and upward fluxes of IR
* radiation at each layer. fd(2) is the downward IR Flux
* at the top of layer 2.
        fd(1)=0.0
        do 780 i=2,19
            if (i.gt.kap) then
                cf=1.0-ac
            else
                cf=1.0
            end if
            fd(i)=cf*sig*em(1,i)*t(1)**4
            do 779 j=1,i-1
                fd(i)=fd(i)+cf*am(j,i)*sig*(t(j+1)**4-t(j)**4)
779    continue
780    continue
            do 785 i=kap+1,19
                fd(i)=fd(i)+ac*sig*t(kap+1)**4
                do 784 j=kap+1,i-1
                    fd(i)=fd(i)+ac*am(j,i)*sig*(t(j+1)**4-t(j)**4)
784    continue
785    continue
            fu(19)=sig*t(19)**4
* cf is the cloud free region of the atmosphere.
        do 792 i=1,18
            if (i.lt.kap+1) then
                cf=1.0-ac

```

```

        else
            cf=1.0
            end if
            fu(i)=cf*sig*t(19)**4+sig*(at(19)**4-t(19)**4)
x*(1-em(19,1))
            do 791 j=i,18
                fu(i)=fu(i)-cf*am(j,i)*sig*(t(j+1)**4-t(j)**4)
791      continue
792      continue
            do 796 i=1,kap
                fu(i)=fu(i)+ac*sig*t(kap)**4
                do 795 j=i,kap-1
                    fu(i)=fu(i)-ac*am(j,i)*sig*(t(j+1)**4-t(j)**4)
795      continue
796      continue
            do 798 i=1,19
                ftot(i)=fd(i)-fu(i)
798      continue
            fw(19)=fd(19)+fr(19)
            fw(18)=ftot(19)+fr(18)
            fw(nt)=ftot(nt)+fr(nt)
            fw(1)=fu(1)+fr(1)
            do 799 i=1,18
* dr1 is divided by .0083224 since it was already mult.
by this in tcool
                dw(i)=dr1(i)/.0083224+(ftot(i+1)-ftot(i))/
x (p(i+1)-p(i))
                dw(i)=dw(i)*.0083224
799      continue
*          do 800 i=1,19
*          write(20,1050) i,fu(i),fd(i)
*800      continue
1050      format (i3,2(4x,f8.3))
*
            return
            end
*
*****
subroutine h2otrans (pa,at,p,tr1,tr2,tr3,tr4,tr5
x ,tr6,trc,kap)
* calculate h2o transmission
* tr1 is trans for 660 - 800 cm-1 h2o
* tr2 is co2 h2o overlap
* tr3 is the ozone overlap (1000 cm-1) and is also
* used as the average transmission of the window
* region (800- 1200 cm-1)
* tr4 is ch4 h2o overlap
* tr5 is 1200-1350 n2o h2o overlap
* tr6 is 520-660 n2o h2o overlap

```

```

*   trc is the emissivity of the 800-1200 cm-1 h2o
*   cont.
*
  real pa(20),at(20),p(20)
  real tr1(20,20),tr2(20,20),tr4(20,20),tr5(20,20)
  real tr6(20,20)
  real trc(20,20),tr3(20,20)
  real th4,tr,tch,u4,sig
  integer kap
      sig=5.67e-8
      do 860 i=2,19
do 859 j=1,i-1
      e=esat(at(j))
      r=rwat(pa(j),e,j,kap)
      if (j.eq.1) then
      u4=r*1033*(p(j+1))
      else
      u4=r*1033*(p(j+1)-pa(j))
      end if
* tave and pave are the average temperature and pressure
* for an atmospheric path weighted according to water
* vapor amount
      tave=at(j)*(p(j+1)-pa(j))*r*1033
      pave=pa(j)*(p(j+1)-pa(j))*r*1033
do 857 k=j+1,i-1
      e=esat(at(k))
      r=rwat(pa(k),e,k,kap)
      u4=u4+r*1033*(p(k+1)-p(k))
      tave=tave+at(k)*r*1033*(p(k+1)-p(k))
      pave=pave+pa(k)*r*1033*(p(k+1)-p(k))
857 continue
      pave=pave/u4
      tave=tave/u4
      e=esat(tave)*.77*pave
      call h2oco2 (tave,pave,u4,tch,e,tr)
      tr1(j,i)=tr
      tr2(j,i)=tch
      call h2och4(pave,u4,tave,th4,e)
      tr4(j,i)=th4
      call n2oh2o1285 (pave,u4,tr)
      tr5(j,i)=tr
      call h2on2o590 (tave,pave,u4,tr)
      tr6(j,i)=tr
      call h2oo3(u4,tave,e,tr)
      tr3(j,i)=tr
      bl=3.742e-16*(100000.**3)/
x((exp(1.438*1000./tave))-1)
      call th2ocont8-12 (u4,tave,e,tr)
      trc(j,i)=40000.*bl*(1-tr)/(sig*tave**4)

```

```

859     continue
860     continue
do 870 i=1,19
do 869 j=1,i
    if (j.eq.19) then
        goto 869
    end if
    e=esat(at(i))
    r=rwat(pa(i),e,i,kap)
    u4=r*1033*(pa(i)-p(i))
    tave=at(i)*(pa(i)-p(i))*r*1033
    pave=pa(i)*(pa(i)-p(i))*r*1033
do 867 k=j,i-1
    e=esat(at(k))
    r=rwat(pa(k),e,k,kap)
    u4=u4+r*1033*(p(k+1)-p(k))
    tave=tave+at(k)*r*1033*(p(k+1)-p(k))
    pave=pave+pa(k)*r*1033*(p(k+1)-p(k))
867  continue
    pave=pave/u4
    tave=tave/u4
    e=esat(tave)*.77*pave
    call h2oco2 (tave,pave,u4,tch,e,tr)
    tr1(i,j)=tr
    tr2(i,j)=tch
    call h2och4(pave,u4,tave,th4,e)
    tr4(i,j)=th4
    call n2oh2o1285 (pave,u4,tr)
    tr5(i,j)=tr
    call h2on2o590 (tave,pave,u4,tr)
    tr6(i,j)=tr
    call h2oo3 (u4,tave,e,tr)
    tr3(i,j)=tr
    bl=3.742e-16*(100000.**3)/
x ((exp(1.438*1000./tave))-1)
    call th2ocont8-12 (u4,tave,e,tr)
    trc(i,j)=40000*bl*(1-tr)/(sig*tave**4)
869  continue
870  continue
        tr1(19,19)=1.0
        tr2(19,19)=1.0
        tr3(19,19)=1.0
        tr4(19,19)=1.0
        tr5(19,19)=1.0
        tr6(19,19)=1.0
        trc(19,19)=0.0
*   write (20,9011) ((tr2(i,j),j=1,19),i=1,19)
9011  format (19(f6.4,1x))
        return

```

end

```

*****
*
  subroutine tempave(at, sg, ta)
  dimension at(20),sg(20)
  dimension ta(20,20)
  real s
*
*   calculate the average temperaure to be used for
*   each path using a pressure weighted average
*   Dp=6sigma(1-sigma)
*
  do 600 i=1,19
  do 599 j=i,19
  ta(i,j)=0.0
  s=0.0
  do 590 k=i,j
  ta(i,j)=ta(i,j)+6.0*sg(k)*(1-sg(k))*at(k)
  s=s+6.0*sg(k)*(1-sg(k))
590  continue
  if(s-0.0) 595,595,596
595  ta(i,j)=at(i)
  goto 597
596  ta(i,j)=ta(i,j)/s
597  ta(j,i)=ta(i,j)
599  continue
600  continue
  return
  end
*****
* Called from h2ocloud to calculate tx and rx for each
* layer. See the detailed disscussion in Chapter 4
  subroutine kdist (tau,omeg,tx,rx)
  real tau,omeg,g,u,t,tx,rx
  g=.85
  t=sqrt(3*(1-omeg)*(1-g*omeg))*tau
  u=sqrt((1-g*omeg)/(1-omeg))
  bot=(u+1)**2-exp(-2*t)*(u-1)**2
  rx=(u+1)*(u-1)*(1.0-exp(-2*t))/bot
  tx=4*u*exp(-t)/bot
  return
  end
*****
*   solar heating for cloudy portion of the sky
*   via Lacis and Hansen 1974. See Chapter 4 of text.
  subroutine h2ocloud (p,pa,at,xk,pk,depth,theta,s0,
  x rg,kap,ac,shc,abs,gw)
  real gw(19),p(20),pa(20),at(20),xk(10),pk(10)

```

```

real shc(20),rx(25,10),tx(25,10)
real up(25,10),d(25,10),ab(25,10),clh(25,10)
real rl(25,10),rls(25,10),r19(25,10),t1(25,10)
real tt,s0,s,depth,abs,u1,mu0,e,r,m,theta
real tau,omeg,ref
* mu0 is the cosine of the average zenith angle
mu0=cos(theta)
m=35.0/sqrt(1224.0*mu0**2+1)
* s is the amount of solar radiation (divided by 2)
* associated with the cloudy portion of the atmosphere.
s=s0*ac
* gw is the downward flux of solar radiation and shc is
* the amount of solar radiation in Watts/m^2 absorbed by
* a layer
do 4500 j=1,19
gw(j)=0.0
shc(j)=0.0
4500 continue
gw(1)=s
abs=0.0
ref=0.0
do 4700 k=2,8
do 4510 j=1,kap-1
* rx and tx are the reflectivity and transmissivity of
* each layer j for each of the k spectral intervals.
rx(j,k)=0.0
e=esat(at(j))
r=rwat(pa(j),e,j,kap)
u1=pa(j)*sqrt(273/at(j))*r*1033*(p(j+1)-p(j))*m
* tau is the optical depth of a clear layer
tau=xk(k)*u1
tx(j,k)=exp(-tau)
4510 continue
e=esat(at(kap))
r=rwat(pa(kap),e,kap,kap)
u1=pa(kap)*sqrt(273/at(kap))*r*1033*
x (p(kap+1)-p(kap))*5/3
* depth is the optical depth of the cloud
tau=depth+xk(k)*u1
omeg=depth/tau
call kdist(tau,omeg,tx(kap,k),rx(kap,k))
do 4520 j=kap+1,18
rx(j,k)=0.0
e=esat(at(j))
r=rwat(pa(j),e,j,kap)
u1=pa(j)*sqrt(273/at(j))*r*1033*
x (p(j+1)-p(j))*5/3
tau= xk(k)*u1
tx(j,k)=exp(-tau)

```

```

4520   continue
      t1(1,k)=tx(1,k)
      r1(1,k)=0.0
      rx(19,k)=rg
      r19(19,k)=rg
      tx(19,k)=0.0
      r1s(1,k)=0.0
      do 4530 j=2,19
         t1(j,k)=t1(j-1,k)*tx(j,k)
         r1(j,k)=r1(j-1,k)+rx(j,k)*t1(j-1,k)**2
         r1s(j,k)=rx(j,k)+r1s(j-1,k)*tx(j,k)**2
*      t1s(j,k) would need to be calculated if there were 2
*      adjacent cloud layers
4530   continue
      do 4540 j=18,1,-1
         tt=tx(j,k)
         r19(j,k)=rx(j,k)+r19(j+1,k)*tt**2/
x      (1-rx(j,k)*r19(j+1,k))
4540   continue
      do 4550 j=1,18
         up(j,k)=t1(j,k)*r19(j+1,k)/(1-r1s(j,k)
x*r19(j+1,k))
         d(j,k)=t1(j,k)/(1-r1s(j,k)*r19(j+1,k))
         gw(j+1)=gw(j+1)+s*pk(k)*d(j,k)
         ab(j,k)=pk(k)*(1-r1(19,k)+up(j,k)-d(j,k))
4550   continue
*      abs is the total absorbed solar radiation by water
*      vapor in the cloudy portion of the sky. and ref is the
*      reflected solar radiation
      abs=abs+ab(18,k)*s*mu0
      ref=ref+r19(1,k)*s*mu0*pk(k)
      clh(1,k)=ab(1,k)
      shc(1)=shc(1)+clh(1,k)*(.0083224/(p(2)-p(1)))
x      *s*mu0
      do 4560 j=2,18
         clh(j,k)=ab(j,k)-ab(j-1,k)
         shc(j)=shc(j)+clh(j,k)*(.0083224/(p(j+1)-p(j)))
x      *s*mu0
4560   continue
      ab(19,k)=t1(18,k)*(1-rg)*pk(k)
      shc(19)=shc(19)+ab(19,k)
4599   format (7(f6.4,3x))
4600   format (9(f6.4,3x))
4700   continue
      gw(19)=shc(19)*mu0*s
      abs=abs+gw(19)
      return
      end

```

```
*****
```



```

subroutine h2ovisclr (s0,theta,pa,p,at,shw,gw,abs
x ,ac,rg,kap)
*   Clear sky calculations for water vapor see Chpt 4
dimension at(20),p(20),pa(20),shw(20)
dimension yl(20),ylb(20),sawd(20),sawu(20)
dimension sawt(20),gw(20)
real m,mu0,theta,e,s,s0,abs
integer kap
*   cos zenith angle mu0
mu0=cos(theta)
m=35./sqrt(1224.0*(mu0)**2+1)
s=s0*(1-ac)
* cp is the specific heat of dry air in J/(kg K)
cp=1005
yl(1)=0.0
sawd(1)=0.0
do 900 k=1,18
    e=esat(at(k))
    r=rwat(pa(k),e,k,kap)
    ul= pa(k)*sqrt(273/at(k))*r*1033*(p(k+1)-p(k))*m
* yl is the total path length of water vapor measured
* from z= infinity to the surface (z=0)
    yl(k+1)=yl(k)+ul
* sawd is the total amount of solar energy absorbed by
* the total path yl as the radiation travels downward
    sawd(k+1)=2.9*yl(k+1)/((1+141.5*yl(k+1))**.635
x +5.925*yl(k+1))
900 continue
* ylb is the total path length measured from the top of
* the atmosphere to the surface and then back up to level
* k. It is the path that a
* ray reflected from the surface would travel. The
* Diffusivity factor of 5/3 is included to account for
* the diffuse nature of the reflected radiation
    ylb(19)=yl(19)
* sawu is the total amount of solar energy absorbed as it
* travels a path ylb
    sawu(19)=sawd(19)
do 910 k=18,1,-1
    e=esat(at(k))
    r=rwat(pa(k),e,k,kap)
    ul=pa(k)*sqrt(273/at(k))*r*1033*(p(k+1)-p(k))
x *(5.0/3.0)
    ylb(k)=ylb(k+1)+ul
    sawu(k)=2.9*ylb(k)/((1+141.5*ylb(k))**.635
x +5.925*ylb(k))
910 continue
gw(1)=mu0*s0
abs=0.0

```

```

do 920 i=1,18
  gw(i+1)=mu0*s*(1-sawd(i+1))
  sawt(i)=mu0*s*(sawd(i+1)-sawd(i)+
  x rg*(sawu(i)-sawu(i+1)))
* .0083224/(delta p) is the conversion between W/m^2 of
* absorbed energy to heating in units of K/day.
* .0083224=86400*9.81/(1005*1.013e5)
  shw(i)=.0083224*(sawt(i))/(p(i+1)-p(i))
  abs=abs+sawt(i)
920 continue
  gw(19)=mu0*(1-rg)*s*(.353-sawd(19))
* abs is the total amount of solar energy absorbed by
* Clear sky water. .353 is included since 35.3 percent
* of the total solar
* energy is influenced by water vapor absorption.
  abs=abs+gw(19)
  return
end
*****
* Calculates the absolute humidity of water vapor based
* upon the assumed relative humidity profile h of Manabe
* and Wetherald 1967. e is the saturation pressure of
* water vapor in (atm).
  function rwat(p,e,j,kap)
  real rwat,h,e,p
  integer j,kap
  if(j.eq.kap) then
    h=.77*(p-.02)/.98
  else
    h=.77*(p-.02)/.98
  end if
  rwat=.622*h*e/(p-h*e)
  if (rwat.lt.3.0e-6) then
    rwat=3.0e-6
  end if
  return
end
*****
* Calculates the saturation vapor pressure of water in
* (atm) according to the Clausius Clapeyron relation
  function esat(t)
  real esat,l,r,t
* l is the latent heat of vaporization
  l=2510.-2.38*(t-273)
  r=.287
  esat=(6.11/1012.34)*exp((.622*l/r)*(t-273)/(t*273))
  return
end
*****

```

```

*
*   Calculates the transmission of water vapor continuum
*   in 8-12 micro meter region via Roberts 1976.  See
*   Chapter 3
  subroutine th2ocont8-12 (u4,t,e,trc)
    real trc,t,e,k,u4
    k=(4.2+5588*exp(-7.87))*exp(1800*(296-t)/(296*t))*e
    trc=(exp(-k*1.66*u4))
    return
  end
*****
*   Calculates the transmission of water vapor continuum
*   in 1042 cm-1 region for ozone overlap via Roberts 1976.
  subroutine h2oo3 (u4,t,e,trc)
    real trc,t,e,k,u4
    k=(4.2+5588*exp(-8.20))*exp(1800*(296-t)/(296*t))*e
    trc=(exp(-k*1.66*u4))
    return
  end
*****
*   calculate the transmission of water vapor Cont. over
*   an arbitrary spectral interval between nu1 and nu2 for
*   an arbitrary water vapor path length u4.  Roberts 1976
  subroutine trcont (nu1,nu2,u4,t,e,trch)
    real trch,nu1,nu2,nu,t,e,k
    integer n1,n2
    n1=int(nu1)
    n2=int(nu2)
    trch=0.0
    do 3000 i=n1,nu2-40,40
      nu=i+10
      k=(4.2+5588*exp(-.00787*nu))
x *exp(1800*(296-t)/(296*t))*e
      trch=trch+(exp(-k*1.66*u4))*40/(nu2-nu1)
3000 continue
    return
  end
*****
*   Calculate the planck function at temperature t and
*   wave number nu
  subroutine planck(b,t,nu)
    real b(20),t(20)
    real nu
    do 5500 i=1,19
      b(i)=3.742e-16*(nu*100)**3/
x ((exp(1.438*nu/t(i)))-1)
5500 continue
    return
  end

```

```

*
*****
* Sets the temperature at the top and bottom of each
* layer after the calculation of the temperature at the
* middle of each layer and the surface.
  subroutine tempset (t,at,p,kap)
    real t(20),at(20),p(20)
    integer kap
    t(1)=at(1)
    t(19)=at(19)
    do 4200 i=2,18
      t(i)=((p(i+1)-p(i))*at(i)+(p(i)-p(i-1))*at(i-1))/
x (p(i+1)-p(i-1))
4200 continue
      return
    end
*
*****
* Used once at the beginning of the main program to set
* the pressures of each layer from the sigma coordinate
* system.
  subroutine presset(sg,p,pa)
    real pa(20),sg(20),p(20)
    sg(2)=1.0/36.0
    pa(1)= (sg(2)**2)*(3.0-2.0*sg(2))
    p(1)=0.0
    p(19)=1.0
    pa(19)=1.0
    sg(1)=0.0
    do 4300 i=2,18
      p(i)=p(i-1)+6.0*sg(i)*(1-sg(i))/18.0
      sg(i+1)=sg(i)+(1.00/18.00)
      pa(i)=(sg(i+1)**2)*(3.0-2.0*sg(i+1))
4300 continue
      return
    end
*
*****
* Generic calculation of IR cooling rates dc and fluxes
* of IR radiation f from planck functions b (at the top
* and bottom of each layer)
* and band absorptances a between layers. ac,kap,and nt
* are the cloud fraction, layer that contains a cloud,
* and trapopause level
  subroutine acool(a,b,p,dc,f,ac,kap,nt)
    real fd(20),fu(20),ftot(20),b(20),dc(20)
    real a(20,20),f(20),p(20)
    real ac,cf
    integer kap,nt

```

```

      fd(1)=0.0
do 4024 i=2,19
  if (i.gt.kap) then
    cf=1.0-ac
  else
    cf=1.0
  end if
  fd(i)=cf*b(1)*a(1,i)
  do 4022 j=1,i-1
    fd(i)=fd(i)+cf*a(j,i)*(b(j+1)-b(j))
4022  continue
4024  continue
  do 4030 i=kap+1,19
    do 4028 j=kap+1,i-1
      fd(i)=fd(i)+ac*a(j,i)*(b(j+1)-b(j))
4028  continue
4030  continue
  fu(19)=0.0
do 4035 i=1,18
  if(i.lt.kap+1) then
    cf=1.0-ac
  else
    cf=1.0
  end if
  fu(i)=0.0
  do 4033 j=i,18
    fu(i)=fu(i)-cf*a(j,i)*(b(j+1)-b(j))
4033  continue
4035  continue
  do 4040 i=1,kap
    do 4038 j=i,kap-1
      fu(i)=fu(i)-ac*a(j,i)*(b(j+1)-b(j))
4038  continue
4040  continue
  do 4042 i=1,19
    ftot(i)=fd(i)-fu(i)
4042  continue
  do 4046 i=1,18
    dc(i)=.0083224*(ftot(i+1)-ftot(i))/(p(i+1)-p(i))
4046  continue
f(1)=fu(1)
  f(18)=ftot(19)
f(nt)=ftot(nt)
  f(19)=fd(19)
*   do 4049 i=1,19
*   write(20,4050) i,fu(i),fd(i)
*4049  continue
4050  format (i3,2(4x,f8.3))
*
```

```

    return
  end
*****
*   Calculates the band absorptances from the spectral
*   interval size dnu and transmissivities between layers.
*   Then call acool.
  subroutine tcool(dnu,tr,b,p,dc,f,ac,kap,nt)
    real a(20,20), tr(20,20)
    real b(20), dc(20), f(20), p(20)
    real dnu,ac
    integer kap,nt
  do 4110 i=1,19
  do 4105 j=1,i
    a(j,i)=(1-tr(j,i))*dnu*100.
    a(i,j)=(1-tr(i,j))*dnu*100.
4105  continue
4110  continue
  call acool (a,b,p,dc,f,ac,kap,nt)
  return
  end
*****
*   Calculates the exponential integral E1 according to a
*   numerical procedur given by Abromowitz and Stegan 1962.
*   Use for water vapor and ozone transmissions calculated
*   by the method of KUO 1977. See Chapter 3 of text.
  subroutine expon (y,e1)
    real gamma, e1,y
*   gamma is Eulers constant
    gamma=.5772157
    e1=0
    if (y.lt.1.) then
      e1=-log(y)-gamma
      e1=e1+.9999919*y-.2499106*y*y+
x .0551997*y**3-.0097600*y**4+.0010786*y**5
    else
      e1=(y**4)+8.5733287*y**3+18.0590170*y*y+
x 8.6347609*y+.26777373
      e1=e1/(y**4+9.5733223*y**3+25.6329561*y*y+
x 21.0996531*y+3.9584969)
      e1=(e1*exp(-y))/y
    endif
    return
  end
*****
  subroutine bcalc (t,bt1,bt2,bt6)
*   subroutine for the calculation of the b temperature
*   correction parameter to be used in the co2 overlap
*   calculation of Kuo 1977
    real bt1,bt2,bt6,t,ts,ts2

```

```

ts=t/100.-2.6
ts2=ts*ts
bt1=0.
bt2=0.
bt6=0.
bt=0.
bt=bt+1.6*.8457*(1-.2569*ts+.1191*ts2)
bt=bt+.60*.4643*(1-.6739*ts+.36*ts2)
bt=bt+.60*1.464*(1-.2605*ts+.1307*ts2)
bt1=bt+1.70*.927*(1-.1641*ts+.0255*ts2)
bt6=1.6*.927*(1-.1641*ts+.0255*ts2)
bt2=bt1+bt6
return
end
*****
* Calculates the water vapor overlap correction for CO2
* H2O overlap. tr1 is the transmission of the vib-rot
* band calculated via Kuo 1977(580-740 cm-1)
* and tr2 is the continuum transmission via Roberts 1976
  subroutine h2oco2 (t,p,u4,tch,e,tr)
    real e,e1,e2,bt1,bt2,bt6,m
    real t,p,u4,tr,tr1,tr2,tch
    real nu1,nu2
    nu1=580.
    nu2=740.
    m=1.66*u4*p
    call bcalc (t,bt1,bt2,bt6)
    y1=51.8845*sqrt(m)
    y5=y1*exp(-bt1)
    y6=y5*exp(-bt6)
    call expon (y5,e1)
    call expon (y6,e2)
    tr1=(e2-e1)/bt6
    call trcont (nu1,nu2,u4,t,e,tr2)
    tch=tr1*tr2
    call trr1(t,p,u4,tr1)
    call trcont(660.,800.,u4,t,e,tr2)
    tr=tr1*tr2
    return
  end
*****
  subroutine co2ir (t,p,pa,dc,fc,ta,tr2,tr3,con2
x,ac,kap,tco2n2,nt,qc,dq,ec,vc,sc,a,nr)
    real ta(20,20), a(20,20),tr2(20,20),tco2n2(20,20)
    real tr3(20,20)
    real qc(4),dq(4,14),ec(14),vc(14),sc(14),a1(20,20)
    real b(20),p(20),dc1(20),dc(20),fc(20),pa(20),t(20)
    real fc1(20)
    real a0,con2,ac,u1

```

```

integer kap,nt
* calculate planck fuctions for each layer for the 15
* micron bands
  call bpl(b,t,667.0)
  if (nr.eq.0.or.nr.gt.10) then
* Calculate the band absorptances once every 10 steps
  do 320 i=1,19
    do 318 j=1,i
      a0=(22.18)*sqrt(ta(j,i)/296.0)
      if (j.eq.1)then
        if(i.eq.1)then
* setting u=1 does nothing here except to prevent a
* divide by zero error
          u=1
        else
* u is the path length of CO2 in atm cm at STP. 1.66 is
* the diffusivity
* factor. and con2 is the CO2 concentration in ppmv.
          u=1.66*.8*con2*p(i)
* w is the dimensionless optical path length of the CO2
* 10 micron band.
* .03 is the band strength of this band.
          w=.03*u/a0
          pave=p(i)/2.0
* uco2 calculates the absorptance of all the 15 micron
* bands via Kiehl and Ramanathan 1983. This is very time
* consuming!
          call uco2(qc,dq,ec,vc,sc,ta(j,i),pave,u,a0,ab)
* ab is muliplied by 100 to change from units of cm -1 to
* m-1
          a(j,i)=ab*100
* a1 are the band absorptances for the CO2 10 micron
* region
          a1(j,i)=200*a0*log(1+w/(4+w*(1+1/
x(pave*.1084*(298/ta(j,i))**.56)))**.5)
          end if
          u=1.66*.8*con2*pa(i)
          w=.03*u/a0
          pave=(p(i+1)+pa(i))/2.0
          call uco2(qc,dq,ec,vc,sc,ta(i,j),pave,u,a0,ab)
          a(i,j)=100*ab
          a1(i,j)=200*a0*log(1+w/(4+w*(1+1/
x(pave*.1084*(298/ta(i,j))**.56)))**.5)
        else
          pave=(pa(j)+p(i))/2.0
          u=1.66*.8*con2*abs(p(i)-pa(j))
          w=.03*u/a0
          call uco2(qc,dq,ec,vc,sc,ta(j,i),pave,u,a0,ab)
          a(j,i)=ab*100

```



```

      a1(j,i)=200*a0*log(1+w/(4+w*(1+1/
x(pave*.1084*(298/ta(j,i)**.56)))**.5)
      u=1.66*.80*con2*abs(pa(i)-p(j))
      w=.03*u/a0
      call uco2(qc,dq,ec,vc,sc,ta(i,j),pave,u,a0,ab)
      a(i,j)=ab*100
      a1(i,j)=200*a0*log(1+w/(4+w*(1+1/
x(pave*.1084*(298/ta(i,j)**.56)))**.5)
      end if
* tco2n2 is use for the N2O CO2 overlap at 590 cm -1
* tr2 is the H2O CO2 overlap for 15 micron region
* tr3 is used for the H2O continuum CO2 overlap in 10
* micron region
      tco2n2(j,i)=1-a(j,i)/30000.
      tco2n2(i,j)=1-a(j,i)/30000.
      a(j,i)=a(j,i)*tr2(j,i)
      a(i,j)=a(i,j)*tr2(i,j)
      a1(j,i)=a1(j,i)*tr3(j,i)
      a1(i,j)=a1(i,j)*tr3(i,j)
318   continue
320   continue
      nr=0
      end if
      nr=nr+1
*
*   write (20,399) ((a1(i,j)/10000,j=1,19),i=1,19)
399   format (19(f5.3,2x))
      call acool(a,b,p,dc,fc,ac,kap,nt)
* Planck functions for each layer for 10 micron CO2
* bands
      call bpl(b,t,1020.0)
      call acool(a1,b,p,dcl,fcl,ac,kap,nt)
      do 400 i=1,19
      dc(i)=dc(i)+dcl(i)
      fc(i)=fc(i)+fcl(i)
400   continue
*
      return
      end
*
*****
* Calculates the 15 micron band absorptances for CO2
* path length u using the method of Kiehl and Ramanathan
* 1983.
      subroutine uco2(qc,dq,ec,vc,sc,t,p,u,a0,ab)
      real qc(4),vc(14),dq(4,14),sc(14),ec(14)
* qc,vc,dq,sc,ec are as defined at the beginning of the
* main program
      real sum(8),f(4,14),s(14)

```

```

* t1,t2, and t3 are used for the correction due to none
* overlapping bands
  real t1,t2,t3,u,a0,uc,t,p
  if (u.lt.0.0) then
    goto 460
  end if
  do 430 i=1,7
    sum(i)=0.0
430  continue
    do 450 j=1,14
*   s is the temperature corrected band strength
      s(j)=sc(j)*(300/t)*(1-exp(-1.439*vc(j)/t))**3/
x   (1-exp(-1.439*vc(j)/300))**3
x   *exp(1.439*ec(j)*(t-300)/(t*300))
      do 440 i=1,4
        if (j.eq.1.and.i.eq.1) then
*   bet is the band width parameter see chapter 3 section
*   2
          bet=(4/dq(i,j))*p*.067*(300/t)**.667
          uc=qc(i)*s(j)*u*exp((-53.5/a0))/a0
          t1=1/(1+uc/(4+uc*(1+1/bet))**.5)
          uc=qc(i)*s(j)*u*exp((-72./a0))/a0
          t2=1/(1+uc/(4+uc*(1+1/bet))**.5)
          uc=qc(i)*s(j)*u*exp((-124./a0))/a0
          t3=1/(1+uc/(4+uc*(1+1/bet))**.5)
        end if
          uc=qc(i)*u*s(j)/a0
          bet=(4/dq(i,j))*p*.067*(300/t)**.667
          f(i,j)=uc/(4+uc*(1+1/bet))**.5
440  continue
450  continue
      do 455 i=1,4
        sum(1)=sum(1)+f(i,1)+f(i,4)+f(i,5)
x   +f(i,9)+f(i,11)+f(i,12)
        sum(2)=sum(2)+f(i,2)+f(i,14)
        sum(3)=sum(3)+f(i,3)+f(i,13)
        sum(4)=sum(4)+f(i,7)
          sum(5)=sum(5)+f(i,8)
        sum(6)=sum(6)+f(i,10)
        sum(7)=sum(7)+f(i,6)
455  continue
        ab=2*a0*(log(1+sum(1))+t1*(log(1+sum(2))
x   +log(1+sum(3)))+t2*(log(1+sum(4))+log(1+sum(5)))
x   +t3*(log(1+sum(6))+log(1+sum(7))))
460  return
      end
*****
* alpha is used by o3ir (ozone cooling) program using
* the method of Kuo 1977 see chapter 3

```

```

function alpha(u,p)
real alpha,u,p,au,al,beta
au=(4.1*u)/(1+9.5*u)
al=.8467*u*(1.9-u)/(1+2.0*u)
if (p.ge..015) then
beta=sqrt((p-.015)/.235)
end if
if (p.le..015) then
alpha=(1.085-.085*p)*au
else
  if((p.ge..015).and.(p.le..25)) then
    alpha=(au**(1-beta))*(al**beta)
  else
    alpha=.6667*(1.75-p)*al
  endif
endif
return
end
*****
* Ozone cooling subroutine using the method of Kuo 1977.
* See chapter 3 of text.
  subroutine o3ir (at,bo,p,pa,uo,uoa,doc,
x fo,ac,kap,nt,tr3)
  dimension abs(20,20),tr3(20,20)
  dimension bo(20), p(20), doc(20), fo(20)
  dimension pa(20),uo(50),uoa(50)
  dimension ua(20),us(20),up(20),a(20),at(20)
  real u,ut,e1,e2,y,alpha
  integer kap,nt
*
  do 610 i=1,18
* u is the ozone path length in atm-cm STP.
  u=(uo(i+1)-uo(i))
  a(i)=alpha(u,pa(i))
  ua(i)=u*1.66*pa(i)**a(i)
  if(i.eq.1)then
    us(i)=uo(i+1)*1.66*pa(i)**a(i)
  else
    us(i)=(uo(i+1)-uoa(i))*1.66*pa(i)**a(i)
  end if
  up(i)=(uoa(i)-uo(i))*1.66*pa(i)**a(i)
610 continue
  do 640 i=2,19
  do 639 j=1,i-1
  ut=us(j)
630   do 635 k=j+1,i-1
    ut=ut+ua(k)
635   continue
  y=.5138*ut/sqrt(1+3.7145*ut)

```

```

    call expon (y,e1)
    call expon (17.778*y,e2)
    trn=.3476*(e1-e2)
    abs(j,i)=13700*(1-trn)*tr3(j,i)
639  continue
640  continue
      do 660 i=1,18
do 659 j=1,i
      ut=up(i)
      do 655 k=j,i-1
      ut=ut+ua(k)
655  continue
    y=.5138*ut/sqrt(1+3.7145*ut)
    call expon (y,e1)
    call expon (17.778*y,e2)
    trn=.3476*(e1-e2)
    abs(i,j)=13700*(1-trn)*tr3(i,j)
659  continue
660  continue
*
*   write (20,399) ((abs(i,j)/10000,j=1,19),i=1,19)
399  format (19(f5.3,2x))
    call acool (abs,bo,p,doc,fo,ac,kap,nt)
*
    return
    end
*
*****
*   Calculates the height of each layer (top, middle, and
*   bottom) using the pressure thickness of each layer and
*   the ideal gas law density of each layer.
    subroutine height (z,za,p,pa,at)
    dimension z(20),za(20),p(20),pa(20),at(20)
    real ao,bo,co,dpr
    z(19)=0.0
    do 900 i=19,2,-1
    dpr=p(i)-p(i-1)
    z(i-1)=z(i)+(dpr*at(i-1)*.02925)/pa(i-1)
    dpr=p(i)-pa(i-1)
    za(i-1)=z(i)+(2*dpr*at(i-1)*.02925)/(pa(i-1)+p(i))
900  continue
    return
    end
*
*****
*   Ozone Clear Skies solar heating see Chapter 4 of
*   text.
    subroutine o3visclr (s0,theta,uo,p,ho,fso
    x ,abo,ac,rg)

```

```

*      Calculate ozone solar heating according to Lacis
* and Hansen 1974 Clear Skies
      real a(20),x(20),xu(20),au(20),ab(20)
      real uo(20), ho(20), fso(20),p(20)
      real mu0, mbar, m, rg, ra2, ra1, theta, ra
      real abo,rrm,rrs
* abo, ho, and fso are the total absorbed solar energy by
* the clear sky ozone, the heating rate in K/day of each
* atmospheric layer (assumed dry), and the contribution
* to the flux of solar radiation from the
* clear sky ozone part of the spectrum.
      s=s0*(1-ac)
* s is the fraction of the total solar energy associated
* with the Clear
* portion of the sky.
      mu0=cos(theta)
      mbar=1.9
      ra2=.144
      ra1=.219/(1+.816*mu0)
      ra=ra1+(1-ra1)*(1-ra2)*rg/(1-ra2*rg)
      m=35./sqrt(1224*mu0*mu0+1)
      do 5000 i=1,19
x(i)=m*uo(i)
a(i)=ao3(x(i))
5000  continue
      do 5010 i=1,19
xu(i)=x(19)+mbar*(x(19)-x(i))/m
au(i)=ao3(xu(i))
5010  continue
      fso(1)=s*mu0
      abo=0.0
      do 5020 i=1,18
ab(i)=s*mu0*((a(i+1)-a(i))+ra*(au(i)-au(i+1)))
ho(i)=.0083224*ab(i)/(p(i+1)-p(i))
fso(i+1)=(s-s*a(i+1))*mu0
      abo=abo+ab(i)
5020  continue
      rrm=.28/(1+6.43*mu0)
      rrs=.0685
      fso(19)=s*(1-rg)*mu0*(.647-rrm-a(19))/(1-rrs*rg)
      abo=abo+fso(19)
      return
      end
*****
*      Calculates solar heating for Cloudy portion of the
* sky for the
* Ozone portion of the spectrum.
      subroutine o3cloud (s0,theta,uo,p,ho,fso,abo
x ,ac,rg,kap,depth)

```

```

*      Calculate ozone solar heating according to lacis
* and hansen 1974 Cloudy Skies.  ho is the heating of
* each layer due to the absorption of solar radiation by
* ozone(each layer is assumed to be dry
* here). fso is the flux of solar radiation for the
* cloudy portion of the sky and for the ozone part of the
* spectrum. and abo is the total absorbed solar energy
* for the cloudy sky and this part of the spectrum.
      real a(20),x(20),xu(20),au(20),ab(20)
      real uo(20), ho(20), fso(20),p(20)
      real mu0, mbar, m, rg, ra2, ral, theta, ra
      real ac,depth,abo,xl,rrm,rrs
      integer kap
* s is the fraction of the total solar energy associated
* with the cloudy portion of the sky
      s=s0*ac
      mu0=cos(theta)
      xl=.85
      mbar=1.9
      ra2=(1-xl)*depth*sqrt(3.0)/
x (2+(1-xl)*depth*sqrt(3.0))
      ral=ra2
      ra=ral+(1-ral)*(1-ra2)*rg/(1-ra2*rg)
      m=35./sqrt(1224*mu0*mu0+1)
      do 5000 i=1,19
      x(i)=m*uo(i)
      a(i)=ao3(x(i))
5000  continue
      do 5010 i=1,19
      xu(i)=x(kap+1)+mbar*(x(kap+1)-x(i))/m
      au(i)=ao3(xu(i))
5010  continue
      fso(1)=s*mu0
      abo=0.0
      do 5020 i=1,18
      ab(i)=s*mu0*((a(i+1)-a(i))+ra*(au(i)-au(i+1)))
      ho(i)=.0083224*ab(i)/(p(i+1)-p(i))
      fso(i+1)=(s-s*a(i+1))*mu0
      abo=abo+ab(i)
5020  continue
      rrm=.28/(1+6.43*mu0)
      rrs=.0685
      fso(19)=s*(1-rg)*(1-ral)*mu0
x (.647-a(19))/(1-ra2*rg)
      abo=abo+fso(19)
      return
      end
*****
      function ao3(x)

```

```

* ao3 is the fraction of incident solar energy absorbed
* by a clear sky path of ozone. Lacis and Hansen 1974.
  a1=.02118*x/(1+.042*x+.000323*x*x)
  a2=(1.082*x/(1+138.6*x)**.805)
  x+.0658*x/(1+(103.6*x)**3)
  ao3=a1+a2
  return
end
*****
* Convective adjustment calculation
  subroutine lapadj (at,gam,za,cp,ch,nt,ce)
  real at(20),gam(20),za(20),cp(20),ch(20),ce(20)
  real s2,d1,d2,d3,db,dt
  integer nt
* nt is the height of the tropopause.
  nt=6
  do 7998 i=1,19
    ch(i)=0.0
7998  continue
7999  s2=0.0
    za(19)=0.0
    do 8002 i=18,2,-1
      d1=at(i+1)-at(i)
      d2=gam(i)*(za(i)-za(i+1))
      if (d1.gt.d2) then
        d3=1.0*(d1-d2)
        db=cp(i)*d3/(cp(i)+cp(i+1))
        dt=cp(i+1)*d3/(cp(i)+cp(i+1))
        at(i)=at(i)+dt
        at(i+1)=at(i+1)-db
        ch(i)=ch(i)+dt
        ch(i+1)=ch(i+1)-db
        s2=s2+d3
        nt=i
      end if
8002  continue
      if (s2.gt..005)then
        goto 7999
      endif
      do 8005 i=2,18
        if (at(19).lt.(at(18)+.04))then
          ce(i)=ce(i)*.95
        end if
        ce(i)=ce(i)+ch(i)/2.0
        if(ch(i).lt..00001) then
          ce(i)=ce(i)*.9995
        end if
8005  continue
      return

```

```

      end
*
*****
* Sets constant Critical lapse rate for convective
* adjustment
  subroutine lap1 (gam,lap)
    real gam(20)
    real lap
    do 8600 i=1,18
      gam(i)=lap
8600  continue
    return
  end
*****
* Set the critical lapse rate equal to the moist
* adiabatic lapse rate
  subroutine lap2 (gam,at,pa)
* moist adiabatic lapse rate from Stone & Carlson
* 1979
    real gam(20),at(20),pa(20)
    real l,r,de,e
    r=.287
    do 8700 i=1,18
      l=2510.-2.38*(at(i)-273)
      e=esat(at(i))
      de=.622*l*e/(r*at(i)**2)
      gam(i)=9.8*(1+.622*l*e/(pa(i)*r*at(i)))/
x (1+(.622*l*de)/(1.005*pa(i)))
8700  continue
    return
  end
*****
* Calculate H2O overlap in methane region 1200-1650
* vib rotation & 950-1200 continuum
  subroutine h2och4 (pa,u4,at,th4,e)
    real pa,u4,th4,e,tr1,tr2,at
    call trr4 (pa,u4,tr1)
    call trcont(920.,1200.,u4,at,e,tr2)
    th4=(280*tr2+450*tr1)/750
    return
  end
*****
* Calculates Vib-rot H2O in CH4 overlap 1200-1650
* Rodgers & Walshaw 1966
  subroutine trr4(p,u4,tr)
    real p,u4,tr,m,kd,kpa
    m=1.66*u4
    kd=248
    kpa=1276

```



```

    tr=exp(-kd*m/sqrt(1+kpa*m/p))
    return
end
*****
*   Calculate methane transmission in N2O 1200-1350 cm-1
*   region using Green's 1964 method see chapter 3 of
*   text. method divides the methane region into 5
*   spectral regions and then calculates an average
*   transmission for part of the methane spectrum that
*   overlaps N2O.
    function tn2c4(w)
    real dn(10),we(10)
    real w,tn2c4
    dn(1)=35.6
    dn(2)=12.0
    dn(3)=18.5
    dn(4)=13.1
    dn(5)=72.0
    we(1)=18.4
    we(2)=9.08
    we(3)=2.60
    we(4)=6.47
    we(5)=14.95
    tn2c4=0.0
    do 9400 i=1,5
    tn2c4=tn2c4+exp(-((w/we(i))**.46))*dn(i)/151.2
9400 continue
    return
end
*****
*   Calculate N2O CH4 overlap using the function tn2c4
*   above
    subroutine n2c41285 (tnc,p,pa,at,c40)
    real tnc(20,20)
    real p(20),pa(20),at(20)
    real f,w,tn2c4,c40
*   f is ch4 mixing ratio 1.6 ppmv
    f=c40
    do 9360 i=2,19
    do 9359 j=1,i-1
    w=f*(1.29/1.6)*pa(j)*(p(j+1)-pa(j))*sqrt(300/at(j))
    do 9355 k=j+1,i-1
    w=w+f*(1.29/1.6)*pa(k)*
x (p(k+1)-p(k))*sqrt(300/at(k))
9355 continue
    tnc(j,i)=tn2c4(w)
9359 continue
9360 continue
    do 9370 i=1,19

```

```

do 9369 j=1,i
  if(j.eq.19)then
    goto 9369
  endif
  w=f*(1.29/1.6)*pa(i)*(pa(i)-p(i))*sqrt(300/at(i))
  do 9365 k=j,i-1
    w=w+f*(1.29/1.6)*pa(k)*
x (p(k+1)-p(k))*sqrt(300/at(k))
9365   continue
      tnc(i,j)=tn2c4(w)
9369   continue
9370   continue
      tnc(19,19)=1.0
      return
      end
*****
*   Calculates Vib-rot H2O in CH4 overlap 1200-1350
*   Rodgers & Walshaw 1966
*   subroutine n2oh2o1285 (p,u4,tr)
      real p,u4,tr,m,kd,kpa
      m=1.66*u4
      kd=12.65
      kpa=142.13
      tr=exp(-kd*m/sqrt(1+kpa*m/p))
      return
      end
*****
*   subroutine h2on2o590 (t,p,u4,tr)
*   transmission of rotation band from 520-660 cm-1
*   using statistical model Goody 1964, Rodgers & Walshaw
*   1966 used for h2o N2O overlap correction
      real kd,kpa,a,a1,b,b1,phi,t,psi,phb,m,mb
      m=1.66*u4
      kd=9.706
      kpa=162.6
      a=.0168
      a1=.0172
      b=-3.63e-5
      b1=-4.86e-5
      phi=exp(a*(t-260)+b*(t-260)**2)
      psi=exp(a1*(t-260)+b1*(t-260)**2)
      mb=phi*m
      phb=psi*p*m/mb
      tr=exp(-(kd*mb)/sqrt(1+kpa*mb/phb))
      return
      end
*****
*   Calculate CH4 cooling via Ramanathan et al 1987
*   subroutine ch4ir (ta,p,pa,t,d4,f4,tr4,

```

```

x c40,ac,kap,nt)
  real p(20),pa(20),d4(20),f4(20),b(20),t(20)
  real tr4(20,20),a4(20,20),ta(20,20),ut(20,20)
  real pe,bet,a0,u,c40,c,ac,a,x,d
  integer kap,nt
  a=3.03
  x=0.104
  d=1.012
  call bpl(b,t,1306.0)
  c=1.66*134*c40*(1.28/1.6)
*   134 (Goody 1989) is the band strength S
*   1.28*(c40/1.6) *delta p is the absorber amount in
*   atm-cm c40 is the concentration of CH4 in ppmv
*   ucalc calculates the total absorber amount for a given
*   atmospheric path assuming that the concentration of CH4
*   decreases above tropopause according to
*   c=c40*(a*p**x-d)/1.6
  call ucalc(p,pa,ut,5,a,x,d,1.6)
  do 9010 i=1,19
  do 9005 j=1,i
    pe=(pa(j)+p(i))/2
    bet=pe*.211*(300./ta(j,i))
*   bet0=.211... and a0=68.2... from Ramanathan et al
*   1987
    a0=68.2*(ta(j,i)/300)**.858
    u=(c/a0)*ut(j,i)
    a4(j,i)=200*a0*
x log(1+(u/(.106+sqrt(3.59+u*(1+1/bet))))))
    u=(c/a0)*ut(i,j)
    a4(i,j)=200*a0*
x log(1+(u/(.106+sqrt(3.59+u*(1+1/bet))))))
    a4(j,i)=a4(j,i)*tr4(j,i)
    a4(i,j)=a4(i,j)*tr4(i,j)
9005   continue
9010   continue
*   write (20,9011) ((a4(i,j)/10000,j=1,19),i=1,19)
9011   format (19(f6.4,1x))
  call acool(a4,b,p,d4,f4,ac,kap,nt)
  return
end
*****
*   Calculate N2O 1200-1350 cooling via Donner and
*   Ramanathan 1980
  subroutine n2o1285 (ta,p,pa,t,d5,f5,tr5,tnc4,
x n20,ac,kap,nt,ut)
  real p(20),pa(20),d5(20),f5(20),b(20),t(20)
  real tr5(20,20),a5(20,20),ut(20,20)
  real ta(20,20),tnc4(20,20)
  real pe,bet,a0,u,n20,c,ac,a,x,d

```

```

integer kap,nt
a=.559
x=.2
d=.096
call bpl(b,t,1285.0)
c=1.66*264*n20*(.239/.30)
* 264 (Goody 1989) is the band strength S
* .239*(n20/.30) *delta p
* is the absorber amount in atm-cm n20 is the
* concentration of n2o in ppmv. ucalc calculates the
* path length of N2O in atm-cm assuming that the profile
* of N2O decreases according to n20*(a*p^x-d)/.3. This
* was obtained from an empirical fit to the profile given
* by Crutzen 1978
call ucalc(p,pa,ut,5,a,x,d,.3)
do 9010 i=1,19
do 9005 j=1,i
pe=(pa(j)+p(i))/2
bet=pe*1.12*(300./ta(j,i))**.5
* bet0=1.12 from Donner and Ramanathan 1980
a0=20.4*(ta(j,i)/300)**.5
u=(c/a0)*ut(j,i)
a5(j,i)=200*a0*log(1+(u/sqrt(4+u*(1+1/bet))))
u=(c/a0)*ut(i,j)
a5(i,j)=200*a0*log(1+(u/sqrt(4+u*(1+1/bet))))
a5(j,i)=a5(j,i)*tr5(j,i)*tnc4(j,i)
a5(i,j)=a5(i,j)*tr5(i,j)*tnc4(i,j)
9005 continue
9010 continue
* write (20,9999) ((a5(i,j)/10000,j=1,19),i=1,19)
9999 format (19(f6.4,1x))
call acool(a5,b,p,d5,f5,ac,kap,nt)
return
end
*****
* Calculate N2O 520-660 cooling via Donner and
* Ramanathan 1980
subroutine n2o590 (p,pa,ta,t,d5,f5,tr6,tco2n2
x ,n20,ac,kap,nt,ut)
real p(20),pa(20),d6(20),f6(20)
real b(20),t(20),d5(20),f5(20)
real tr6(20,20),a6(20,20),tco2n2(20,20)
real ta(20,20),ut(20,20)
real pe,bet,a0,u,n20,c,ac
integer kap,nt
call bpl(b,t,589.0)
c=1.66*24*n20*(.239/.30)
* 24 (Ramanathan 1985) is the band strength S
* .239*(n20/.30) *delta p

```

```

*      is the absorber amount in atm-cm n2o is the
* concentration of n2o in ppmv
      do 9010 i=1,19
      do 9005 j=1,i
      pe=(pa(j)+p(i))/2
      bet=pe*1.08*(300./ta(j,i))**.5
*      bet0=1.12 from Donner and Ramanathan 1980
      a0=23.0*(ta(j,i)/300)**.5
      u=(c/a0)*ut(j,i)
      a6(j,i)=200*a0*log(1+(u/sqrt(4+u*(1+1/bet))))
      u=(c/a0)*ut(i,j)
      a6(i,j)=200*a0*log(1+(u/sqrt(4+u*(1+1/bet))))
      a6(j,i)=a6(j,i)*tr6(j,i)*tco2n2(j,i)
      a6(i,j)=a6(i,j)*tr6(i,j)*tco2n2(i,j)
9005  continue
9010  continue
*      write (20,9990) ((a6(i,j)/10000,j=1,19),i=1,19)
9990  format (19(f6.4,1x))
      call acool(a6,b,p,d6,f6,ac,kap,nt)
      do 9991 i=1,19
      d5(i)=d5(i)+d6(i)
      f5(i)=f5(i)+f6(I)
9991  continue
      return
      end
*****
* Calculates the absorber path length divided by the
* ground level concentration for N2O and CH4 which are
* both assumed to have decreasing mixing ratios above the
* tropopause.
      subroutine ucalc (p,pa,ut,nt,a,x,d,c0)
      real u(20),c(20),p(20),pa(20)
      real ut(20,20)
      integer nt
      do 9520 i=1,19
      if(i.le.nt)then
      c(i)=(a*(pa(i)**x)-d)/c0
      else
      c(i)=1.0
      end if
      u(i)=c(i)*(p(i+1)-p(i))
9520  continue
      do 9540 i=1,19
      do 9535 j=1,i
      ut(i,j)=0.0
      ut(j,i)=0.0
      if (j.eq.1) then
      ut(j,i)=u(j)
      else

```

```

ut(j,i)=c(j)*(p(j+1)-pa(j))
end if
if (i.eq.j) then
ut(i,j)=c(i)*(pa(i)-p(i))
else
ut(i,j)=u(j)+c(i)*(pa(i)-p(i))
end if
do 9530 k=j+1,i-1
ut(i,j)=ut(i,j)+u(k)
ut(j,i)=ut(j,i)+u(k)
9530 continue
9535 continue
9540 continue
return
end
*****
* Calculates solar heating due to CO2 following the
* parameterization given by Sasamori 1972
subroutine co2vis (p,pa,shco2,abco2,c20,s0,
x theta,kap,ac)
real p(20),pa(20),shco2(20),a2(20)
real u2,abco2,c20,theta,s0,mu0,ac
integer kap
mu0=cos(theta)
abco2=0.0
u2=0.0
a2(1)=0.0
do 9600 i=1,18
u2=u2+c20*.8*(p(i+1)-p(i))*pa(i)
a2(i+1)=(2.35e-3)*((u2+.0129)**.26)-7.5e-4
9600 continue
do 9610 i=1,18
if (i.gt.kap-1) then
shco2(i)=(1-ac)*s0*mu0*(a2(i+1)-a2(i))
else
shco2(i)=s0*mu0*(a2(i+1)-a2(i))
end if
abco2=abco2+shco2(i)
shco2(i)=shco2(i)*.0083224/(p(i+1)-p(i))
9610 continue
return
end
*****
* Calculates solar absorption due to molecular
* Oxygen following Sasamori 1972
Subroutine oxyvis (p,sho2,abo2,s0,theta,kap,ac)
real p(20),sho2(20),a4(20)
real abo2,theta,mu0,s0,ac
integer kap

```

```

      mu0=cos(theta)
      abo2=0.0
      a4(1)=0.0
      do 9700 i=1,18
9700  a4(i+1)=7.5e-3*(p(i+1)/mu0)**.875
      continue
      do 9710 i=1,18
      sho2(i)=s0*mu0*(a4(i+1)-a4(i))
      abo2=abo2+sho2(i)
      sho2(i)=sho2(i)*.0083224/(p(i+1)-p(i))
9710  continue
      return
      end
*****
*   Calculates IR heating/Cooling for atmospheric trace
*   gases that have small mixing ratios (less than 5 ppbv)
*   especially useful for global warming due to CFCs etc..
      subroutine smallir (ta,p,pa,t,ds,fs,cs0,ac,
x kap,nt,v0,strength)
      real ta(20,20),p(20),pa(20),t(20)
      real b(20),ds(20),fs(20),as(20,20)
      real dst(20),fst(20)
      real cs0,ac,v0,strength
* strength is the band strength in atm-1 cm-2 at a temp
* of 300K
      integer kap,nt
      call bpl(b,t,v0)
      c=1.66*strength*.8*cs0/1e6
* when cs0 is in pptv then c*(p(i+1)-p(i))/strength is
* the path length of the gas in atm-cm STP. using the
* linear limit c*(p(i+1)-p(i)) is the band absorptance of
* layer i at a temperature
* of 300 K.
      do 9808 i=1,19
      do 9806 j=1,i
      if(j.eq.1) then
      as(j,i)=100*c*ta(j,i)*p(i)/300
* ta/300 is a temperature correction to the band strength
      as(i,j)=100*c*(ta(i,j)/300)*pa(i)
      else
      as(j,i)=100*c*(ta(j,i)/300)*abs(p(i)-pa(j))
      as(i,j)=100*c*(ta(i,j)/300)*abs(pa(i)-p(j))
      end if
9806  continue
9808  continue
      call acool(as,b,p,dst,fst,ac,kap,nt)
      do 9810 i=1,19
      ds(i)=ds(i)+dst(i)
      fs(i)=fs(i)+fst(i)

```

```
9810  continue
      return
      end
```

Biographical Note

The author was born 21 September 1956, in Oroville, California. In 1963 he moved from a small rural mountain community in the Sierra Nevada to Chico, California and subsequently graduated from Chico High School in 1974. In December 1978 he received a Bachelor of Arts in Physics and Mathematics from California State University Chico.

In September 1979 the author began Graduate school at Portland State University, Portland, Oregon and after an 18 month interruption to work for an oil exploration company, received a Masters of Science in Physics in 1983.

The author then accepted a position as Physics Instructor at Clark College, Vancouver, Washington in September 1983 and has been active in the teaching profession since that time. He began work at the Oregon Graduate Institute in 1988 and after completion of his Masters of Science work will continue his studies at the Institute towards the requirements for the degree of Doctor of Philosophy.

In addition to his professional interests the author has a wife, of ten years, two step sons ages 22 and 24, and throughly enjoys the outdoors.